

ADVERTIMENT. L'accés als continguts d'aquesta tesi queda condicionat a l'acceptació de les condicions d'ús establertes per la següent llicència Creative Commons:  <https://creativecommons.org/licenses/?lang=ca>

ADVERTENCIA. El acceso a los contenidos de esta tesis queda condicionado a la aceptación de las condiciones de uso establecidas por la siguiente licencia Creative Commons:  <https://creativecommons.org/licenses/?lang=es>

WARNING. The access to the contents of this doctoral thesis it is limited to the acceptance of the use conditions set by the following Creative Commons license:  <https://creativecommons.org/licenses/?lang=en>

**DECELLULARIZED ALLOGRAFTS FOR REPAIRING
SEVERE PERIPHERAL NERVE INJURIES**

ACADEMIC DISSERTATION

To obtain the degree of PhD in Neuroscience by the

Universitat Autònoma de Barcelona

May 2023

PhD Candidate

Estefanía Contreras Carretón

Thesis supervisors

Dr. Xavier Navarro Acebes

Dr. Esther Udina Bonet

Academic Tutor

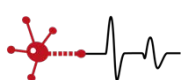
Dr. Xavier Navarro Acebes

Group of Neuroplasticity and Regeneration,

Departament de Biologia Cel·lular, Fisiologia i Immunologia,

Institut de Neurociències

NeuroPlasticity
& Regeneration



This thesis was funded by:

- Project E10668. Eurostars, EUREKA. 2016-2019. "eBIONERVE: personalized nerve grafts for treating human nerve injuries".
- Research agreement with Banc de Sang i Teixits 2017-2019. Design of a decellularized nerve matrix to generate peripheral nerves.
- Project SAF 2017-84464R from Ministerio de Economía y Competitividad, 2018-2021. "Modulation of axonal transloma to promote selective regeneration after peripheral nerve injuries".
- Project RD21/0017/0008 from Grupo de la Red de Terapias Avanzadas (TERAV RICORS) , Instituto de Salud Carlos III, 2022-2025.
- Centro de Investigación Biomédica en Red sobre Enfermedades Neurodegenerativas (CIBERNED).

A mi padre

INDEX

I. SUMMARY	9
II. ARTICLES PRODUDUCED IN THIS THESIS	13
III. ABBREVIATIONS	17
IV. INTRODUCTION	21
1. Peripheral Nervous System	23
1.1. Extracellular matrix in the PNS.....	26
2. Peripheral Nerve Injuries	28
2.1. Classification of PNI	28
3. Degeneration and regeneration following PNI	30
3.1. Neuronal response after PNI.....	30
3.2. Wallerian degeneration	32
3.3. Axonal regeneration	33
3.4. Functional recovery	35
4. Surgical repair strategies	35
5. Nerve decellularization strategies.....	39
6. Recellularization of decellularized nerve grafts	43
7. Experimental models of PNI and regeneration	47
7.1. <i>In vivo</i> models of nerve injury and repair	48
7.2. Sciatic nerve and tributaries.....	49
7.3. Nerve size and length of regeneration	49
7.4. Large animal models for translational research on nerve repair ...	50
V. OBJECTIVES.....	53
VI. STUDY DESIGN AND METHODOLOGIES.....	57
VII. RESULTS	65

INDEX

Chapter I: Repair of long peripheral nerve defects in sheep: a translational model for nerve regeneration.....	67
Chapter II: Evaluation of a decellularized nerve graft optimized by the BST to repair severe peripheral nerve injuries in rats and in sheep	105
Chapter III: Evaluation of a decellularized allograft optimized by Verigrift to repair severe peripheral nerve injuries in rats and in sheep	157
VIII. GENERAL DISCUSSION	199
IX. CONCLUSIONS.....	209
X. REFERENCES	213
XI. ACKNOWLEDGMENTS	233

I. SUMMARY

Peripheral nerve injuries result in loss of sensory, motor and autonomic functions of the area innervated by the injured nerves. Although peripheral neurons have the capability to regenerate after a lesion, functional recovery is usually unsatisfactory, specially after severe nerve injuries where nerves are completely transected. Surgical repair is mandatory after nerve section; if the lesion generates a gap too large to allow apposition and direct suture of the nerve stumps, a nerve graft is used to bridge this gap, being the autologous nerve graft the gold standard technique. However, it has some drawbacks, such as limited availability of healthy nerves, donor site morbidity, and longer intraoperative time. Allografts can be an alternative to the use of the autografts, although the immune rejection against Schwann cells and myelin sheaths impedes their use. To avoid rejection, these allografts can be decellularized.

The aim of this thesis is to evaluate two different enzymatic protocols, one also combined with detergents for rat, sheep and human nerves. The regenerative capacity of these decellularized allografts has been tested for the repair of critical injuries in the rat sciatic nerve and in the sheep peroneal nerve.

Both decellularization protocols were highly efficient for removing the cells present in the nerve while preserving the extracellular matrix structural and biomechanical properties. *In vivo* results in the rat sciatic nerve model showed that the decellularized allografts supported nerve regeneration along a critical nerve injury inducing a 15 mm gap. However, the lack of cellularity implied slight delay in the regenerative process in comparison to the ideal autograft. On the other hand, the use of human decellularized xenografts in the rat did not sustain well nerve regeneration. An inflammatory and fibrotic reaction was observed at early-phases of regeneration. *In vitro* studies showed that the components of the extracellular matrix play also a role in axonal regeneration being less effective inter-species.

In the sheep, we evaluated the regenerative capacity of the decellularized allografts in a 5 or 7 cm long gap injury of the peroneal nerve. In both cases, the grafts assayed supported effective axonal regeneration along the gap and distal target reinnervation, although slower regenerative progression was observed in the gap of 7 cm than in the gap of 5 cm. The regeneration outcomes were lower than the ones reached with the autograft repair in both allografts due to the lack

SUMMARY

of cellularity. In summary, decellularized allografts emerge as the most suitable alternative to autografts, since they guarantee regeneration in long gap nerve injuries in contrast to nerve conduits reported in the literature.

II. ARTICLES PRODUCED IN THIS THESIS

Research papers

- Contreras E, Bolívar S, Nieto-Nicolau N, Fariñas O, López-Chicón P, Navarro X, Udina E. A novel decellularized nerve graft for repairing peripheral nerve long gap injury in the rat. *Cell Tissue Res.* 2022 Dec;390(3):355-366.

Peer reviewed publication

- Contreras E, Traserra S, Bolívar S, Forés J, Jose-Cunilleras E, García F, Delgado-Martínez I, Holmgren S, Strehl R, Udina E, Navarro X. Repair of Long Nerve Defects with a New Decellularized Nerve Graft in Rats and in Sheep. *Cells.* 2022 Dec 16;11(24):4074.
- Contreras E, Traserra S, Bolívar S, Forés J, Jose-Cunilleras E, Delgado-Martínez I, García F, Udina E, Navarro X. Repair of Long Peripheral Nerve Defects in Sheep: A Translational Model for Nerve Regeneration. *Int J Mol Sci.* 2023 Jan 10;24(2):1333.
- Contreras E, Traserra S, Bolívar S, Nieto-Nicolau N, Jaramillo J, Forés J, Jose-Cunilleras E, Moll X, García F, Delgado-Martínez I, Fariñas O, López-Chicón P, Vilarrodona A, Udina E, Navarro X. Decellularized graft for repairing severe peripheral nerve injuries in sheep. Accepted for publication in *Neurosurgery*.

Review

- Contreras E, Bolívar S, Navarro X, Udina E. New insights into peripheral nerve regeneration: The role of secretomes. *Exp Neurol.* 2022 Aug;354:114069.

Other collaborations

- Nieto-Nicolau N, López-Chicón P, Torrico C, Bolívar S, Contreras-Carreton E, Udina E, Navarro X, Casaroli-Marano RP, Fariñas O, Vilarrodona A. "Off-the-Shelf" Nerve Matrix Preservation. *Biopreserv Biobank.* 2022 Feb;20(1):48-58.

ARTICLES PRODUCED IN THIS THESIS

- Redolfi E, Özkan M, Contreras E, Pawar S, Zinno C, Escarda-Castro E, Kim J, Wieringa P, Stellacci F, Micera S, Navarro X. Beyond the limiting gap length: peripheral nerve regeneration through implantable nerve guidance conduits. Submitted to Biofabrication
- Redolfi E, Pérez-Izquierdo M, Zinno C, Contreras E, Rodríguez-Meana B, Iberite F, Ricotti L, Micera S, Navarro X. A novel 3D-printed/porous conduit with tunable properties to enhance nerve regeneration over the critical nerve gap length. Submitted to Advanced Materials Technologies

III. ABBREVIATIONS

- ADSCs: adipose-derived mesenchymal stem cells
- AG: autograft
- AG5: 5 cm autograft
- AG7: 7 cm autograft
- BMSCs: Bone-marrow-derived mesenchymal stem cells
- BST: Barcelona Tissue Bank
- CMAP: compound muscle action potential
- CNS: central nervous system
- CSPG: chondroitin sulfate proteoglycans
- DC: 7 cm decellularized nerve allograft
- DC-RA: decellularized rat allograft
- DC-HX: decellularized human xenograft
- DCA: decellularized allograft
- DRA: decellularized rat allograft
- DRG: dorsal root ganglia
- DPI: days post injury
- ECM: extracellular matrix
- EMG: electromyography
- FDA: Food Drug Administration
- FT: functional tests
- GM: gastrocnemius
- IHC: immunohistochemistry
- iPSCs: induced pluripotent stem cells
- JNK: c-jun N-terminal kinase
- MPO: months post operation
- MPS: months post surgery
- MSC: mesenchymal stem cell
- NAD⁺: nicotinamide adenine dinucleotide
- NMNAT2: nicotinamide nucleotide adenylyltransferase 2
- PB: phosphate buffered
- PBS: phosphate buffered solution
- PDL: poly-D-lysine
- PL: plantar interosseus
- PN: peripheral nerve
- PNI: peripheral nerve injuries
- PNS: peripheral nervous system
- RT: room temperature
- SC: Schwann cell
- SD: Sprague Dawley
- SFI: sciatic functional index
- SGCiE: Servei de Granges i Camps Experimentals
- TA: tibialis anterior
- VERI: Verigraft AB

IV. INTRODUCTION

1. Peripheral Nervous System

The main function of the peripheral nervous system (PNS) is to connect the central nervous system (CNS) with the organs, muscles, and skin to enable sensations, perform movements and control the visceral organs. The PNS can be divided into two functional categories: the somatic nervous system and the autonomic nervous system. The somatic nervous system control actions under conscious control, body movements and receives information from external stimuli, while the autonomic nervous system controls the functions and receives information of the internal organs.

The human PNS consists of 12 pairs of cranial nerves, 31 pairs of spinal roots and their associated nerves, and the peripheral nerves (PN). The cranial nerves make the connections between the head and the upper body while the spinal nerves make the connections between the head and the rest of the body.

PN are composed by motor axons that extend from motor neurons located in the ventral horn of the grey matter of the spinal cord, sensory neurons located in the dorsal root ganglia (DRG) and autonomic neurons; their axons innervate their target organs: skeletal muscles, sensory receptors and visceral muscles and glands respectively.

Peripheral nerve fibers were classified by Erlanger and Gasser (1937) according to their myelination, diameter, and velocity of impulse conduction. Motor neurons can be divided into α motor neurons, that innervate the skeletal muscle fibers, and γ motoneurons, that innervate the intrafusal fibers of the muscle spindle, and play an important role in adjusting the sensitivity of the spindle receptors. Sensory axons transduce specific stimuli into electrical signals that will be transported from the periphery to the CNS.

INTRODUCTION

Depending on the stimuli and their function, sensory neurons can be classified as:

- Proprioceptors: are located in the muscles, joints, and other deep structures. The main function is to provide information about the tension and length of the muscles, and the position of different body parts.
- Fine touch receptors: mechanoreceptors with specialized end organs that transmit fine information about pressure or touch.
- Gross touch receptors: mechanoreceptors with free nerve endings that transmit information about gross touch.
- Thermoceptors: either cold or warm receptors, provide information about temperature of the skin.
- Nociceptors: process damaging stimuli, and can be high threshold mechanoreceptors, thermal receptors, or chemical receptors, but a majority are polymodal.
- Itch receptors: convey irritation and tingling sensations (Usoskin et al., 2015).

Neurons that innervate cutaneous receptors project to the skin mainly via cutaneous nerves, while neurons that carry sensory information from muscles, such as proprioceptive neurons, project to the muscles or tendons via muscular nerves. Sensory fibers are usually classified by roman numbers (in parenthesis in Table 1), in contrast to the broad classification used to classify any type of nerve fiber by using combined Latin and Greek letters (Table 1).

Table 1. Classification of peripheral nerve fibers. Adapted from Erlanger & Gasser (1937).

	Fiber	Diameter (μm)	Conduction velocity (m/s)	Myelin	Function
Motor fibers	A α	12-22	60-120	Yes	Skeletal muscle control
	A γ	3-5	30-45	Yes	Muscle spindle control
Sensory fibers	A α (Ia)	12-22	60-120	Yes	Muscle spindle proprioception
	A α (Ib)	12-22	45-80	Yes	Golgi tendon organs proprioception
	A β (II)	6-12	5-30	Yes	Proprioception and fine touch
	A δ (III)	1-5	5-30	Yes	Temperature, fast pain and gross touch
	C (IV)	0.3-1.5	0.5-2	Yes	Temperature and slow pain
Autonomic fibers	B	6-12	45-80	Yes	Preganglionic
	C	0.3-1.5	0.5-2	No	Postganglionic

PN are made up of fascicles of axons, each surrounded by a layer of connective tissue, the endoneurium, which contains the endoneurial space. The endoneurium consists of collagen fibrils that run longitudinally along the nerve fibers between the Schwann cell (SC) basal lamina and the perineurium. The endoneurial tubules contain the axons and their associated glial cells. SC myelinate the thick axons, insulating them with high resistance and low capacitance myelin sheaths, allowing ion flow to create a saltatory conduction between the nodes of Ranvier, which increases the speed of nerve impulses.

Non myelinating SC, called Remak cells, surround a group of unmyelinated axons, that due to the lack of myelin, conduce nerve impulses slowly in a continuous manner.

INTRODUCTION

The perineurium is the connective tissue assembled around each fascicle. It is the nerve layer that offers more tensile resistance, since it is composed of several layers of flattened fibroblasts, compacted, and surrounded by basal lamina.

Finally, the epineurium is the outermost covering connective tissue which connects the nerve fascicles in a single trunk. It is composed by longitudinal collagen fibers, fibroblasts, mast cells, and fat. Collagen fibers prevent nerve stretching and, therefore, injuries during limb motion. It also contains the blood vessels that supply the PN, that branch out and penetrate the perineurium. However, the endoneurium is poorly vascularized and axonal nutrition relies primarily on diffusive mass transfer from perineural capillaries (Figure 1).

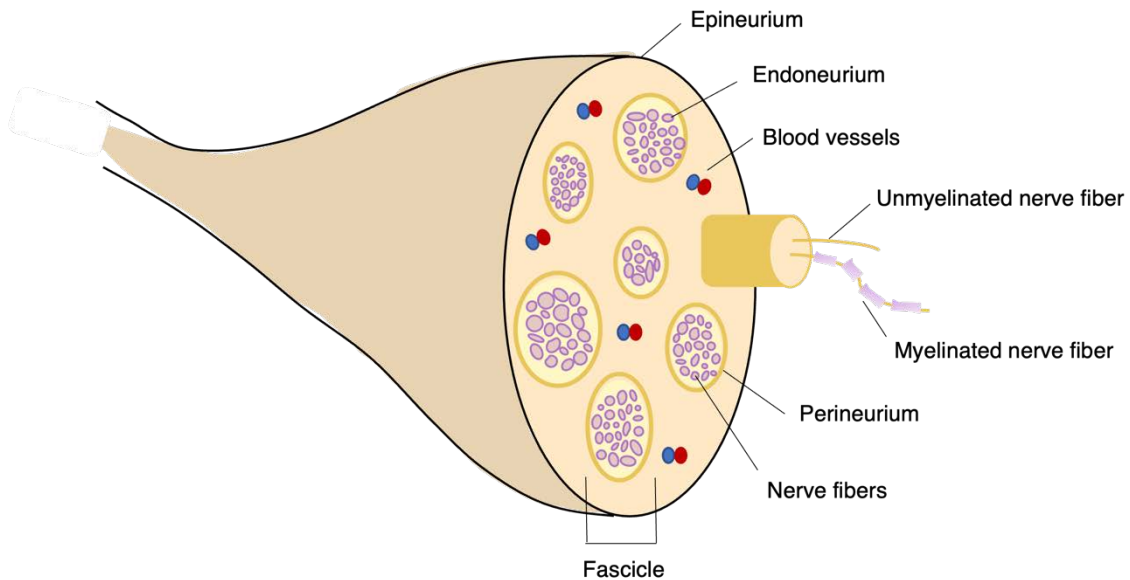


Figure 1. Structure of the peripheral nerve. Transverse view of a peripheral nerve composed by different layers of connective tissue, endoneurium, perineurium and epineurium. Nerve fibers can be myelinated or unmyelinated and are packed in fascicles.

1.1. Extracellular matrix in the PNS

The extracellular matrix (ECM) is a three-dimensional network matrix of a complex molecular nature in which axons and supporting cells are immersed. It

is located in the interstitial space of all tissues and contains proteins and carbohydrates synthesized and secreted by cells. The ECM plays an important role in the migration, proliferation, and differentiation of cells, provides structural support, and regulates cell-to-cell communication, contributes to the mechanical properties of tissues, enables cells to form tissues, facilitates cell communication, and forms pathways through which cells can migrate. In the PNS, the ECM is found in the basal lamina of SC and endoneurium (Gonzalez-Perez et al., 2013).

The components of the ECM can be divided into two main categories: proteoglycans and glycoproteins. Three of the glycoproteins have an important role in axonal regeneration and their effects have been proved both *in vitro* and *in vivo*: collagen (Babington et al., 2005), laminin (Werner et al., 2000) and fibronectin (Gardiner et al., 2007).

- Collagen is a trimeric molecule consisting of three α -chains. It can be divided into several subfamilies depending on the type of structure they form: fibrillar (types I, II, III, V, XI), facet-fibril-associated collagens with broken triple helices (types IX, XII, XIV), short chains (types VIII, X), basement membranes (type IV) and other types with different structural types (types VI, VII, XIII). Also, is associated with fibril formation (type I collagen) and basement membrane (type IV collagen) in the establishment of axonal pathfinding during neurodevelopment, as well as in the maintenance of synaptic connections and maintenance (Fox, 2008).

- Laminin is the major ECM protein involved in cell differentiation, adhesion, and migration activities. It is mainly found in the basal lamina and different isoforms, such as laminin-2 ($\alpha 2, \beta 1, \gamma 1$) and laminin-8 ($\alpha 4, \beta 1, \gamma 1$) are secreted by SC and are found in PN (Wallquist et al., 2002), whereas laminin-10 ($\alpha 5, \beta 1, \gamma 1$) is located in sensory end organs (Caissie et al., 2006). Laminin provides the adhesion component that confers pro-regenerative capabilities to the basal lamina scaffolds after nerve injury (Wang et al., 1992) and has been shown to promote neuritogenesis *in vitro* (Agius and Cochard, 1998).

- Fibronectin is a glycoprotein found in the ECM. It forms a fibrous network and maintains the interactions with laminin and collagen IV, promoting cell

INTRODUCTION

proliferation and differentiation. Furthermore, fibronectin mainly binds to integrins, but also has binding sites for collagen, heparin, fibrin, and syndecan (Mao and Schwarzbauer, 2005). In the nervous system, fibronectin is shortly up-regulated after peripheral nerve injuries (PNI) (Lefcort et al., 1992) and is secreted by fibroblasts and SC (Baron-Van Evercooren et al., 1986; Chernousov and Carey, 2000).

2. Peripheral Nerve Injuries

PNI result in partial or complete loss of motor, sensory and autonomic functions mediated by the involved nerves. The injury of the axons leads to degeneration of distal nerve fibers and consequent denervation of the territories and organs innervated by the injured nerves. Eventually, axotomized neurons can die. These deficits can be recovered by reinnervation of denervated targets following two compensatory mechanisms: regeneration of damaged axons and sprouting of nearby undamaged axons. However, clinical, and experimental evidence generally indicates that these mechanisms are insufficient to ensure effective functional recovery, especially after severe injuries (Kline, 2000; Lundborg, 2000).

PNI have a variety of etiologies, including trauma, laceration, compression, ischemia, or stress-related injuries (Campbell, 2008). Besides, PNI are a major clinical and public health problem because severe injuries have a devastating impact on patients' quality of life. Worldwide, more than a million people suffer from peripheral nerve damage per year. In Europe, more than 300,000 PNI are reported each year, while severe injuries affect 14 cases per 100,000 inhabitants per year (Asplund et al., 2009). In the United States, 20 million cases by trauma and medical disorders (Lundborg, 2003) result in approximately \$150 billions spent in annual healthcare (Taylor et al., 2008).

2.1. Classification of PNI

The severity of the injury determines the need for surgical repair and the appropriate technique. There are two classifications to evaluate PNI severity,

made by Seddon (1943) and Sunderland (1990). The most detailed classification was made by Sunderland and is more useful from a surgical point of view. It differentiates five degrees of injury.

The first degree (named also as neurapraxia in Seddon's classification) corresponds to the interruption of conduction, usually due to compression. It affects the myelin sheaths but do not disturb axonal continuity, preventing degeneration of distal fibers. This injury recovers within a short time once the cause is removed. In the second degree (Seddon's axonotmesis) the axons are disrupted, but the connective sheaths remain intact, often due to crush injuries. Axons distal to the lesion degenerate and severed axons have to regenerate. Recovery is good as the regenerating axons grow within the original endoneurial tubules and can reconnect to their original targets. The third degree implies the rupture of axons and endoneurial tubules without affecting the perineurium, leading to a distal degeneration and internal disorganization of the nerve fascicles. In the fourth degree the perineurium is also damaged (in which the epineurium remains intact), leading to disrupt and disorganize the fascicular architecture, intraneural scar formation, and loss of directional guidance for regenerating axons. In addition, neuroma formation is common. In the last degree of injury, the fifth degree (Seddon's neurotmesis) there is a complete transection of the nerve.

After transection of a nerve, the elastic forces generate a separation between the two nerve stumps. The length of the resulting gap depends on the size of the nerve and the adherences to surrounding tissue. When a segment of the PN is damaged, such as in severe trauma or in transection lesion, the gap between the proximal and the distal stumps is correspondingly longer. In these situations, the prognosis for spontaneous recovery is low, and therefore, surgical repair is required. The purpose of the repair is to re-establish the continuity of the nerve trunk, prevent the formation of scar tissue at the lesion site, and providing the injured axons growing from the proximal stump with an appropriate substrate which supports nerve regeneration, such as the distal degenerating nerve.

regeneration after axotomy mainly depends on the ability of injured neurons to survive and to switch from a transmission state to a pro-regenerative state, which implies changes in the expression genes that encodes for transcription factors (Herdegen et al., 1991; Leah et al., 1991; Schwaiger et al., 2000), that regulate other genes involved in cell survival and neurite growth (Navarro et al., 2007).

After axotomy, the arrival of injury-induced signals is followed by the induction of transcription factors, adhesion molecules, growth-related proteins, and structural components in the soma, all of which are required for axonal regeneration (Rishal and Fainzilber, 2014). A back-propagating calcium wave generated at the site of damage (Cho et al., 2013) when the axoplasm is exposed to the extracellular environment. Also, a high frequency burst of action potentials quickly inform the cell body of the damage caused due to axonal injury and activating several protein kinase pathways (Ghosh and Greenberg, 1995). Another set of signals includes the early absence of target-derived trophic factors (Lee et al., 1998; Raivich et al., 1991) and the arrival of activation signals not only from the injured axons themselves but also from other non-neuronal cells. Finally, the axoplasm is sealed, and expresses various receptors for neurotrophic factors or cytokines that can be activated, internalized, and delivered to the neuron body by retrograde transport when SCs and infiltrating macrophages release these molecules in the degenerative environment, contributing to the preservation of the regenerative function of neurons (Curtis et al., 1993, 1994, 1998).

These neuronal activation signals also trigger multiple signaling pathway genes in neuronal cells that can lead to two opposite outcomes: cell death or regenerative response. Among them are some kinases, such as MAPKs Erk1 and Erk2, c-jun N-terminal kinase (JNK) and p38 kinase. Changes in gene expression affect the encoding of cell adhesion and guidance molecules, transcription factors, cytoskeletal proteins, trophic factors, cytokines, neuropeptides, and neurotransmitter synthesizing enzymes, ion channels and membrane transporters. Finally, one of the most important changes after peripheral axotomy is the increase of regeneration-related proteins such as growth-related proteins GAP-43 (Skene, 1989), ion channels (Goldberg, 2003), tubulins and neurofilaments (Hoffman et al., 1987) and neuropeptides (Hökfelt et

INTRODUCTION

al., 2000). GAP-43 is upregulated from the first day after axonal injury and is usually used as a label to identify growing axonal profiles. Besides, GAP-43 is rapidly transported along the axon to growth cones, where the protein accumulates to regulate neurite formation and synaptic plasticity (Li et al., 1997).

Tubulins are significantly increased in axotomized motor and sensory neurons, while the neurofilament proteins NF-L, NF-M and NF-H are decreased, probably reflecting an increase in axoplasmic fluidity to facilitate axonal transport (Hoffman et al., 1987; Tetzlaff et al., 1996; Wong and Oblinger, 1990).

3.2 Wallerian degeneration

After PNI that implies the rupture of PN fibers, axons, and myelin sheaths distal to the lesion are degraded by a process known as Wallerian degeneration. It is a well-characterized molecular and cellular event for clearing distal segment debris (Zochodne, 2012), creating a permissive environment that will allow axons to re-grow to their original targets. This degeneration is important in the process, since an intact nerve does not support axonal regeneration due to the presence of inhibitory factors (Mueller, 1999; Tang, 2003), such as chondroitin sulfate proteoglycans (CSPGs) of the ECM and myelin-associated inhibitors of nerve regeneration (Mukhopadhyay et al., 1994).

The process requires guidance signals different from those produced during developing stages (Dudanova & Klein, 2013). When the distal nerve stump undergoes Wallerian degeneration, the activation of SCs and the infiltration of hematogenous macrophages (Stoll and Müller, 1999) eliminate distal axons and myelin debris to clear all the inhibitory factors. On the contrary, the proximal axon segment and cell soma remain intact. Nerve injury results in impaired supply of nicotinamide nucleotide adenylyltransferase 2 (NMNAT2) synthesized in the soma to the axon, resulting in diminished levels of this protein as well as nicotinamide adenine dinucleotide (NAD⁺). Axonal injury also leads to SARM1 activation, that promotes NAD⁺ depletion. Lack of NAD⁺ leads to increase of Ca²⁺ in the axoplasm, thus activating Ca²⁺-dependent proteases that initiate degradation of axonal cytoskeletal components (Gerdtts et al., 2016). The

degenerative end-products are eliminated by the cooperative action of SCs and infiltrating macrophages (Stoll and Müller, 1999). The first signs of Wallerian degeneration are observed within 24 hours after nerve injury, and they continue distally for approximately two weeks, following a proximo-distal progression. Denervated SCs can engulf their myelin sheath to some extent, but recruitment of hematogenous macrophages is the main pathway for phagocytosing myelin and axonal debris (Tanaka et al., 1992). From 2-3 days after injury there is an important infiltration of macrophages into the degenerating nerve, attracted by chemotactic and inflammatory cytokines secreted by reactive SCs.

At the distal nerve segment, SCs are stimulated by the loss of axonal contact and by cytokines secreted by macrophages, and they shift from a quiescent phenotype to a pro-regenerative state (Jessen and Mirsky, 2016). The de-differentiated cells proliferate and line up within the endoneurial tubules forming the bands of Büngner. The rate of SC proliferation increases fast after lesion until a three-fold increase in number. There is also an increase in the ECM and collagen fibrils of the distal nerve segment resulting in reduction of the lumen size of denervated endoneurial tubules.

3.3 Axonal regeneration

The regenerative response at the neuronal body promotes the protrusion of growth cones from the proximal stump of the cut axons, that sense the surrounding environment and elongate if they found a favorable substrate. If the growth cones cannot reach the distal stump, they twist and sprout within the proximal stump forming a neuroma. If the regenerating axons gain the distal nerve, then elongate within the endoneurial tubules in association with the SCs and the basal lamina.

The orientation of the advancing growth cones is guided by gradients of neurotrophic and neurotropic factors mainly produced by reactive SCs and the ECM within the degenerated nerve (Fu and Gordon, 1997; Allodi et al., 2012). In this scenario, SCs play a key role in nerve regeneration because they constitute

INTRODUCTION

the most favourable substrate for axonal growth and synthesize several trophic factors that stimulate neuronal survival and regeneration.

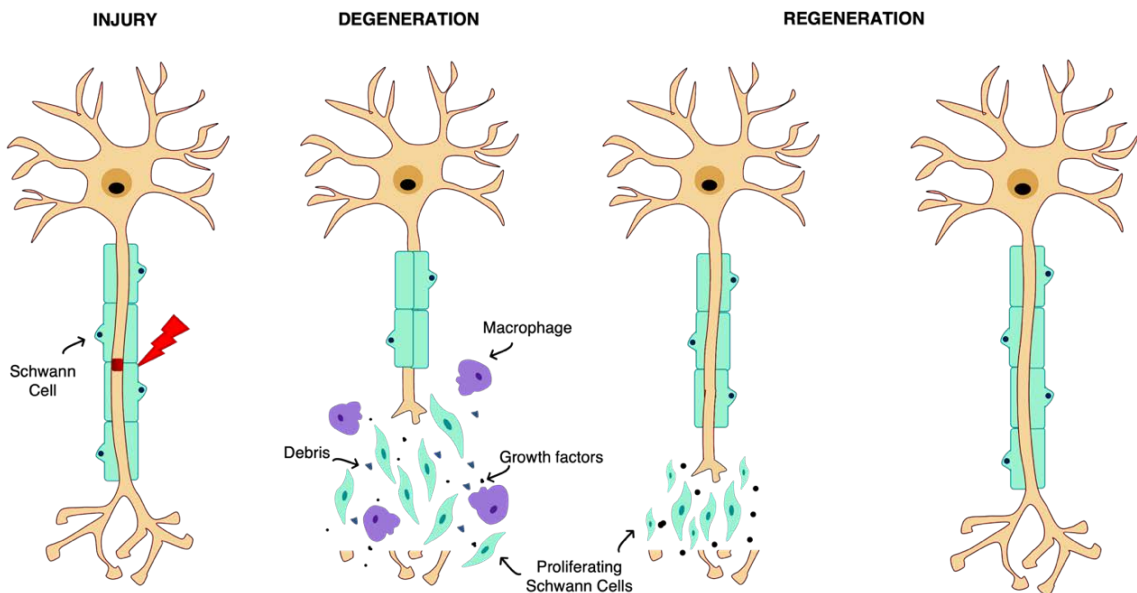


Figure 3. Degeneration and regeneration after axotomy. After nerve injury, SCs detach from the axons and start proliferating helping the recruited macrophages to clear the cellular and myelin debris. At the same time, the expression of stimulating factors by SCs creates a favorable environment for nerve regeneration towards the target organs.

The rate of axonal regeneration is initially very slow but after some days reaches a constant value of about 1-3 mm/day. The regenerating axons follow the distal nerve to eventually reach target tissues in the periphery, that can be reinnervated. Axons that regenerate through incorrect distal pathways to targets that cannot reinnervate, such as motor axons to the skin or cutaneous axons to muscle, tend to withdraw and may be eliminated. Despite regeneration may be successful, the normal nerve structure and function are not restituted. After nerve injury and repair, the diameter and conduction velocity of regenerated axons remain below normal.

3.4. Functional recovery

Peripheral axons are capable to regenerate after nerve injury, but functional recovery does not always occur in lesions from Sunderland's grade III. The reason of poor functional recovery in neurotmesis lesions is in good part the misdirection of the axons since endoneurial tubules loss their continuity (Lundborg and Rosén, 2001; Valero-Cabré and Navarro, 2002) leading axons to reinnervate incorrect target organs.

Factors contributing to poor functional recovery after nerve injuries includes: 1) death of neurons due to axotomy and retrograde degeneration; 2) inability for axons to regenerate through the injury, leading to atrophy of denervated targets; 3) poor specificity of reinnervation by regenerating axons, that after a complete nerve section grow randomly along the distal endoneurial tubules. All these limitations are more marked when the lesion creates loss of continuity in the nerve and the outcome is dependent upon the interstump gap length.

4. Surgical repair strategies

After neurotmesis or complete transection, both nerve stumps have to be reapposed by surgical repair to facilitate that proximal axons invade the distal stump and reinnervate the target organs. However, matching of proximal and distal endoneurial tubules is impossible, and thus, misdirection of axons to a wrong distal pathway is common after this type of lesion (Gonzalez-Perez et al., 2013). Repair techniques are described below (Navarro and Verdú, 2004) and will vary depending on the distance between proximal and distal stumps.

- Direct suture: The ideal method is to reappose both nerve stumps by epineural sutures, however this is only possible if the lesion is a clean cut, the distance between both nerve stumps is short (0.5 to 2 cm in humans), and the repair takes place soon after the injury to avoid an excessive retraction of nerve stumps (Papalia et al., 2007; Bell and Haycock, 2012). This technique causes a minimal trauma associated to the surgical intervention. After removing the scarred part of the injured tissue, fascicular patterns and longitudinal surface vessels will help to

INTRODUCTION

guarantee accurate re-organization by suturing individual fascicles (Brushart et al., 1983). Nevertheless, although microsurgical identification and coaptation of individual fascicles is possible by means of perineurial sutures, direct suture does not ensure correct matching of the fascicular organization of the nerve trunk.

- Fibrin Glue: Fibrin glue is a blood-derived adhesive that can be used to directly attach both nerve endings without sutures. The main advantages of fibrin glue are the shortening of surgical time, reduced fibrosis, and inflammation, and coaptation of severed nerve fascicles with minimal induced trauma. In addition, general axonal regeneration, fiber alignment and recovery of nerve conduction velocity were found to be similar in fibrin glue as in direct suture repairs (Sameem et al., 2011).

- Autograft: when the length of the gap created by tissue destruction and nerve retraction is too long to allow the apposition of the nerve stumps with direct suture without applying tension, a nerve graft is necessary to bridge the nerve stumps (Lundborg, 1988). Autografts provide an aligned microstructure with endoneurial tubules for mechanical guidance, and essential pro-regenerative elements, such as SCs and their basal lamina with neurotropic and neurotrophic molecules (Hall, 1986). The autologous nerve graft is the closest structure to the distal segment of the severed nerve, preserving the internal structure and the physicochemical properties without causing an immune response. This nerve graft undergoes Wallerian degeneration providing a mechanical guidance for re-growing axons. Donor nerves are limited to cutaneous sensory nerves of lower functional hierarchy, such as the sural or the medial antebrachial nerve (Isaacs, 2010), that may be divided in several segments for a fascicular grafting in larger injured nerves. Experimental studies have shown that autograft repair sustain similar degree of axonal regeneration and thus, allow close functional recovery to the direct suture repair. Thus, repair of a nerve section with an autograft requires two surgical interventions and involves sacrificing a healthy donor nerve (Kornfeld et al., 2019). Autograft repair has some drawbacks, such as morbidity in the donor area, causing paresthesia or neuroma formation, and transferring the problem from one area of the body to another (Ducic et al., 2012) and longer postoperative recovery. Moreover, motor nerve repair typically involves donor sensory nerves,

compromising the risk-benefit ratio of autotransplantation (Moradzadeh et al., 2008) and nerve used are limited in length and caliber, resulting in a lack of donor tissue (Whitlock et al., 2009).

Alternatives to the use of autografts are:

- Tube repair: Artificial nerve conduits should mimic the natural environment found in a degenerating distal stump or and autograft (Doolabh et al., 1996; Deumens et al., 2010). Both proximal and distal nerve stumps can be introduced within the ends of a tube and hold in place by means of epineural sutures, leaving a gap between nerve stumps. The regenerative process starts with the formation of a fibrin cable (Lundborg et al., 1982) that will be replaced by collagen and laminin secreted by fibroblasts and SCs, respectively (Deumens et al., 2010; Gonzalez-Perez et al., 2013). Success of regeneration differs with the material properties, the physical characteristics of the conduit, and the length of the nerve gap. There is a limitation depending upon the length of the gap (Navarro and Verdú, 2004). For nerve gaps longer than 40 mm recovery is minimal to non-existent (Reyes et al., 2005), as well as in the rat, tubes do not ensure repair of gaps longer than 10 mm (Butí et al., 1996).

- Allograft: Biological materials, such as donor nerves from cadaveric donors may be available, with relative abundance, offering different length, caliber, and specificity (sensory or motor) suitable for the type of the nerve to repair (Squintani et al., 2013). Nevertheless, the alternative use of allografts or xenografts has been discouraging, since the immune rejection, mainly directed against SCs and myelin sheaths of the graft, impedes axonal regeneration (Evans et al., 1994). Rejection can be prevented by administration of systemic immunosuppressants, such as cyclosporine or tacrolimus, that effectively allow for host tolerance to foreign tissue, and even in the case of tacrolimus, accelerates the rate of axonal regeneration (Udina et al., 2003a, b). However, the risks associated to systemic immunosuppression, even if it is temporary, limit the widespread translation of allograft repair in the clinic (Matsuyama et al., 2000; Fox and Mackinnon, 2007). The removal of the immunogenic components of the nerves can be a good strategy to overcome this limitation. Acellular nerve allografts appear as a good

INTRODUCTION

alternative for autografts, considering that they come from a natural and abundant source, are not immunogenic given that the cellular components are effectively eliminated, and may keep a normal-like ECM structure which helps guiding regenerating axons (Hall, 1986; Moore et al., 2011). Nerve decellularization involves several processes and strategies to obtain an immunogenic free scaffold while preserving the composition and biomechanical properties of the ECM (Szynkaruk et al., 2013; Nieto-Nicolau et al., 2021). The decellularized graft can provide adequate support for the migration of fibroblasts, endothelial cells, and SCs, from the host nerve stumps into the grafted segment, and still contains neurotropic cues, such as laminin, fibronectin, and collagen, that are essential for guiding the regenerative growth cones (Wang et al., 1992). Nevertheless, decellularized allografts also have some limitations, mainly related to the lack of cell support for axonal regeneration. Indeed, the lack of cellular component causes a slower regeneration into decellularized grafts compared to the cellular autografts. However, this slower regeneration does not necessarily imply poorer functional recovery if long time is allowed (Moore et al., 2011).

Any other tissue containing basal lamina can be used as a bridge for nerve repair, in a similar fashion to that of acellular nerve grafts. This option has been used primarily with segments of skeletal muscle, once made acellular by freezing-thawing or chemical extraction. Regenerative axons grow into the empty cylinders of muscle basal lamina that contain neurotropic molecules, such as laminin and fibronectin, following the migration of SCs. It appears to exist a limiting length for muscle grafts, due to the limited migration of SCs. Myelination and maturation of regenerated axons have been found to take place more slowly in the muscle graft than in the distal nerve segment.

The use of blood vessels as a conduit to close a gap in PN has also received attention. Vein grafts are easily available from autologous origin and have been used for bridging nerve gaps in animal studies and in human patients. Vascular grafts act as a conduit, but also provide molecular and cellular elements from their own wall. Invaginated vein grafts that expose regenerating axons directly to the collagen-rich adventitia resulted in increased vascularity and earlier regeneration in comparison to standard vein conduits. However, veins tend to

collapse, hampering the regenerating nerve fibers, and they are only considered for repairing short nerve gaps. The “muscle-in-vein” construct has been also assayed by placing a cylinder of acellular muscle within a vein, so that the vein prevents muscle fiber dispersion, while the muscle prevents vein collapse and provides neurotropic support, however the reported results are controversial (Heinzel et al., 2021).

5. Nerve decellularization strategies

Removal of the antigens responsible for immunological rejection is possible through a controlled decellularization process that preserves the regenerative components of the ECM (Whitlock et al., 2009). After freezing and freeze-thawing, usually three to five times, nerve segments were first introduced for assaying axonal regeneration along acellular peripheral nerve allografts and for investigating the regenerative capabilities of the connective layers and ECM of a decellularized nerve (Zalewski and Gulati, 1982; Hall 1986; Gulati and Cole 1994). Despite being a rapid method, it produces tissue expansion and contraction and, it can damage the basal lamina tubules. Moreover, cell debris can remain in the nerve tissue, difficulting axonal regeneration (Lovati et al., 2018). In addition, it has been considered that there is a limit for an effective decellularization related with the length of such acellular nerve grafts, that should be no more than 20-mm in the rat (Gulati, 1988). More recently, modification to the freeze-drying process by unidirectional freezing has been shown to produce axially aligned channels in the acellular nerve, resulting in enhanced cellular penetration into the graft when compared to non-freeze dried and standard freeze-dried scaffolds (Sridharan et al., 2015).

Cold preservation has been also extensively used. Harvested nerve segments can be stored in tissue preservation solutions, such as the University of Wisconsin Cold Storage Solution, and stored at 5°C. Resident cells and myelin are not completely eliminated by this procedure, although increasing storage time led to decreasing immune response and improved axonal regeneration (Evans et al., 1998). After 5-7 weeks prolonged cold storage nerve allografts allowed good

INTRODUCTION

axonal regeneration, that was better than with fresh allografts, but clearly lower than autografts (Evans et al., 1999; Fox et al., 2005).

Later developments introduced detergent based decellularization procedures, mostly using Triton X-100 to permeate the cell membranes. The protocol developed by Sondell and co-workers (1998) was based on two sequential baths with 3% Triton X-100 solution followed by 4% sodium deoxycholate solution, thus combining a non-ionic surfactant with an anionic detergent to chemically lyse the cells. They demonstrated complete removal of SCs and myelin sheaths with preserved basal lamina tubule, and good nerve regeneration when assessed *in vivo*. Hudson et al. (2004) proposed a milder and less toxic chemical treatment to better preserve the structure of the ECM, with combination of an amphoteric detergent consisting of 125 mM sulfobetaine-10 solution followed by an anionic detergent solution of 0.14% Triton X-200 and 0.6 mM sulfobetaine-16. They compared *in vivo* their optimized acellular allograft with an isograft and reported that the axonal density at the midgraft was similar, whereas it was considerably higher than in grafts decellularized by freeze-thawing and by Sondell's method. More recently, Nagao et al. (2011) made another comparative study of Hudson's, Sondell's, and freeze-thawing protocols for decellularizing allografts in rats. They found that the animals reached a plateau in the recovery of the sciatic functional index (SFI), and that until 52 weeks of follow-up the Hudson's grafts allowed better recovery than the Sondell's and the freeze-thawing grafts. However, the walking track method and the derived SFI index has a low discrimination after complete section or resection of the sciatic nerve in rodents and therefore, limits the ability to compare therapeutical strategies (Shenaq et al., 1989; Navarro, 2016).

Further refinements to allograft preparation can be implemented to improve regenerative capability of these grafts. Elimination of CSPG, a component that inhibits axonal growth, can be achieved by incubating frozen-thawed acellular grafts in 2 U/ml chondroitinase ABC solution. This additional degradation step significantly increased the length that axons regenerated along the acellular graft, over 40-mm in the rat sciatic nerve and improved the preservation of the distal graft structure (Neubauer et al., 2010). This incubation with chondroitinase ABC

enzyme was adopted by more authors to optimize protocols by adding this degradation step at the end of the decellularization process, either detergent-based or thermal. Indeed, the Avance® nerve graft (Axogen Inc., Alachua, FL, USA), undergoes detergent based decellularization by Triton X and sulfobetaine-16 and sulfobetaine-10 following the Hudson protocol, followed by CSPG degradation according to the protocol of Neubauer et al. (Lovati et al., 2018). This graft is the first processed nerve allograft approved by the Food and Drug Administration (FDA) to be used in humans, although limited to the American market. Among the well-established decellularization protocols, the one used for Axogen is considered as one of the most effective and good results have been obtained for repairing long gaps up to 20 mm. When tested in such long gaps in rats, the processed acellular graft was inferior to an autograft but superior to a collagen conduit (Whitlock et al., 2009).

The Michigan group adopted a modified detergent-based protocol, using five steps including ethylenediaminetetraacetic acid, sodium deoxycholate, azide and Triton X-100 detergent, and showed that the produced allografts were immunologically inactive, and were not populated by macrophages as seen Wallerian degeneration, unlike protocols that do not remove cellular content such as freeze-thawing cell destruction (Rovak et al., 2005). These chemically acellularized grafts supported axonal regeneration and functional reinnervation across 20-mm but not 40-mm nerve gaps in the rat (Haase et al., 2003).

Other authors have reported variations in the detergent components used for chemical decellularization of PN, with combination of Triton-X100 or 200, and SDS, an anionic surfactant with amphiphilic properties or peracetic acid, an oxidizing agent that permeabilizes the tissue (for review see Lovati et al., 2018; Phillips et al., 2018a). Phillips and coworkers (2018b) used a novel method consisting of subsequent incubations with Triton X-100, DNase, RNase, and trypsin. They thoroughly compared the resulting decellularized nerve segments with those following Sondell's and Hudson's methods. Decellularization by the method described by Sondell et al. resulted in reduction of the cell content, but disruption of the endoneurial tubules with loss of ECM molecules such as laminin and glycosaminoglycans. Decellularization by a modified Hudson's method did

INTRODUCTION

not alter the ECM composition of the nerves, but cell removal was incomplete. In contrast, decellularization by their new method led to successful removal of cell and nuclear material, while maintaining the structure and composition of the ECM, thus offering a promising scaffold for peripheral nerve regeneration.

Similarly, addition of elastase to previous protocols of detergent decellularization significantly reduced the immunogenicity and amount of SCs, while maintaining good structural properties of the processed grafts (Hundepool et al., 2017). Interestingly, in the same study the authors found that storage at -80°C after the decellularization process deteriorated the ultrastructure of the nerve compared with cold storage at 4°C . Among six possible combinations of detergent- and nuclease-based decellularization protocols, the combination of amphoteric detergent and nuclease was found as the most suitable for nerve decellularization in terms of cell removal and preservation of the ECM (Shin et al., 2019). Following the advances during the last decades, there are several protocols that may yield decellularized PN that are devoid of cells, maintain the ECM architecture without affecting its composition and preserves biomechanical properties similar to the native nerve. Nevertheless, these and future acellular allografts should be quantitatively evaluated, by means of accurate histological, ultrastructural, biochemical, and biomechanical analyses, and compared to previous protocols. To this end, general guidelines have been proposed (Phillips et al., 2018a) to establish standardized criteria and testing methods, enabling reliable comparison of decellularization protocols, and increasing the quality of further *in vivo* experiments.

Regarding the application to human nerves, Bae et al (2021) decellularized median and sural nerves from human cadavers with two different methods: nonionic and anionic detergents (Triton X-100 and sodium deoxycholate), similar to Sondell's protocol, and amphoteric detergent and nucleases (CHAPS, DNase, RNase), derived from a protocol assayed in rat nerves (Shin et al., 2019). Decellularization with amphoteric detergent and nucleases removed cellular components and preserved the ECM structure better than decellularization with classical detergents and had biomechanical properties comparable to those of fresh nerves, indicating that the method may be effectively used in large human

PN. A combination of cell lysing methods was used by Suss et al (2021) to decellularize human median and ulnar nerve segments. They used first a hypotonic shock, followed by incubations with Triton X-100, sodium dodecyl sulfate and peracetic acid, and in a modified protocol added sonication at 40 KHz. They reported that sonication increased the effectiveness of the detergent-based protocols for removal of cell components from PN allografts. In another study fulfilling the guidelines for decellularization (Phillips et al., 2018b), Nieto-Nicolau and co-workers (2021) proved a combination of zwitterionic, non-ionic detergents, hyperosmotic solution and nuclease enzyme treatment removed cell remnants, maintained collagen and laminin tubules, and preserved the biomechanical properties of long human nerve segments without generating cytotoxic products. Although further optimization of the decellularization protocols can be performed, there is a delicate equilibrium between preserving nerve architecture and completely decellularizing the graft to avoid immune rejection. In general, the detergent-based methods optimized during the last decade have efficiently achieved these goals.

6. Recellularization of decellularized nerve grafts

The use of a decellularized allografts, mainly of those processed by detergent-based methods, allows for significant nerve regeneration in preclinical and clinical settings but still inferior to the autologous nerve graft (Kornfeld et al., 2021).

Further experimental improvements may be addressed to add mild and preferably local immunosuppression to avoid immune reaction against antigenic components remaining in the ECM. On the other hand, improvement of the regenerative potential of these grafts can be achieved by enriching them with either neurotrophic factors or pro-regenerative autologous cells, such as SCs or mesenchymal stem cells (MSCs), to overcome the current limitation in length and diameter of the acellular allografts (Peters et al., 2021). Promising results in rodent models underline that the combination of autologous or immune-compatible cells and acellular nerve allografts may be beneficial for nerve

INTRODUCTION

regeneration in critical nerve defects and represent the most likely early future alternative to autografts in the clinic.

One of the initial experimental strategies employed to enhance the regenerative efficacy of nerve allografts was supplementation with SCs previously isolated in culture, demonstrating positive effects on nerve regeneration by adding autogenic or isogenic SCs to previously decellularized nerve allografts (Gulati et al., 1995; Fansa et al., 1999; Frerichs et al., 2002; Brenner et al., 2005). It must be pointed out that acellular allografts repopulated with isogenic SCs supported axonal regeneration through them, whereas allogenic SCs underwent rejection and impaired regeneration (Gulati, 1995; Rodríguez et al., 1999), or did not produce any enhancement (Dumont and Hentz, 1997). These observations indicate that SCs continue to exhibit immunogenicity even after being isolated and cultured *in vitro*.

In general, studies that have applied a non-limiting nerve gap of 10–12 mm found little to no enhanced effect of adding SCs to acellular grafts, due primarily to the fact that endogenous host cells are able to infiltrate short grafts within short time (Szynkaruk et al., 2013). Therefore, supplementation of acellular grafts with SCs may be of actual benefit in the case of long gap nerve injuries, in which host SC migration and persistence with a repair phenotype appear compromised (Saheb-Al-Zamani et al., 2013). Thus, SCs from different nerve sources transplanted into cold-preserved acellular nerve grafts improved functional recovery compared with nerve isografts in a 14-mm rat sciatic injury model (Jesuraj et al., 2014). Similarly, autologous SCs repopulated cold-preserved grafts demonstrated significantly enhanced nerve regeneration compared to unseeded grafts after repair of 6 cm nerve defects in the ulnar nerve of non-human primates (Hess et al., 2007).

SCs can be engineered by viral vectors to deliver neurotrophic support (BDNF, CNTF, NT3, GDNF or NGF). When implanted into previously decellularized nerve grafts, each factor used had different effects on the overall regenerative process (Godinho et al., 2013, 2020) and can have specific effects on different axonal populations.

Although these experimental results are encouraging, there are some obstacles to overcome before therapeutic SC-seeded nerve allografts may be translated to the clinic. Among them, the need for autologous source of the cells, likely requiring the sacrifice of a healthy nerve, and the time and conditions needed for culturing human SCs (Levi, 1996), and the relatively low survival of cells injected in decellularized nerves under common methods (Jesuraj et al., 2011). Nevertheless, the demonstration that human SCs isolated in culture enhance axonal regrowth and myelinate regenerated axons after grafting in the peripheral nerve of immune deficient rodents (Levi et al., 1994), is important for clinical expectations. Indeed, there is an ongoing phase one clinical trial with the purpose to assess the safety of autologous human SC augmentation of nerve autograft repair in subjects with severe PNI.

To facilitate the potential clinical application and to enhance the efficacy of decellularized nerve grafts, the use of multipotent cells such as MSCs or their derived secretome is receiving more attention, with the aim to further optimize the outcome following allograft nerve repair (Pedrini et al., 2019; Contreras et al., 2022). Bone-marrow-derived mesenchymal stem cells (BMSCs) and adipose-derived mesenchymal stem cells (ADSCs) were differentiated into SC-like phenotype and used to enrich acellular allografts. MSCs are adult multipotent progenitor cells found in many organs and tissue types. Due to their relative ease of isolation and expansion in culture, MSCs have been used as a multi-purpose cell-based therapy, in which transplanted MSCs would reach damaged tissues and help to reduce neuroinflammation and even differentiate in specific cell types (Wu et al., 2020).

BMSCs and ADSCs promoted sciatic nerve regeneration and functional recovery comparable to that with a nerve autograft for repair a 15-mm long gap in rats (Wang et al., 2012). Similarly, skin precursor cells-derived SCs were able to improve nerve regeneration across a 12-mm gap in the sciatic nerve of rats bridged by a freeze-thawed nerve graft (Walsh et al., 2009). MSCs from different sources can represent a clinically relevant and abundant source of transplantable cells that may be obtained from in adults from autologous origin and appear to enhance nerve regeneration in nerve injuries.

INTRODUCTION

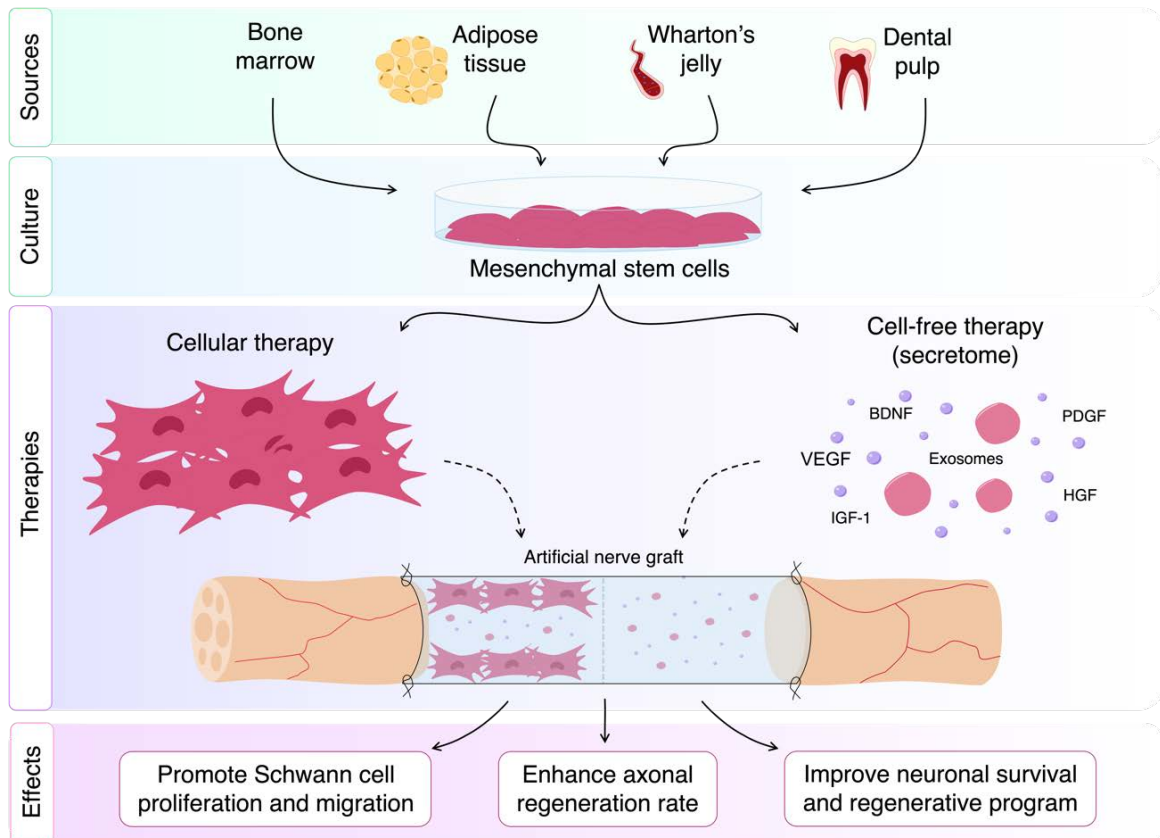


Figure 4. Therapies based on mesenchymal stem cells to improve nerve regeneration. MSCs are relatively easy to isolate from bone marrow, adipose tissue, Wharton's jelly, or dental pulp. These cells have been widely used as regenerative therapy for the damaged nervous system. An alternative repair method for severe nerve lesions is the use of artificial nerve grafts filled with different factors to bridge the nerve stumps. The use of MSCs in the nerve conduits as well as the secretome of these cells (conditioned medium) has been proved to have beneficial effects in axonal regeneration after nerve injuries. Extracted from Contreras et al., 2022.

The group of Shin developed an approach to seed MSCs in acellular nerve allografts with improved reproducibility and a more uniform distribution by using a dynamic bioreactor compared to microinjection (Rbia et al., 2018; Bedar et al., 2022). Interestingly, labelled ADSCs could be detected for up to 29 days after *in vivo* implantation within a recellularized graft, longer than in previous methods. However, a limited survival of MSCs after *in vivo* implantation was observed (Rbia

et al., 2019). Subsequently they studied the outcomes of nerve allografts seeded with undifferentiated and differentiated MSCs, finding that undifferentiated cells improved functional outcomes to a greater extent than differentiated cells, and similar to autografts, although the model was a mid-gap of 10 mm in the sciatic nerve of rats (Mathot et al., 2021).

Further preclinical investigations on recellularized nerve allografts should clarify which type of differentiated cells, the time maintained *in vitro*, and their optimal density is the best option for improving nerve regeneration in well standardized long gap nerve injury models before clinical translation can be proposed.

Cell-free therapies are an emerging alternative to cell therapies in the field of tissue regeneration. Considering the limited time that grafted cells survive within the host tissue, it is generally considered that the therapeutic effects of MSCs or other derived stem cells are related with the secretion of bioactive molecules and extracellular vesicles, that constitute their secretome (Wu et al., 2020; Contreras et al., 2022). Thus, cells secretome may be used as therapeutic approach, avoiding risks associated with the transplantation of cells, such as immune rejection, and reducing the problems associated with cell procurement. In a recent study, induced pluripotent stem cells (iPSCs) derived exosomes were used to supplement acellular nerve grafts bridging a 15-mm defect in the sciatic nerve of rats. The results showed satisfactory regenerative outcomes, especially motor function, and muscle reinnervation were comparable to those achieved with a nerve autograft (Pan et al., 2021), opening an avenue of therapeutic interest.

7. Experimental models of PNI and regeneration

A large variety of both animal models and nerve models have been used in PN regeneration research. Rodents, specifically rats, are the most widely used model because they have a similar PNS than humans and have low costs compared to large animals. Numerous knock-out and transgenic rodent models have been developed as approaches to study regeneration-related mechanisms and pathways. Non-human primates have been used for devices and/or drugs in final

INTRODUCTION

stages before clinical application, but high costs, required facilities, and ethical dilemma have limited their use. Large non-human primate animals, such as sheep or pigs, are a good model as they have a similar anatomy to humans.

Several different nerves have been used in experimental studies. The most frequently used nerves are the sciatic, facial, median, femoral, and the brachial and lumbar spinal roots. Some of these nerves simulate relevant clinical lesions that occurs in humans, on the same nerve and on similar nerves. Other nerves make it possible to address specific cellular, molecular, or behavioral problems to expand knowledge.

7.1. In vivo models of nerve injury and repair

The ability of severed axons to regenerate and recover functional connections after PNI depends on several parameters, such as the type of injury, the location, the injured trunk, and the distance between the two nerve ends that determine the need for surgical repair and the prognosis of functional recovery. The most common lesions performed in experimental studies are focal lesions by crushing or freezing the nerve, which induce axonal interruption but preserve the connective sheaths (axonotmesis), complete transection of the entire nerve trunk (neurotmesis), and resection of a segment nerve that induces a long gap (Rodríguez et al., 2004).

After nerve crush, regeneration is usually successful thanks to the favorable terrain provided by repair SCs and the preservation of the endoneurial tubules. Both facts enhance axonal elongation and facilitate adequate target reinnervation (Valero-Cabré et al., 2004). This type of injuries is adequate to investigate the intrinsic cellular and molecular events that participate in PN regeneration, and to evaluate factors, such as drugs (Udina et al., 2003b) that may increase the speed of regeneration.

In contrast, surgical repair is needed after complete transections because axonal growth is limited across a gap imposed after nerve section. In this type of injury, the classical method of repair is the epineural suture. When a long gap is induced by resecting a segment of the peripheral nerve, repair requires a graft or artificial

bridge for supporting regeneration. The gold standard for repairing a nerve long gap is the autograft. Autograft repair allows for similar number of regenerated axons and functional recovery compared to direct suture repair. The autograft is mainly used to assay new techniques for nerve repair, including the use of nerve allografts or xenografts, decellularized grafts of nerves or other tissues (Fansa et al., 2002), and most often new artificial alternative grafts based on nerve tubes or conduits.

7.2. Sciatic nerve and tributaries

The sciatic nerve is the most used model for studies on PNI. It is a nerve trunk with suitable length in the mid-thigh for surgical manipulation and the use of grafts or guides for repair. The sciatic nerve divides above the popliteal fossa into three branches: tibial, peroneal, and sural nerves. Each of the branches conveys different proportions of sensory, motor, and autonomic axons to muscles, vessels, skin receptors or sweat glands located in different areas of the hindlimb. Injury to one branch leads to regional paralysis and anesthesia on particular regions. Although sciatic nerve injuries themselves are rare in humans, this model provides a realistic testing bench for injuries and repair methods in plurifascicular mixed nerves with axons of different size and types competing to reach distal endoneurial tubules and reinnervate targets. Injuries to one of the branches, mainly on the tibial or peroneal nerve, have also been reported. Comparisons with the normal distribution allow the efficiency of reinnervation using electrophysiological and retrograde tracing methods (Valero-Cabr e and Navarro, 2002). Behavioral recovery during walking has been widely assessed through detailed analysis of footprints during walking (Varej o et al., 2001).

7.3. Nerve size and length of regeneration

The dependence due to the gap created makes the length and the nerve size of great relevance for nerve regeneration studies. The success of tubulization depends on the capability of the injured nerve to provide sufficient cellular and humoral elements to produce the initial regenerative wire, although length is the

INTRODUCTION

main limitation. This limit gap depends on the animal species, since it implies both the number of non-neuronal cells present and the nerve mass, being up to 4 mm in mice (Butí et al., 1996; Gómez et al., 1996), up to 10 mm in rat (Lundborg et al, 1982; Williams et al, 1983) and less than 30 mm in non-human primates (Mackinnon and Dellon, 1990; Archibald et al, 1995).

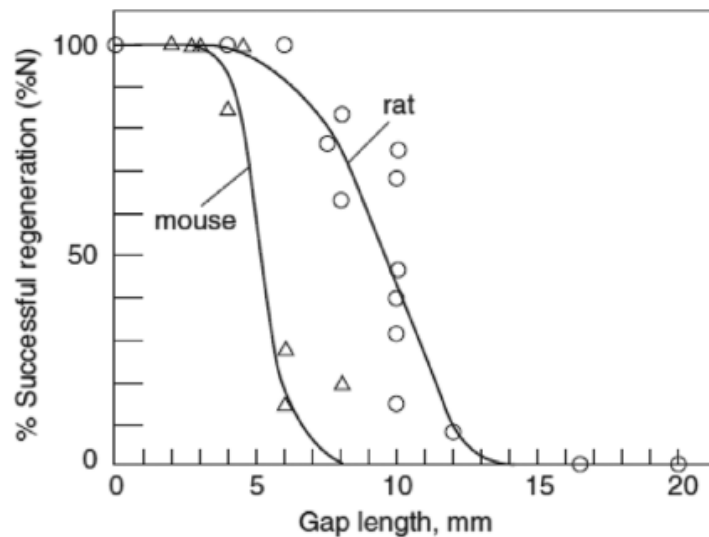


Figure 5. Graph of the nerve gap dependence of regeneration in silicone tubes. Successful regeneration depends on the length of the nerve gap, the limiting gap length. Is defined as the length as which regeneration occurs in 50% of treated animals (Extracted from Yannas & Hill, 2004).

Within a short or mid-length gap, tubes provide a window to study the role of molecular factors and cell types in the regeneration process (Liu, 1996; Navarro et al., 2003). In addition, it should be considered that in the case of long gaps, regeneration fails in most cases. Tube repair is the basis for the artificial development that can replace the autograft as a gold standard in the clinics. Many studies have looked at the introduction of ECM components, neurotrophic factors, or transplanted cells within nerve tubes (Schmidt et al., 2003, Navarro et al., 2003, Deumens et al., 2010).

7.4. Large animal models for translational research on nerve repair

The rat sciatic nerve transection and repair model is the most widely used rodent model in peripheral nerve regeneration (Tos et al., 2009; Siemionow et al., 2009;

Angius et al., 2012; Geuna, 2015; Gordon and Borschel, 2017). Nerve anatomy of rodents has been well studied, but regeneration is faster than in humans and, only short nerve gaps can be studied (Glasby et al., 1999; Angius et al., 2012; Diogo et al., 2017). In addition, the recovery of limb function may be better because of the short regeneration distances between the injured nerve and the target organs in rodents (Kettle et al., 2013).

Large animal models allow for longer gaps and longer regeneration distances that mimic the clinical conditions often found in human nerves. The development of new clinical approaches in peripheral nerve regeneration includes preclinical animal testing in animal models that reproduce the regeneration process that occurs in human nerve injuries (Angius et al., 2012). There is no standard large animal model for nerve repair studies (Kornfeld et al., 2019). The large animals used for peripheral nerve injury and regeneration studies include primates, dogs, cats, pigs, and sheep (Atchabahian et al., 1998; Forden et al., 2011; Angius et al., 2012; Alvites et al., 2021).

Non-human primates have been used in experimental studies to assess nerve regeneration between autograft and decellularized allografts treated with FK-506 in the distal ulnar motor nerve (Auba et al., 2006) or recellularized with autologous mesenchymal cells in the ulnar nerve (Hu et al., 2007). Synthetic and biologic conduits were also evaluated in up to 5 cm ulnar/radial nerve defects (Mackinnon and Dellon, 1990; Archiblad et al., 1995).

The sciatic nerve model was used to repair a 5 cm with a biodegradable artificial nerve guide in the cat (Suzuki et al., 1999; Sufan et al., 2001). Peroneal nerve of dogs has been also used to assess both allografts (Ide et al., 1998) and conduits (Matsumoto et al., 2000). Conventional pigs have been used to test the efficacy of allograft nerve regeneration in the ulnar nerve (Atchabian et al., 1998; Jensen et al., 2005; Brenner et al., 2005) while Burrell et al. (2020) used minipigs to repair 5 cm gap injuries in the common peroneal nerve and the deep peroneal nerve. Studies have been carried out in rabbits to investigate nerve regeneration with autograft in nerve defects between 3 and 7 cm in the saphenous nerve (Koller et al., 1997) and muscle grafts in lesions up to 10 cm in the sciatic nerve (Hems et

INTRODUCTION

al., 1993). Veins were also evaluated in defects from 4 to 6 cm in the tibial nerve (Zhang et al., 2002) and in the peroneal nerve (Strauch et al., 1996, 2001) of rabbits.

The sheep has gained interest as one of the most relevant animal models for preclinical studies (Hems and Glasby, 1992; Glasby et al., 1993; Al Abri et al., 2014; Alvites et al., 2021). Compared to other large animals, sheep have advantages because of their availability, simplicity of care and housing, cost, and social acceptance (Turner, 2007; Ozturk et al., 2015; Diogo et al., 2017). They have generated interest for the study of long nerve gap repair because their peripheral nerves resemble human nerves in terms of their length, diameter, and function (Diogo et al., 2017; Costa et al., 2018; Kornfeld et al., 2019). Protocols for nerve surgery and the clinical evaluation of deficits and histological processing have been recently proposed (Alvites et al., 2021).

V. OBJECTIVES

PNS neurons have the ability to regenerate their axons after an injury. However, functional recovery is not always satisfactory, with important consequences for patients' quality of life. The degree of functional recovery depends on the type and severity of the injury. The current gold standard for repairing severe PNI, the autograft, has several drawbacks, such as the sacrifice of an uninjured nerve to bridge both nerve stumps. Therefore, it is essential to study alternatives as a potential replacement to the use of autograft in human clinics.

In this thesis, we have collaborated with two different companies, Verigraft AB (VERI), a private biotech company from Sweden, and the Barcelona Tissue Bank (BST), a public company from Spain. Both companies are interested in optimizing nerve graft decellularization protocols with the aim to use decellularized nerve allografts to repair long nerve defects in patients. We have evaluated these grafts in both rat and large animal models, for upcoming clinical trials and market approval.

The main objectives of this thesis are:

- To develop a large animal model for the study of severe peripheral nerve injuries.
- To test the regenerative capacity of decellularized nerve allografts in the sheep.

The specific objectives of this thesis are:

- To assess different functional tests to quantify regeneration and reinnervation in the sheep model.
- To evaluate the degree of axonal regeneration and reinnervation in different size nerve gaps in the sheep.
- To evaluate histologically different protocols for decellularization of donor grafts from humans, rats, and sheep.
- To evaluate the regenerative capacity of decellularized nerve grafts in a severe resection model in rats.

OBJECTIVES

- To study the early phases of regeneration of the decellularized allograft and decellularized xenograft in a severe resection model in rats.
- To evaluate the regenerative capacity of decellularized nerve grafts in a severe resection model in sheep.

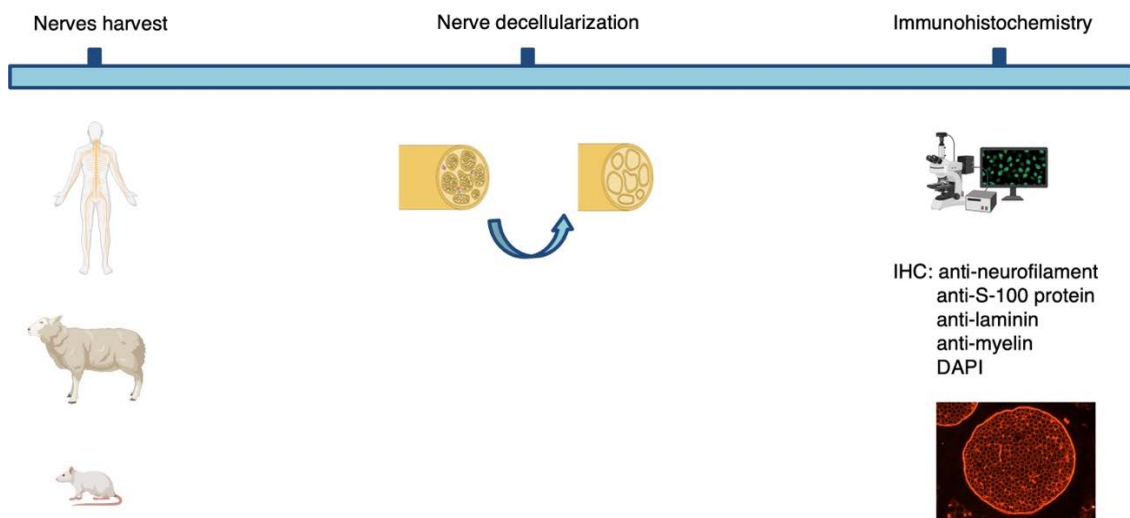
VI. STUDY DESIGN AND METHODOLOGIES

All the experimental procedures were approved by the Ethics Committees of Universitat Autònoma de Barcelona and Generalitat de Catalunya. For the rat study protocol, code is 10306 and date of approval is 07/09/2018 whereas for the sheep study protocol, code is 10314 and date of approval is 20/11/2018.

1. IN VITRO STUDIES

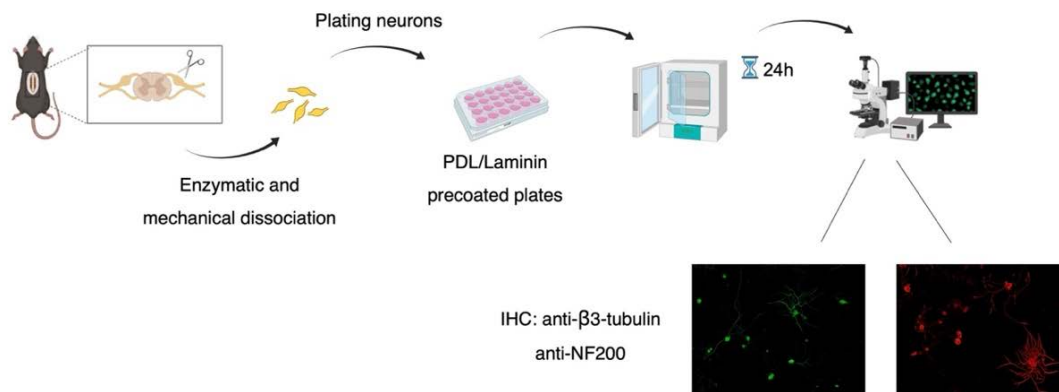
1.1 Nerve decellularization

Rat sciatic nerves, sheep peroneal nerves and human sural nerves were harvested from donors and processed by Verigrift and BST. After the decellularization, immunohistochemistry (IHC) was performed to evaluate the efficiency of the protocols for removing the cellularity and maintaining the ECM components.



1.2. Dissociated culture of DRG

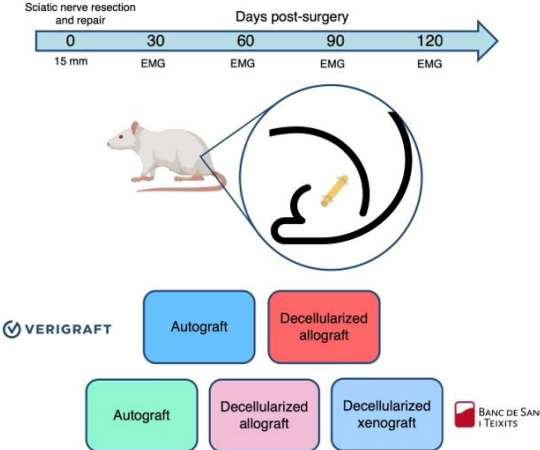
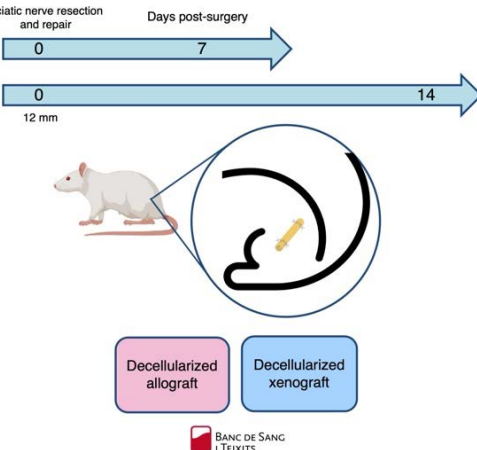
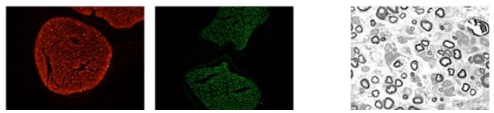
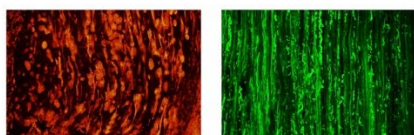
Dissociation and culture of mice DRG were performed through enzymatic digestion and mechanical dissociation. Coverslips coated with poly-D-lysine (PDL) plus human or mice laminin were used to test if the laminin, an important component of the ECM can contribute to poorer regeneration potential in grafts from different species.



2. IN VIVO STUDIES

2.1 Rat

- Long-term studies: A resection of 15 mm was performed in the sciatic nerve of Sprague Dawley (SD) rats. The repair was carried out with the gold standard, autograft and with a decellularized nerve allograft. In the BST study, a decellularized nerve xenograft from human origin was also used. We performed nerve conduction tests at 30-, 60-, 90- and 120-days post injury. After the euthanasia, samples of the nerve grafts were taken to perform immunohistochemical and histological analyses.
- Short-term study decellularization: A resection of 12 mm was performed in the sciatic nerve of SD rats in two different batches. The repair was carried out with a decellularized nerve allograft and decellularized nerve xenograft. Both nerves were decellularized with the optimized decellularization protocol provided by BST. After the euthanasia, samples from the nerve graft were taken to perform immunohistochemical analyses.

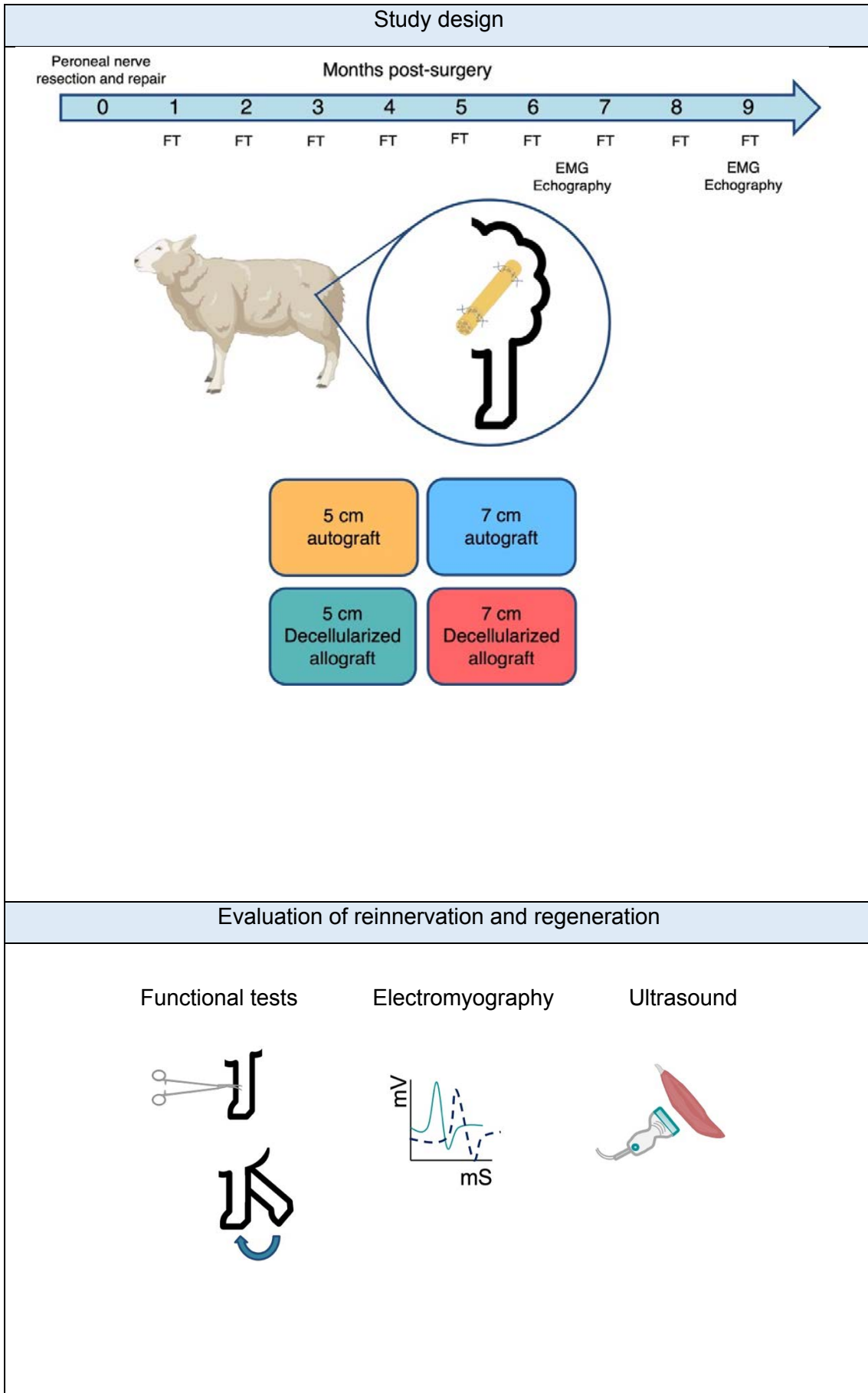
Long-term studies	Short-term study
Study design	Study design
 <p>Sciatic nerve resection and repair</p> <p>Days post-surgery</p> <p>0 30 60 90 120</p> <p>15 mm EMG EMG EMG EMG</p> <p>VERIGRAFT</p> <p>Autograft Decellularized allograft</p> <p>Autograft Decellularized allograft Decellularized xenograft</p> <p>BANC DE SANG I TEIXITS</p>	 <p>Sciatic nerve resection and repair</p> <p>Days post-surgery</p> <p>0 7 14</p> <p>12 mm</p> <p>Decellularized allograft Decellularized xenograft</p> <p>BANC DE SANG I TEIXITS</p>
Immunohistochemistry and histology	Immunohistochemistry
<p>IHC: anti-neurofilament anti-S-100 protein anti-laminin anti-iba1</p> <p>Epon and toluidine blue stain</p> 	<p>IHC: anti-neurofilament anti-S-100 protein anti-vimentin anti-iba1</p> 

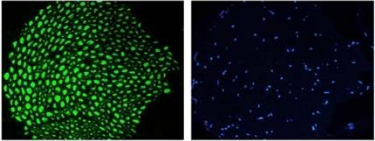
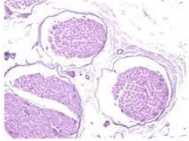
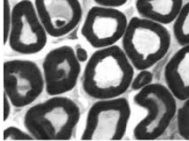
2.2. Sheep

This thesis focuses on the establishment of the sheep as a large animal model to test new therapeutic alternatives to the use of the autograft. Therefore, it was necessary to establish the animal model, as well as the tests to assess nerve regeneration.

We have used a resection of 5- or 7- cm in the peroneal nerve of the sheep. The repair was carried out using the gold standard, the autograft or a decellularized nerve allograft of the same length. The studies lasted 9 months, during which monthly functional tests (FT) were performed to assess the degree of reinnervation. Electromyography (EMG) and ultrasound test of the TA muscle were also performed at 6.5- and 9-months post-surgery (mps). Furthermore, immunohistochemical and morphological analyses were performed.

STUDY DESIGN AND METHODOLOGIES



Immunohistochemical and morphological analyses		
<p>IHC: anti-neurofilament anti-S-100 protein anti-laminin anti-macrophages DAPI</p>	<p>H&E stain</p>	<p>Epon and toluidine blue stain</p>
		

VII. RESULTS

Chapter I

Repair of long peripheral nerve defects in sheep: a translational
model for nerve regeneration

Repair of Long Peripheral Nerve Defects in Sheep: A Translation Model for Nerve Regeneration

Estefanía Contreras^{1,2}, Sara Traserra^{1,2}, Sara Bolívar^{1,3}, Joaquím Forés^{1,4}, Eduard Jose-Cunilleras⁵, Ignacio Delgado-Martínez^{1,3}, Félix García⁵, Esther Udina^{1,3} and Xavier Navarro^{1,3}

1. Institute of Neurosciences, Department Cell Biology, Physiology and Immunology, Universitat Autònoma de Barcelona, 08193 Bellaterra, Spain

2. Integral Service for Laboratory Animals (SIAL), Faculty of Veterinary, Universitat Autònoma de Barcelona, 08193 Bellaterra, Spain

3. Centro de Investigación Biomédica en Red Sobre Enfermedades Neurodegenerativas (CIBERNED), 28031 Madrid, Spain

4. Hand and Peripheral Nerve Unit, Hospital Clínic i Provincial, Universitat de Barcelona, 08036 Barcelona, Spain

5. Department of Animal Medicine and Surgery, Universitat Autònoma de Barcelona, 08193 Bellaterra, Spain

International Journal of Molecular Sciences **2023**, *24*,1333.

Abstract: Despite advances in microsurgery, full functional recovery of severe peripheral nerve injuries is not commonly attained. The sheep appears as a good preclinical model since it presents nerves with similar characteristics to humans. In this study, we induced 5 or 7 cm resection in the peroneal nerve and repaired with an autograft. Functional evaluation was performed monthly. Electromyographic and ultrasound tests were performed at 6.5 and 9 months post surgery (mps). No significant differences were found between groups with respect to functional tests, although slow improvements were seen from 5 mps. Electrophysiological tests showed compound muscle action potentials (CMAP) of small amplitude at 6.5 mps that increased at 9 mps, although they were significantly lower than the contralateral side. Ultrasound tests showed significantly reduced size of TA muscle at 6.5 mps and partially recovered size at 9 mps. Histological evaluation of the grafts showed good axonal regeneration in all except one sheep from autograft 7 cm (AG7) group, while distal to the graft there was a higher number of axons than in control nerves. The results indicate that sheep nerve repair is a useful model for investigating long gap peripheral nerve injuries.

1. Introduction

Peripheral nerve injuries results in partial or total loss of motor, sensory, and autonomic functions of the affected nerve territory [1]. When the axon is transected, the segment distal to the lesion disconnects from the neuronal body and undergoes Wallerian degeneration [1–4] to create a permissive environment for regeneration. In parallel, the axotomized neuron switches to a pro-regenerative state, with phenotypic changes to support axon re-growth [5]. Despite adult peripheral neurons having this intrinsic regenerative capability and being able to reinnervate their target organs eventually, functional outcome is not always complete [1,6,7], leading to chronic functional impairments and decreased patient quality of life.

The severity of the nerve injury is one of the main factors that determines the degree of recovery. Therefore, mild injuries, such as compression or crush, in which only the axons are transected but all the connective layers, including the endoneurial tubules, are preserved, usually recover normal function. In contrast, when both axons and connective tissue are transected, functional outcomes are worse. After a complete nerve transection, surgical repair is mandatory to suture the proximal and distal nerve stumps together and, thus, facilitate that axons can cross the gap and grow along the distal stump. When direct suture of the two stumps is not possible because the separation is too large, a bridge is required to guarantee continuity between the two nerve stumps. Currently, the gold standard for this type of lesion is the interposition of a segment of another nerve from the same patient, called an autologous graft [6,8]. However, long nerve defects cannot always be repaired with an autograft due to the limited availability of nerve sources for the repair of extensive or multiple nerve injuries. In addition, autograft harvesting can lead to neuroma formation and permanent loss of sensation in the territory of the donor nerve [9].

Thus, regeneration of long nerve defects remains a challenge in the clinic, and further research is needed to find alternatives to autograft repair. Tube repair, the implantation of a tube or conduit from natural or synthetic biomaterials to bridge

a nerve gap, emerged as a potential alternative to the autograft repair of transected peripheral nerves [10]. However, depending on the size of the injured nerve and the species, the regeneration across nerve conduits is limited by the length of the gap. Experimental studies showed that regenerating axons can bridge empty tubes made of silicone or synthetic materials along a gap of up to 4 mm in the mouse [11], up to 10 mm in the rat [10], and 30 mm in primates [12,13], but fail in most cases with longer gaps. Therefore, the most relevant clinical need for alternative repair methods in human patients are lesions resulting in gaps between 3–30 cm in length [14].

The rat sciatic nerve transection and repair model is the most widely used rodent model in peripheral nerve regeneration [15–19]. Nerve anatomy of rodents has been well studied, but regeneration is faster than in humans and, obviously, only short nerve gaps can be studied [17,20,21]. In addition, the recovery of limb function may be better because of the short regeneration distances between the injured nerve and the target organs in rodents [22]. It is fundamental to provide good experimental models with the aim to explore and design new and innovative therapies with translational potential.

Large animal models allow for longer gaps and longer regeneration distances that mimic the clinical conditions often found in human nerves. The development of new clinical approaches in peripheral nerve regeneration includes preclinical animal testing in animal models that reproduce the regeneration process that occurs in human nerve injuries [17]. There is no standard large animal model for nerve repair studies [9]. The large animals used for peripheral nerve injury and regeneration studies include primates, dogs, cats, pigs, and sheep [17,23–25]. The sheep has gained interest as one of the most relevant animal models for preclinical studies [25–28]. Compared to other large animals, sheep have advantages because of their availability, simplicity of care and housing, cost, and social acceptance [20,29,30]. They have generated interest for the study of long nerve gap repair because their peripheral nerves resemble human nerves in terms of their length, diameter, and function [9,20,31]. Protocols for nerve surgery

and the clinical evaluation of deficits and histological processing have been recently proposed [25].

The aim of this study is to standardize a model of peripheral nerve injury in sheep and adequate methods for evaluation during a long follow-up period that will be useful for the investigation of new therapeutic alternatives to the autograft for the repair of severe, long-gap nerve injuries. We include the surgical approach, functional monitoring, electrophysiological and ultrasound tests, and histological analyses, for a comprehensive and detailed quantification of nerve regeneration and reinnervation.

2. Materials and Methods

2.1. Animals and Study Design

Nine adult, female ripollesa sheep (*Ovis aries*) were used. Their age was 2–5 years and their body weight was 55–69 kg. They were obtained from Servei de Granges i Camps Experimentals (SGiCE, Bellaterra, Spain) of the Universitat Autònoma de Barcelona (UAB, Bellaterra, Spain). The animals were housed in groups in a conventional manner, in stable on straw at the SGiCE from one week post-surgery until the end of the study. The light cycle was natural as well as the temperature and the humidity.

Animals were divided in two experimental groups: autograft 5 cm (AG5; n = 4) and autograft 7 cm (AG7; n = 5) depending on the length of the graft used. Blood samples were taken and general health assessment was performed before inclusion in the study. Clinical signs, including general state, behavior, claudication, water and food intake, and wound healing during the observation period were assessed twice a day for 3 days after the surgery, once a day for one week, and then once a week until the end of the follow-up at 9 months post-surgery. In the operated and the contralateral (as control) hindlimbs, clinical evaluation of motor and sensory functions was performed prior to and at monthly intervals after surgery to evaluate nerve regeneration and reinnervation (Figure

CHAPTER I

1). Electrophysiological and echography testing was carried out at 6.5 and 9 months post surgery (mps).

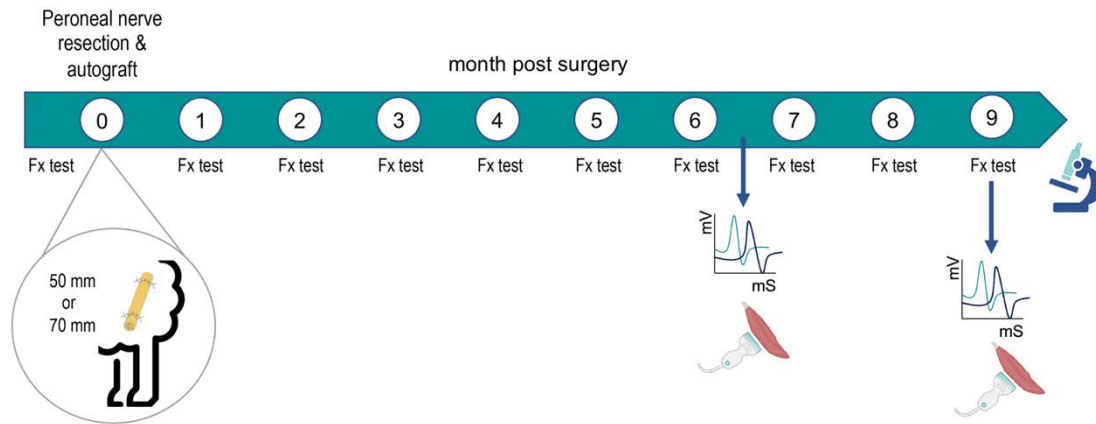


Figure 1. Schema of the design of the study. Following the surgery, functional tests (Fx test) were performed each month, electrophysiological tests and echography were made at 6.5 and 9 months, and samples were taken for histology at the end of the follow-up. Both operated and contralateral hindlimbs were tested at each interval.

2.2. Surgical Procedure

Animals were fasted 16 h prior to the surgery to reduce the ruminal content and to prevent deviant swallowing and consequent risk of provoking aspiration. For the surgery, the sheep were sedated with an intramuscular injection of a mixture of midazolam (0.2 mg/kg) and morphine (0.4 mg/kg). A venous catheter was inserted in the cephalic vein and anesthesia was induced with propofol (4 mg/kg i.v.). Animals were intubated to maintain a proper anesthesia level by means of isoflurane (2 L/min) mixed with 100% oxygen. Fluid therapy was given with 10 mL/kg of Ringer solution, and a preoperative antibiotic dose of cefazoline (22 mg/kg) was administered intravenously. A gastric catheter was also placed in the stomach to avoid reflux during anesthesia.

The sheep was placed in a lateral decubitus position and the incision zone was shaved and cleaned with chlorhexidine solution. The peroneal nerve was exposed using a longitudinal lateral skin incision along the right thigh followed by

splitting the semitendinosus and biceps femoris muscles. Under the operating microscope, a length of 50 or 70 mm of the common peroneal nerve was resected 1 cm above the iliac vein to create a nerve gap (Figure 2). The distance between the proximal cut of the peroneal nerve and the entrance of the distal nerve into the TA muscle was 34–36 cm. The two nerve stumps were then bridged with the resected nerve segment in the same orientation by means of 8/0 epineural sutures. The resistance of the coaptation was tested by slightly stretching the nerve. The incision was closed by layers and disinfected with povidone iodine solution.

After the surgery, the animals were transferred to the SGiCE, where they were housed in couples for one week in a controlled enclosure, and thereafter housed in groups at the regular sheep barn. Postoperative care included buprenorphine (0.01 mg/kg s.c.) twice a day for 2 days and meloxicam (0.2 mg/kg s.c.) once daily for 3 days. Long-term antibiotic ceftiofur (5 mg/kg s.c.) was administered after the surgery.

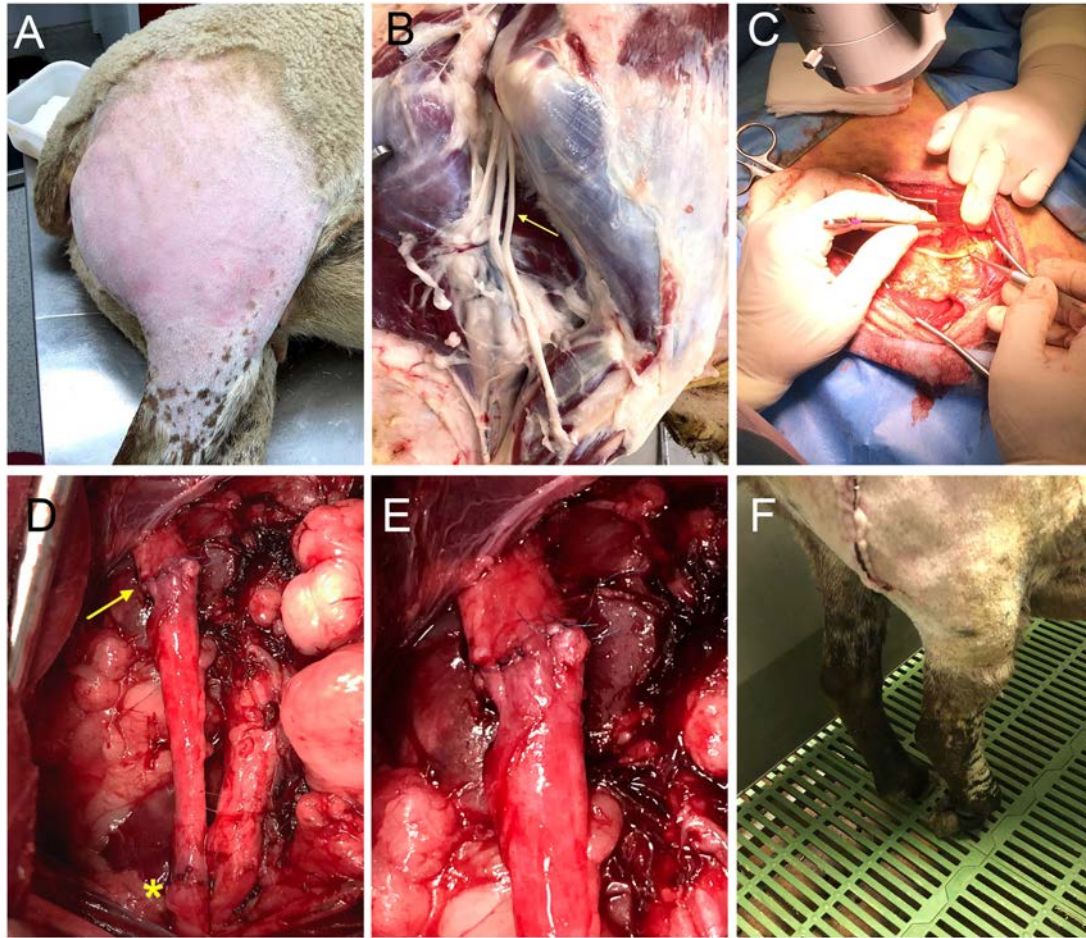


Figure 2. Photographs of the surgical procedure for the peroneal nerve injury and repair. (A) The surgical approach was performed with the animal in lateral recumbency through a lateral longitudinal skin incision. (B) Wide dissection showing the peroneal nerve location (arrow) after the sciatic nerve bifurcation into the tibial and peroneal nerve in a cadaveric sheep. (C) Resection of the common peroneal nerve under the operating microscope to create the nerve gap. (D) A 5 cm autograft was sutured again to the nerve stumps with epineural sutures (proximal suture marked with yellow arrow and distal suture marked with a yellow asterisk). (E) Detail of the 8 stitches made to join the nerve graft with the healthy nerve stump without tension. (F) After the surgery, some animals showed foot drop in the standing position.

2.3. Functional Testing

Prior to the surgery and afterwards at monthly intervals, animals were tested for functional evidence of regeneration and reinnervation of the operated hindlimb compared with the contralateral hindlimb (Figure 7). Each parameter assessed was scored on a semiquantitative scale of 0 (no deficit), -1 (partial deficit or functional loss), or -2 (complete loss of response to the maneuver). In all the sessions, each functional test was validated by first performing the test on the non-operated control hindlimb of the same animal. Ankle and foot placement were assessed in the orthostatic position. Locomotion was evaluated during free walking in the pen and during fast walking to assess the ability to maintain plantar support and paying particular attention to the foot drop position of the operated hindlimb (0 = normal walk and maintenance of the plantar support; -1 = few failures on the plantar support maintenance; -2 = foot drop in most of the steps). The mass of the TA muscle was assessed by manual palpation comparing the contralateral hindlimb with the operated one (0 = similar mass; -1 = slight reduction; -2 = large reduction). The proprioceptive response was tested by the ability to replace the hoof from a forced plantar flexion position to a plantar support three times (0 = consistent response; -1 = one failure; -2 = two or three failures). The hindfoot withdrawal reflex was tested by assessing whether the animal withdrew the hindlimb when pinching with a forceps in three areas of the dorsal area of the hindfoot, proximal, middle, and distal (Figure 3). Each site was tested two different times and the score was independent between the three zones (0 = fast and brisk withdrawal response of the limb; -1 = weak or non-consistent response in 2 trials; -2 = no response in 2 trials). Two researchers, who were blind regarding the group allocated throughout the study period, scored on a 0–1–2 scale each of the above maneuvers for all the animals and test days; the score given was by agreement between the observers (Table 1).

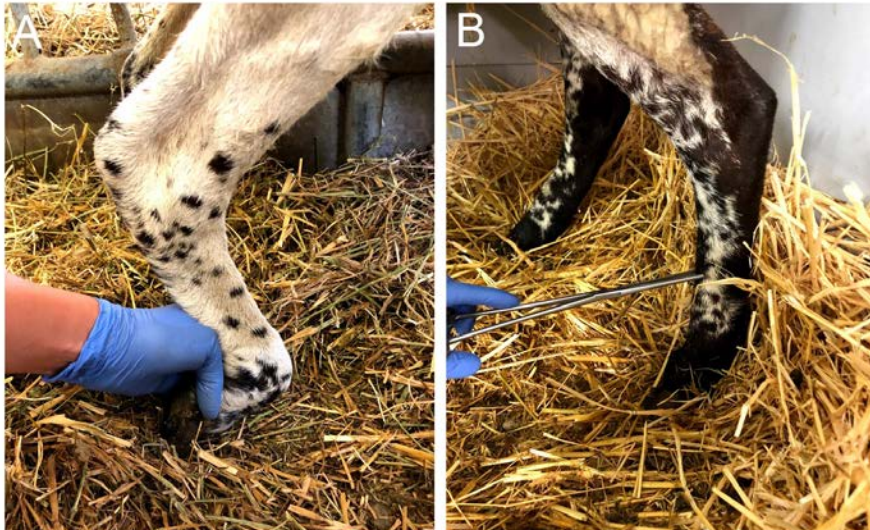


Figure 3. Photograph of the maneuver used for the proprioception test, assessing the capability of dorsiflexion of the hindfoot from a forced plantar flexion position (A). The flexor withdrawal reflex assesses the response to pinching the dorsum of the foot with a hemostat in a proximal point, a middle point (B) and a distal point.

Table 1. Items used in the functional evaluation of sheep after injury and repair of the peroneal nerve. The score points negative values in the case of deficit or loss of response.

Parameter	0	-1	-2
Locomotion	Normal gait	Limp	Drag the limb
Muscle loss (TA)	No loss	Reduced	Atrophy
Proprioception	Present	Decreased	Absent
Flexor withdrawal reflex (proximal point)	Present	Decreased	Absent
Flexor withdrawal reflex (middle point)	Present	Decreased	Absent
Flexor withdrawal reflex (distal point)	Present	Decreased	Absent

2.4. Electrophysiological Tests

Electrophysiological tests to evaluate reinnervation of the TA muscle were performed at 6.5 and 9 mps under general anesthesia. Animals were sedated with intravenous diazepam (0.25 mg/kg), and then anesthesia was induced with an intravenous injection of diazepam and ketamine (0.25 mg/kg and 5 mg/kg, respectively). The sciatic nerve was stimulated with transcutaneous needle electrodes placed at the sciatic notch using an EMG apparatus (Sapphire 4ME Medelec, Vickers Healthcare Co., Surrey, UK). The compound muscle action potential (CMAP) of the TA muscle was recorded with monopolar needle electrodes (Figure 4) from the control hindlimb and the operated hindlimb; the amplitude and onset latency were measured from the maximal response obtained. The stimulus intensity was progressively increased until a maximal amplitude CMAP was obtained, and the recorded CMAP corresponded with contraction of the TA muscle and hindlimb movement. In addition, free-running EMG recordings were made to detect fibrillation potentials as a sign of muscle denervation.

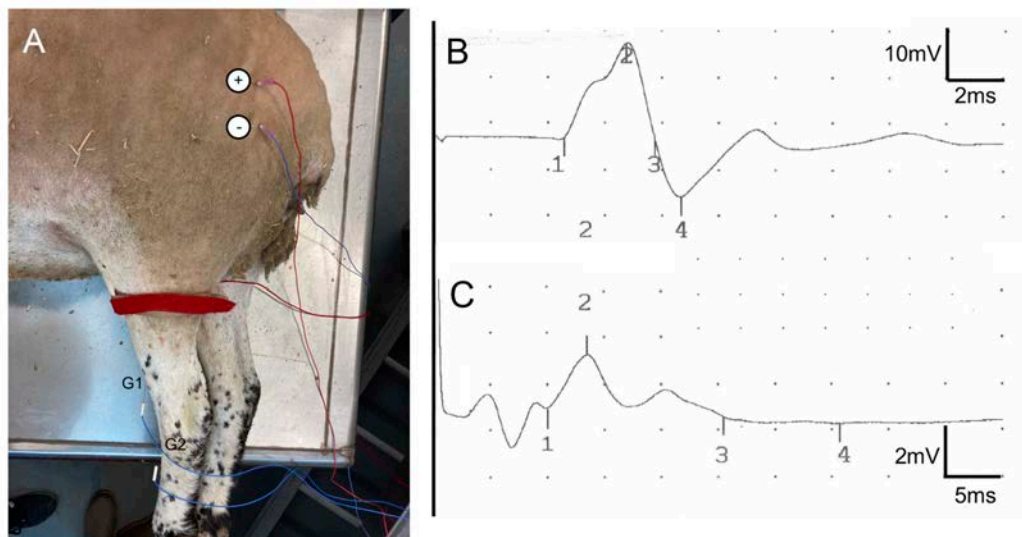


Figure 4. (A). Setup used for the nerve conduction studies. Stimulating needle electrodes were placed at the sciatic notch to stimulate the nerve (+ –), whereas recording needle electrodes were placed at the TA muscle (active electrode, G1)

and at the distal tendon (reference, G2). The red band corresponds to the ground electrode. (B,C) Sample EMG recordings at 9 mpo. Top trace (B) shows the CMAP in the control hindlimb, and the bottom trace (C) in the operated hindlimb of a sheep of AG7 group. The onset of the CMAP is labeled with mark 1, the negative peak of the CMAP with mark 2, and the end with mark 3. Note the differences in time and voltage scales, noted at the right of each trace.

2.5. Ultrasound Test

Echographic evaluation of the leg anterior compartment was performed with a MyLab® Gamma apparatus (Esaote, Genova, Italy) at the same time of the electrophysiological tests, 6.5 and 9 mpo, under general anesthesia. Hair of the dorsal area of the leg was shaved, and the skin was cleaned with water and mild soap. To optimize image acquisition, acoustic gel was used. The size of the TA muscle, calculated as area and perimeter, was determined using the B-mode ultrasound (15 MHz), with a linear ultrasound probe in the cranial aspect of the crus at the midpoint between the tibial crest and the tuber calcanei (Figure 5). The control hindlimb of all animals was used as a control.

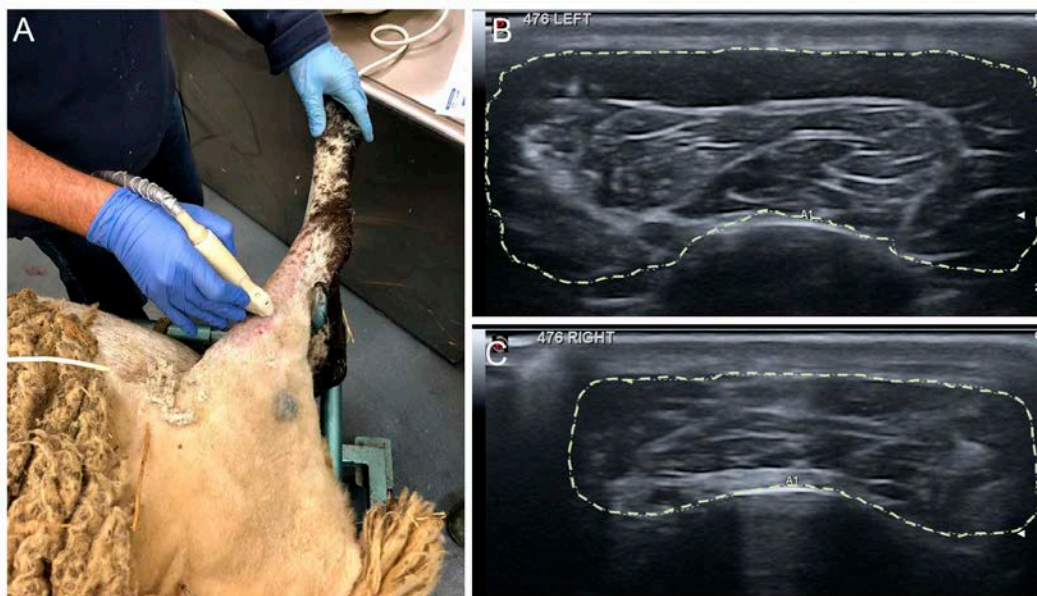


Figure 5. Procedure for the echographic imaging. The ultrasound probe was placed with conductive gel on the mid of the TA muscle mass (A). Sample images

of the echography of TA muscle, delineated by discontinuous line in a control hindlimb (B), and in an operated hindlimb (C).

2.6. Histological Evaluation

At the end of the follow-up at 9 mpo, following electrophysiological and ultrasound tests and under general anesthesia, the sheep were euthanized with an intravenous administration of Euthasol (400 mg/kg). The sciatic nerve and branches were exposed under surgical dissection. The nerve graft, including the proximal and distal suture lines, was harvested, and fixed in 4% paraformaldehyde for 5 days at 4 °C. The TA muscle was dissected and weighted. Samples from the TA muscle and a piece of skin of the dorsum of the hindfoot were taken and fixed in paraformaldehyde 4% for 7 days at room temperature (RT). Samples from the contralateral hindlimb were taken as control samples.

The nerve graft was divided into different segments to analyze the middle segment of the graft and the nerve distal to the graft. Each segment was also divided in two halves. The first half of the nerve graft of section 2 and section 4, corresponding to the middle and distal to the nerve graft, respectively, were transferred to 70° ethanol for 48 h. Samples were embedded in paraffin and 5 mm thick cross-sections were cut on a microtome. Some slides were deparaffinated and stained with hematoxylin and eosin to visualize the general structure of the nerve graft under light microscopy. Other slides were processed for immunohistochemistry. The latter slides were deparaffinated and blocked with a solution of normal goat serum and normal donkey serum (10%) in phosphate-buffered solution (PBS) containing 0.3% Triton. The sections were incubated overnight at RT with primary antibodies against neurofilament (NF200; myelinated axons; 1:400; AB5539-Millipore) and against S100 protein (S100; Schwann Cells; 1:50; 22520-DiaSorin). Following washes, sections were incubated against secondary antibodies bound to Alexa Fluor 488 and Alexa Fluor 594. Immunolabeled sections were viewed under epifluorescence microscopy (Olympus BX51). The total number of regenerated myelinated axons

CHAPTER I

was estimated by measuring the cross-sectional area of the nerve grafts and counting myelinated axons labeled with NF200 in selected fields distal to the nerve grafts.

The second half of the sections were post-fixed in 3% paraformaldehyde and 3% glutaraldehyde in cacodylate-buffer solution (0.1 M, pH 7.4) at 4 °C. The samples were post-fixed in osmium tetroxide (2% for 2 h), dehydrated with ethanol, and embedded in Epon resin. Semithin sections 0.5 µm thick were cut on an ultramicrotome (Leica, Wetzlar, Germany) and stained with toluidine blue. Representative light microscopic images were selected.

Samples from TA muscle and skin of the dorsum of the hindfoot were embedded in paraffin, sectioned, and stained with hematoxylin and eosin to visualize the general structure.

2.7. Data Analysis

All the data are expressed as mean \pm standard error of the mean (SEM). Statistical comparisons of functional and histology results were analyzed by using Student's t test and two-way ANOVA after testing for normal distribution. The GraphPad Prism 9 software was used for analysis and graphic representations. Statistical significance was considered if $p < 0.05$.

3. Results

3.1. Clinical Observations

The surgical approach allowed the dissection of the peroneal nerve over a long distance, its resection, and its repair by interposing the same nerve segment with either a 5 or a 7 cm autograft, AG5 and AG7, respectively. All the sheep recovered well from the surgery and survived to the end of the study. In addition, no significant clinical signs were observed during the experimental study. After the surgery, animals were able to stand and walk and showed good mobility. As a result of the peroneal nerve injury, two animals from AG7 group had a marked foot drop posture and developed pressure ulcers. A molded plastic splint was

placed at 1 mps, and the skin ulcers were treated with clorexhydine and Blastoestimulin cream and covered with Vetrap bandage. After one month, one of the sheep recovered and the splint was removed. In contrast, the other sheep continued with the food drop posture until the end of the study.

3.2. Functional evaluation

After the surgery, all sheep showed deficit in locomotion score based on the occurrence of foot drop during fast walking. In the resting orthostatic position, all the sheep, except the two animals of AG7 group indicated above, were able to maintain the plantar support of the right hindlimb. In all the sheep, we observed evidence of foot drop during fast walking, as they failed to maintain the plantar support in some steps (scored as -1 or -2) (Figure 6A). The proprioceptive response was not significantly reduced after the surgery and did not change during the follow-up (Figure 6B). The muscle mass of the right reinnervated tibialis anterior (TA) muscle showed a clear reduction one month after the surgery in comparison to the contralateral muscle. A significant improvement ($p < 0.01$) was detected in AG5 group at the end of the follow-up with respect to values at 30 days (Figure 6C). The withdrawal reflex response to pinching the skin of the dorsum of the foot was abolished at the first test after the surgery and recovered slowly during the follow-up to close to normal levels, early in proximal ($p < 0.0001$) (Figure 6D) and middle ($p < 0.05$) (Figure 6E) sites, likely due to collateral reinnervation. In contrast, the reflex in the distal site showed a return of response compatible with peroneal reinnervation, reaching full recovery in all the sheep of AG5 group at the end of the study ($p < 0.001$ vs. values at 30 days), and in all except one in the AG7 group ($p < 0.05$ vs. values at 30 days) (Figure 1F).

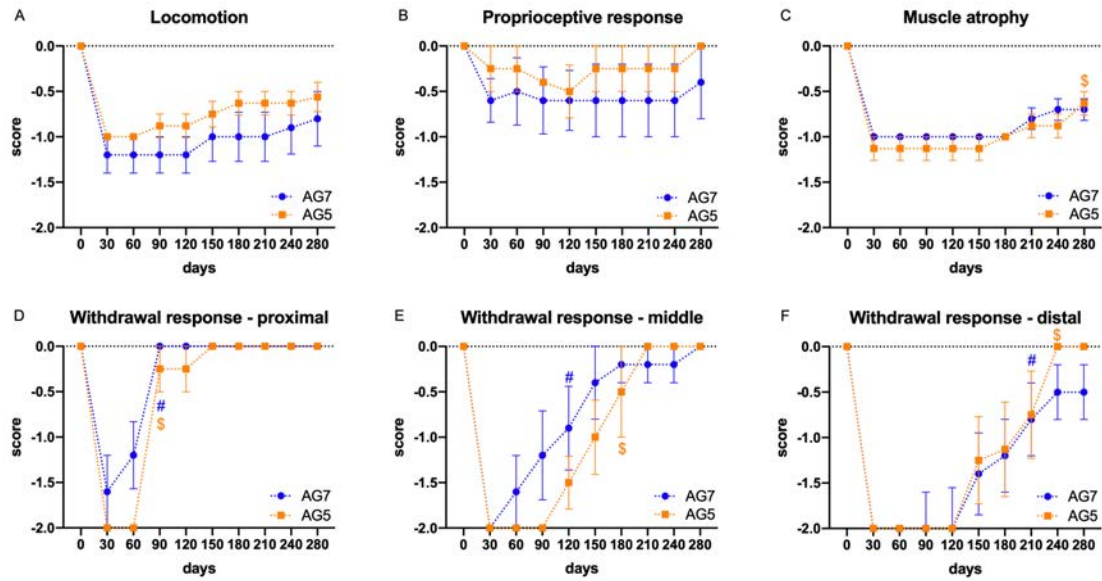


Figure 6. Plots of the monthly functional tests during the follow-up (9 months) in the AG5 and AG7 groups. Results are expressed as mean \pm SEM. (A): Locomotion, scored based on the occurrence of foot drop during fast walking, was reduced and did not have significant recovery. (B): The proprioceptive response was slightly impaired and did not show noticeable changes. (C): The mass of the TA muscle was reduced postinjury and significantly recovered ($\$p < 0.01$) vs. baseline at 30 days postoperation, at the end of the follow-up in AG5 group. (D–F): The withdrawal response to pinching the skin of the dorsum of the foot recovered to close to normal levels in AG5 group. D: The responses recovered significantly in AG5 and AG7 groups at 90 days postoperation ($\$p < 0.0001$ and $\#p < 0.0001$ vs. baseline at 30 days postoperation, respectively) in the proximal site. E: In the middle site, recovery was observed at 120 days postoperation in the AG7 group ($\#p < 0.05$) and at 180 days postoperation in the AG5 group ($\$p < 0.01$), compared to baseline at 30 days postoperation. In both cases, the responses were earlier than in the distal site, likely due to collateral reinnervation. F: Pinching the distal site showed a response compatible with peroneal reinnervation, with significant improvement at 210 days postoperation in AG7 group ($\#p < 0.05$) and at 240 days postoperation in AG5 group ($\$p < 0.001$) vs. baseline at 30 days post surgery.

3.3. Electrophysiological Results

Motor nerve conduction tests were performed at 6.5 and 9 months after the surgery under general anesthesia (diazepam 0.25 mg/kg and ketamine 5 mg/kg i.v.), to assess reinnervation of TA muscle with an electromyography (EMG) apparatus (Sapphire 4ME, Vickers Healthcare Co., Surrey, UK). In the left control hindlimb, the TA compound muscle action potential (CMAP), evoked by stimulation of the sciatic nerve at the sciatic notch, appeared at an average of 4.3 ± 0.1 ms of latency and had a mean amplitude of 21.2 ± 0.7 mV considering the nine sheep of the study (Figure 7). In the right, operated hindlimb, at 6.5 mps, 75% of the animals from AG5 group and 60% of the animals from AG7 showed consistent evidence of reinnervation with CMAPs at long latency, with disperse shape and small amplitude (1.53 ± 0.67 mV in group AG5 and 0.97 ± 0.48 mV in group AG7). At 9 mps, all the sheep of group AG5 but only 80% of group AG7 group had a positive CMAP. The mean CMAP amplitude of group AG7 (1.87 ± 0.72 mV) was significantly lower than in group AG5 (5.00 ± 2.13 mV) (Figure 7A), and the onset latency was significantly longer in AG7 group (11.58 ± 1.06 ms) compared to AG5 group (9.46 ± 0.6 ms) (Figure 7B).

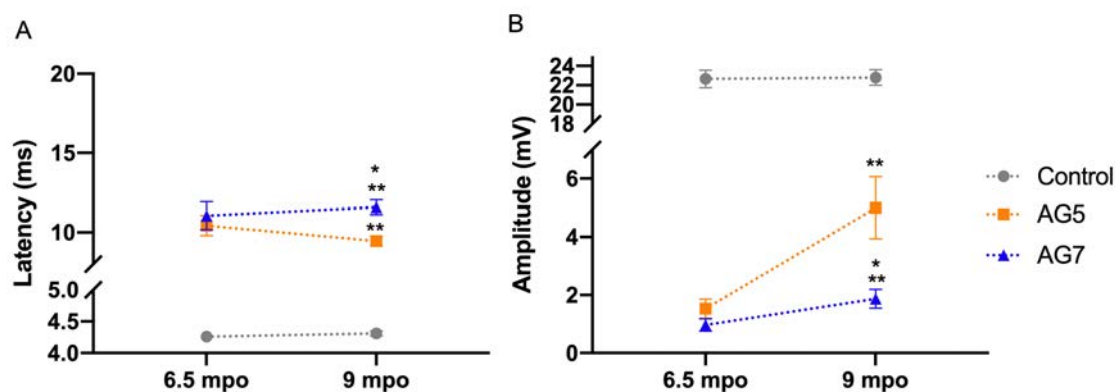


Figure 7. Plots of the latency (A) and the amplitude (B) of the TA CMAP evoked by stimulation of the sciatic nerve at the sciatic notch and recorded at 6.5 and 9 months after surgical insertion of autografts of 5 and 7 cm length, AG5 and AG7, respectively, and compared with the measurements made in the control contralateral hindlimb. A. Small and long latency CMAPs were recorded in 3 of the sheep of each experimental group at 6.5 mps. B. The CMAP amplitudes

increased at 9 mps, although they were much lower than in control muscles. Values are represented as mean \pm SEM. * $p < 0.05$ AG7 vs. group AG5; ** $p < 0.0001$ AG5 and AG7 groups vs. Control.

3.4. Echographic Evaluation of TA Muscle

Echography of TA muscle was performed following the electrophysiological tests, at 6.5 and 9 mps, under general anesthesia. In the operated hindlimb, the size of the TA muscle was significantly decreased, and the echo density changed due to muscle atrophy secondary to denervation. At 9 mps, the muscle size, the perimeter (Figure 8A), and the area (Figure 8B) were still below control values, although the muscle area was significantly lower ($p < 0.5$) in the group AG7 ($2.44 \pm 0.21 \text{ cm}^2$) compared to the group AG5 ($3.43 \pm 0.23 \text{ cm}^2$) (Figure 3B). The TA muscle size of the sheep without EMG recovery was the smallest, linking muscle size to degree of reinnervation. The TA muscle was weighed fresh after extraction. The mean values in the experimental sheep of AG5 and AG7 were $38.5 \pm 1.4 \text{ g}$ and $33.0 \pm 4.5 \text{ g}$, and were significantly lower ($p < 0.05$) than $78.8 \pm 4.8 \text{ g}$ for the left control muscles.

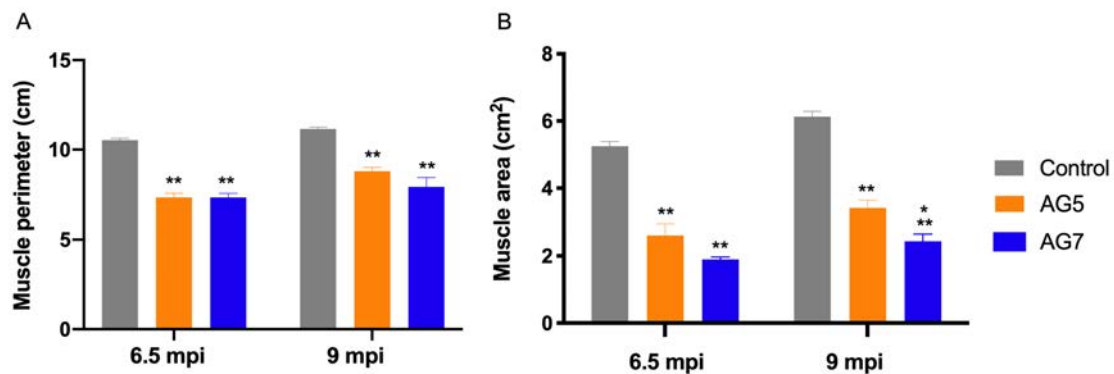


Figure 8. Histogram of the measurements of perimeter (A) and area (B) of the TA muscle obtained by echographical imaging. Values are mean \pm SEM. * $p < 0.05$ group AG7 vs. AG5; ** $p < 0.0001$ groups AG7 and AG5 vs. Control.

3.5. Histological Results of the Grafted Nerve

After harvesting, the nerve autografts of all the sheep showed neuromata that were visible at both proximal and distal suture lines, but the autograft had a well-preserved appearance. The sheep peroneal nerve is composed of multiple fascicles, usually more than 30, each containing numerous nerve fibers densely packed in the endoneurium. The fascicular structure was maintained in the autografted segment in both experimental groups. Regenerative axons were seen both inside and outside the nerve fascicles (Figure 9).

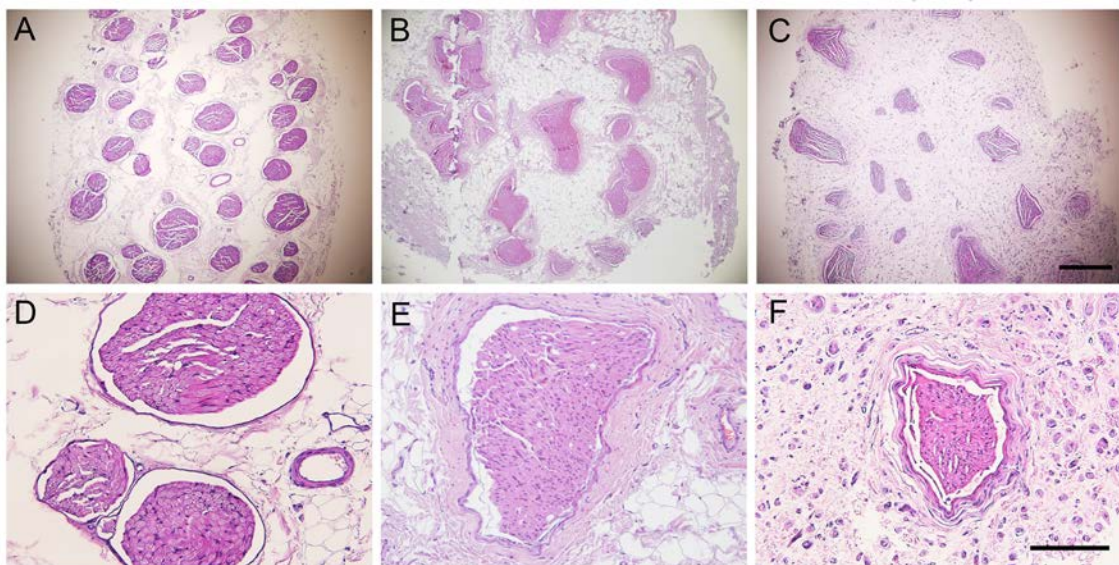


Figure 9. Representative micrographs of cross-sections of the middle part of the nerve graft stained with hematoxylin and eosin. (A,D) control nerve, (B,E) nerve of a sheep of group AG5, and (C,F) of group AG7, viewed at 40 \times magnification (A–C), scale bar 500 μ m, and at \times 200 magnification (D–F), scale bar 150 μ m.

Immunohistochemical labeling for NF200 and S100 in sections taken at the middle of the nerve grafts showed the presence of myelinated axons and Schwann cells in the intrafascicular and extrafascicular space of the autografts. In contrast, distal to the nerve autograft, myelinated axons and Schwann cells were only observed within the fascicles (Figure 10). In semithin transverse sections of the mid segment of the nerve autograft of both experimental groups, we found that myelinated axons were grouped in small regenerative units and

CHAPTER I

were distributed throughout the autograft structure, as well as unmyelinated axons and Schwann cells (Figure 10M–O).

Regarding the quantitative analysis of NF200 positive myelinated axons, one animal of group AG7 did not show regenerated axons, likely attributable to suture dehiscence in early phases after the surgery. The estimated mean number of myelinated axons in the control peroneal nerve was $18,022 \pm 2040$ axons. At the mid-level of the autograft, there was a significantly higher number of myelinated axons in the AG5 group compared to group AG7 ($57,294 \pm 1368$ axons and $26,213 \pm 2798$ axons, respectively, $***p < 0.001$). Distal to the nerve graft, there were also significantly more axons in group AG5 ($36,185 \pm 3533$ axons) compared to group AG7 ($20,600 \pm 6082$ axons) ($***p < 0.001$).

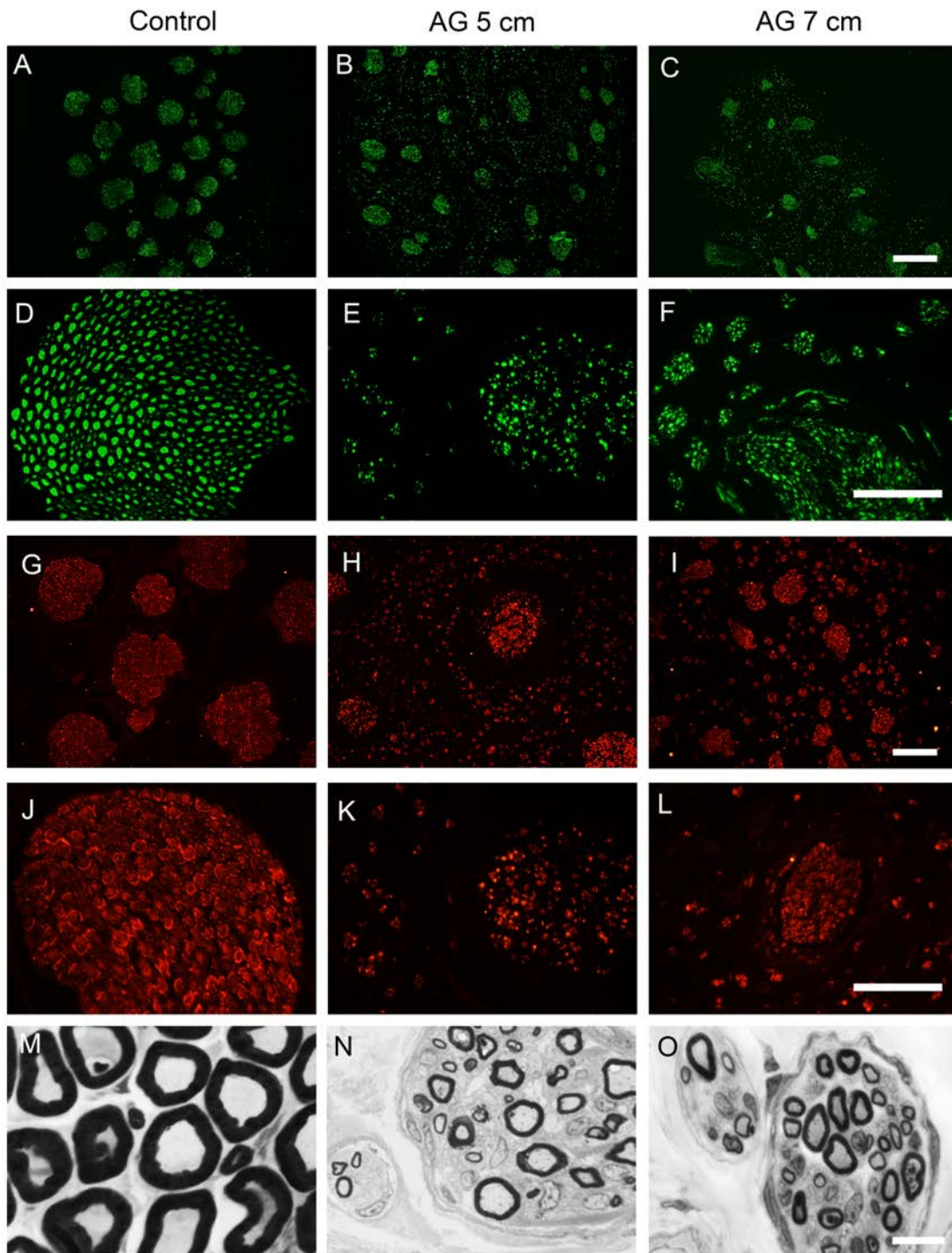


Figure 10. Representative immunohistochemical images of transverse sections of a control peroneal nerve (A,D,G,J) and of an autograft of group AG5 (B,E,H,K) and of group AG7 (C,F,I,L). Sections were immunolabeled against NF200 for myelinated axons (A–F), and against S100 for Schwann cells (G–L). Images were taken at $\times 40$ magnification (A–C,G–I), scale bar 200 μm , and at $\times 400$ magnification (D–F,J–L), scale bar 100 μm . The bottom panels show

representative semithin transverse sections of the middle segment of the nerve graft stained with toluidine blue. (M) control nerve, (N) AG5, and (O) AG7 graft, at 10,000 \times magnification, scale bar 10 μ m.

3.6. Histological Evaluation of Reinnervated Targets

The intact TA muscle showed an organized structure of elongated muscle fibers with the nuclei at the periphery. In cross-sections, histological images showed compact muscle fibers, polygonal in shape and surrounded by basal lamina (Figure 11A, D). In the operated hindlimb, the TA muscle showed an irregular structure in both experimental groups. Some areas appeared with a normal structure, although the muscle fibers had smaller diameter than normal, likely corresponding to reinnervated areas of the muscle, whereas other areas showed signs of atrophy and inflammatory cell infiltration (Figure 11B-C, E-F).

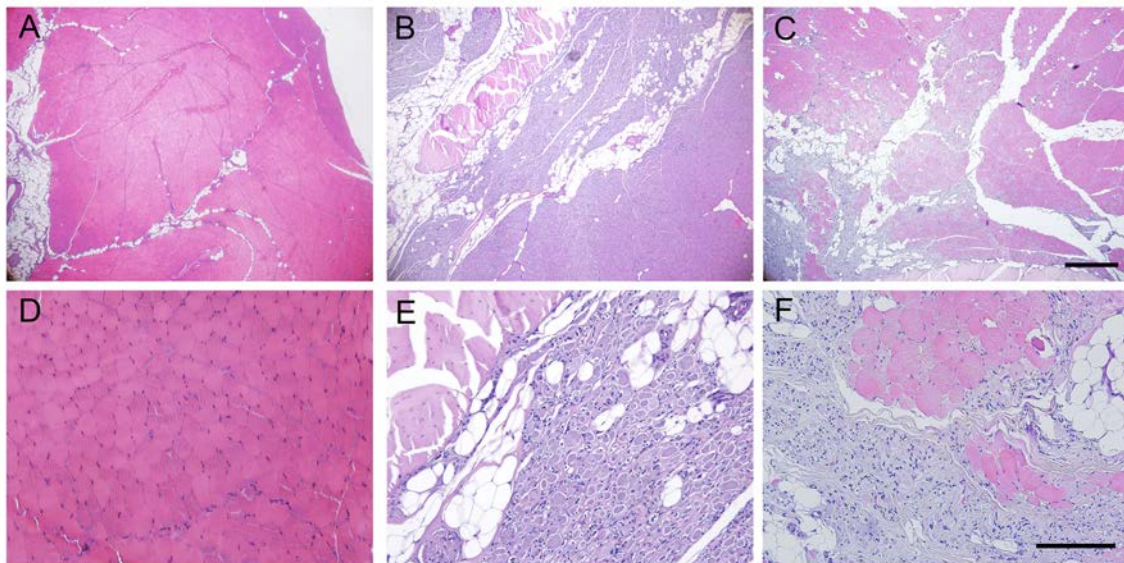


Figure 11. Representative micrographs of cross-sections of the TA muscle stained with hematoxylin and eosin from (A,D) a control muscle, (B,E) a sheep of group AG5, (C,F) a sheep of group AG7, taken at $\times 40$ magnification (A–C), scale bar 200 μ m, and at $\times 200$ magnification (E–F), scale bar 100 μ m. Note the areas of hypotrophic muscle fibers with inflammatory cell infiltration in the denervated muscle areas of AG sheep.

The skin samples of control hindlimb, in sagittal sections, showed distinct organization in three layers: epidermis, dermis, and subcutaneous tissue. The skin samples of the operated hindlimb showed a similar aspect to the skin from the contralateral side, without signs of inflammatory cell infiltration or tissue atrophy.

4. Discussion

In this study, we have shown that nerve regeneration is successful after autograft repair of a large defect in the peripheral nerve of sheep and can be objectively evaluated. Thus, we propose that the sheep is a suitable model to evaluate regeneration through long nerve gaps. Sheep represent an adequate large animal model because they have similar body weight and peripheral nerve dimensions to humans. Unlike rodent species, sheep have plurifasciculated nerves [32] and a regeneration rate identical to humans [33,34]. Compared to other large animals used, including pigs, sheep are calm, easy to obtain, and cost-effective, and they allow the evaluation of sensory and motor functions with the same methods used in the clinic. In addition, their life expectancy is sufficiently long to allow long-term studies to compare with studies of recovery after human peripheral nerve injuries, requiring at least 2 years for recovery to plateau values [35–37]. Other useful models in preclinical studies, like conventional pigs, would be unusable for long-term studies due to their high growth rate, in addition to their stressful and nervous behavior. Other large species, which include nonhuman primates and dogs, present more ethical concerns.

For nerve injury in an animal model to be a useful model with translational potential, the injured nerve must be also relevant. In humans, the most frequently injured nerve in the lower limb is the common peroneal nerve [25,38]. In sheep, this nerve is similar in size to the human nerve [34,37] and it is also plurifascicular, giving rise to the deep peroneal nerve branch that innervates muscles in the anterior compartment of the hindleg, and to the superficial peroneal nerve providing sensory innervation to the dorsum of the paw. Surgical access to the

peroneal nerve is an easy procedure with blunt dissection of the semitendinosus and biceps femoris muscles. Since the common peroneal nerve is a mixed nerve, both motor and sensory functional losses in the denervated targets are expected [39]. The injury of this nerve in sheep mimics the symptoms of the inversion of the foot and inability to dorsiflex the ankle [25,40]. However, the motor deficits are limited, and do not markedly disturb standing and walking of the animals [32,37]. We observed that the sheep did not show disabling consequences of the nerve surgeries in their locomotor motion or a reduced quality of life. This was so despite two animals showing a sustained foot drop position that, together with the lack of sensitivity in the dorsum of the foot, led to focal pressure ulcerations.

Other studies producing a transection and relatively long gaps in the sheep used the median nerve in the forelimb, with gaps ranging from 5 mm to 5 cm [22,24,30,34,41,42], or the facial nerve inducing just transection or gaps up to 5 cm [27,43]. However, injuries of the forelimb nerves lead to more functional deficits, since compensation for animal weight support and movement is more effective in the hindlimbs [37]. The sciatic and the tibial nerves have also been subjected to gap lesions and repair with different conduits bridging a 1 cm gap [44–46], and with recellularized allografts in a 2 cm gap [47] in comparison with autologous nerve grafts. The sheep peroneal nerve has been used in a few studies prior to the present study. Strasberg and colleagues [32] compared the outcomes of the surgical repair of the peroneal nerve via insertions of 8 cm long nerve autografts and allografts. Histological and electrophysiologic analyses were carried out at 6 and 10 months. Roballo et al. [37] compared electrophysiological and histological outcomes after peroneal nerve transection and a 5 cm autograft in adult sheep. Alvites et al. [25] compared only functional outcomes 3 and 6 months after peroneal transection and repair by direct suture or via a chitosan conduit leaving a ~24 mm gap. In the study by Tamez-Mata et al. [48], a peroneal nerve segment of 30 mm in length was excised, and repair was performed by an autograft or an allograft recellularized with Schwann-like cells. Altogether, the peroneal nerve in sheep is a good model for preclinical trials in which several-centimeter-long gaps can be repaired with newly developed grafts or synthetic conduits in comparison with the standard autologous graft.

Importantly, the long distance that axons must grow in the sheep hindlimb requires a considerably long follow-up for assessment of reinnervation of distal targets and meaningful functional recovery. We measured the distance between the proximal section of the peroneal nerve and the entrance of the distal nerve into the TA muscle, and it was between 34–36 cm. Considering a rate of regeneration of 1–2 mm/day, similar to humans, 6 to 12 months would be needed for regaining muscle innervation, and even longer for reinnervation of the dorsum of the hindfoot. Our evidence of TA muscle reinnervation by nerve conduction tests at 6.5 months suggests a regeneration rate \sim 2 mm/day, in line with previous results reported by Strasberg et al. [32], Radtke et al. [45], and Roballo et al. [37], who performed similar electrophysiological tests. Indeed, an average axonal regeneration velocity of 1.57 mm/day was estimated in sheep that received an autologous nerve graft in the tibial nerve [46]. It is worth noting that the time courses of functional recovery for surgical repair of both 5 and 7 cm lengths of the autografts used to repair the transected peroneal nerve were parallel, even though the functional recoveries were less when 7 cm long autografts rather than 5 cm long grafts were inserted. These observations indicate that the length of the autograft plays a role.

We used clinical evaluations for assessing functional recovery of sensory-motor functions after autograft repair in sheep that are used regularly in human patients. These quantifiable functional behavioral measures provided important indicators of recovery that were complemented by electrophysiological measures. We established monthly intervals for a functional evaluation to assess the deficits produced by the peroneal nerve injury and the recovery course. Peroneal nerve injury, as in humans, results in inability to dorsiflex the ankle [25,40]. In the standing position, most sheep were able to correctly place the hoof and make plantar contact with the ground; however, two of the sheep were unable to do so and showed persistent contact with the dorsum of the foot that led to skin lesions. Whilst we do not know why some sheep presented more marked motor deficits, mechanical factors may be involved. Alvites et al. [25] reported overextension of the hock and overflexion of the distal joints in their sheep, with only slight improvement from 10–12 weeks after neurotmesis and direct suture repair.

Testing foot placement during open locomotion in the barn allowed us to detect foot drop in the operated paw in all the sheep. The incidence of foot drop partially improved in two sheep of each group from 5 mps onwards, but the mean score of the groups did not change significantly during follow-up. That the proprioceptive response in the animal's hoof was only diminished slightly after the injury may be accounted for by the proprioception conveyed by the tibial and sural nerves that remained intact. Evaluating the time to response using a similar maneuver, Alvites et al. [25] found a small reduction in time but already at 6–8 weeks after direct suture. Therefore, measurement of the proprioceptive response has limited use in this model. A fast recovery of the withdrawal reflex induced by painful stimulation in the peroneal cutaneous territory, was observed at early times in proximal and mid sites of the dorsum of the foot, as reported also by Alvites et al. [25]. This may be explained by reinnervation of the foot by collateral sprouting of neighbor intact nerves that branch from tibial and sural nerves. For this test, the distal third appears to be the one sensitive to peroneal nerve regeneration (see Figure 6F).

Electrophysiological tests are commonly used to objectively evaluate nerve regeneration and muscle reinnervation after nerve injuries in humans and in animals [49,50]. In contrast to small animal models, large animal models allow for easier access to stimulation and recording sites, limiting electrical artifacts [51]. Some animals from both experimental groups showed recordable CMAPs at 6.5 mps, indicating that regenerating axons had crossed the nerve autograft and into the denervated distal nerve stump to reinnervate the TA muscle. At 9 months, all sheep but one showed positive CMAPs with increasing amplitude and decreasing latency, indicating regeneration and myelination of motor axons. Based on our electrophysiological findings, 9 months appeared to be the minimum timepoint to reliably evaluate different therapies after long nerve gap neurotmesis in the sheep, in agreement with other studies [32,37,45], and the amplitude of the CMAP is the most valuable parameter [50]. Complementing electrophysiology, we used high-resolution echography to evaluate the degree of atrophy of the TA muscle as an indirect measure of reinnervation. This is the first

time that ultrasound has been used to quantitatively assess muscle mass after nerve injury in experimental studies.

When the nerve samples were harvested, a small amount of fibrosis was observed around the suture lines in both experimental groups, whereas the diameter of the autografts and the host nerve stumps were similar, contrary to observations when the autograft was from a smaller nerve [51]. In both experimental groups, the peroneal nerve fascicles were preserved but they were slightly smaller than in the control nerve. Myelinated axons and Schwann cells were seen within but also some outside of the fascicles, as commonly reported after neurotmesis [24]. This can be explained by the difficulty of surgically aligning the two ends of the autograft and the proximal and distal stumps of the host nerve. As a result, regenerating axons are likely to be misdirected into pathways that they were not in previously, that in turn, likely result in poor recovery [52,53]. In both experimental groups, myelinated axons of smaller size than normal were seen both within the nerve graft and distal to the graft. The higher number of axons counted compared to the control nerve can be explained by the well-known phenomenon of multiple regenerative sprouts emitted by each axon [54] that, despite a tendency to reduce with time, persist even months after injury in the distal stump [55].

In conclusion, sheep provide an excellent opportunity to study peripheral nerve regeneration in long-nerve gap injuries allowing assays of new repair strategies for the translation towards clinical treatments of nerve injuries. This large animal model addresses key factors for assessing regeneration and can be adequately evaluated by functional tests in addition to electrophysiological and ultrasound tests, as shown in this study.

References

1. Navarro, X.; Vivó, M.; Valero-Cabré, A. Neural Plasticity after Peripheral Nerve Injury and Regeneration. *Prog. Neurobiol.* 2007, 82, 163–201.
2. Allodi, I.; Udina, E.; Navarro, X. Specificity of Peripheral Nerve Regeneration: Interactions at the Axon Level. *Prog. Neurobiol.* 2012, 98, 16–37.
3. Fu, S.Y.; Gordon, T. The cellular and molecular basis of peripheral nerve regeneration. *Mol Neurobiol.* 1997, 14, 67–116.
4. Fawcett, J.W.; Keynes, R.J. Peripheral nerve regeneration. *Annu Rev Neurosci.* 1990, 13, 43–60.
5. Arthur-Farraj, P.; Coleman, M.P. Lessons from Injury: How Nerve Injury Studies Reveal Basic Biological Mechanisms and Therapeutic Opportunities for Peripheral Nerve Diseases. *Neurotherapeutics* 2021, 18, 2200–2221.
6. Kline, D.G.; Hudson, A.R. Nerve Injuries. In *Operative Results for Major Nerve Injuries, Entrapments, and Tumors*, 2nd ed.; Saunders: Philadelphia, PA, USA, 1995.
7. Lundborg, G. A 25-Year Perspective of Peripheral Nerve Surgery: Evolving Neuroscientific Concepts and Clinical Significance. *J. Hand Surg. Am.* 2000, 25, 391–414. <https://doi.org/10.1053/jhsu.2000.4165>.
8. Ray, W.Z.; Mackinnon, S.E. Management of Nerve Gaps: Autografts, Allografts, Nerve Transfers, and End-to-Side Neuroorrhaphy. *Exp. Neurol.* 2010, 223, 77–85.
9. Kornfeld, T.; Vogt, P.M.; Radtke, C. Nerve Grafting for Peripheral Nerve Injuries with Extended Defect Sizes. *Wien Med. Wochenschr.* 2019, 169, 240–251. <https://doi.org/10.1007/s10354-018-0675-6>.
10. Lundborg, G.; Dahlin, L.B.; Danielsen, N.; Gelberman, R.H.; Longo, F.M.; Powell, H.C.; Varon, S. Nerve Regeneration in Silicone Chambers: Influence of Gap Length and of Distal Stump Components. *Exp. Neurol.* 1982, 76, 361–375.

11. Butí, M.; Verdú, E.; Labrador, R.O.; Vilches, J.J.; Forés, J.; Navarro, X. Influence of Physical Parameters of Nerve Chambers on Peripheral Nerve Regeneration and Reinnervation. *Exp. Neurol.* 1996, 137, 26–33.
12. Mackinnon, S.E.; Dellon, A.L. A study of nerve regeneration across synthetic (Maxon) and biologic (collagen) nerve conduits for nerve gaps up to 5 cm in the primate. *J. Reconstr. Microsurg.* 1990, 6, 117–121.
13. Archibald, S.J.; Shefner, J.; Krarup, C.; Madison, R.D. Monkey Median Nerve Repaired by Nerve Graft or Collagen Nerve Guide Tube. *J. Neurosci.* 1995, 15, 4109–4123.
14. Kaplan, H.M.; Mishra, P.; Kohn, J. The Overwhelming Use of Rat Models in Nerve Regeneration Research May Compromise Designs of Nerve Guidance Conduits for Humans. *J. Mater. Sci. Mater. Med.* 2015, 26, 226.
15. Tos, P.; Ronchi, G.; Papalia, I.; Sallen, V.; Legagneux, J.; Geuna, S.; Giacobini-Robecchi, M.G. Chapter 4 Methods and Protocols in Peripheral Nerve Regeneration Experimental Research: Part I-Experimental Models. *Int. Rev. Neurobiol.* 2009, 87, 47–79.
16. Siemionow, M.; Brzezicki, G. Chapter 8 Current Techniques and Concepts in Peripheral Nerve Repair. *Int. Rev. Neurobiol.* 2009, 87, 141–172.
17. Angius, D.; Wang, H.; Spinner, R.J.; Gutierrez-Cotto, Y.; Yaszemski, M.J.; Windebank, A.J. A systematic review of animal models used to study nerve regeneration in tissue-engineered scaffolds. *Biomaterials* 2012, 33, 8034–8039.
18. Geuna, S. The Sciatic Nerve Injury Model in Pre-Clinical Research. *J. Neurosci. Methods* 2015, 243, 39–46.
19. Gordon, T.; Borschel, G.H. The Use of the Rat as a Model for Studying Peripheral Nerve Regeneration and Sprouting after Complete and Partial Nerve Injuries. *Exp. Neurol.* 2017, 287, 331–347.
20. Diogo, C.C.; Camassa, J.A.; Pereira, J.E.; da Costa, L.M.; Filipe, V.; Couto, P.A.; Geuna, S.; Maurício, A.C.; Varejão, A.S. The Use of Sheep as a Model for Studying

CHAPTER I

Peripheral Nerve Regeneration Following Nerve Injury: Review of the Literature. *Neurol. Res.* 2017, 39, 926–939.

21. Glasby, M.A.; Gilmour, J.A.; Gschmeissner, S.E.; Hems, T.E.; Myles, L.M. The Repair of Large Peripheral Nerves Using Skeletal Muscle Autografts: A Comparison with Cable Grafts in the Sheep Femoral Nerve. *Br. J. Plast. Surg.* 1990, 43, 169–178.

22. Kettle, S.J.A.; Starritt, N.E.; Glasby, M.A.; Hems, T.E.J. End-to-Side Nerve Repair in a Large Animal Model: How Does It Compare with Conventional Methods of Nerve Repair? *J. Hand Surg. Eur. Vol.* 2013, 38, 192–202.

23. Atchabahian, A.; Genden, E.M.; Mackinnon, S.E.; Doolabh, V.B.; Hunter, D.A. Regeneration through long nerve grafts in the swine model. *Microsurgery* 1998, 18, 379–382.

24. Forden, J.; Xu, Q.G.; Khu, K.J.; Midha, R. A Long Peripheral Nerve Autograft Model in the Sheep Forelimb. *Neurosurgery* 2011, 68, 1354–1362. <https://doi.org/10.1227/NEU.0b013e31820c08de>.

25. Alvites, R.D.; Branquinho, M.V.; Sousa, A.C.; Zen, F.; Maurina, M.; Raimondo, S.; Mendonça, C.; Atayde, L.; Geuna, S.; Varejão, A.S.P.; et al. Establishment of a Sheep Model for Hind Limb Peripheral Nerve Injury: Common Peroneal Nerve. *Int. J. Mol. Sci.* 2021, 22, 1401. <https://doi.org/10.3390/ijms22031401>.

26. Al Abri, R.; Kolethekkat, A.A.; Kelleher, M.O.; Myles, L.M.; Glasby, M.A. Effect of Locally Administered Ciliary Neurotrophic Factor on the Survival of Transected and Repaired Adult Sheep Facial Nerve. *Oman Med. J.* 2014, 29, 208–213.

27. Glasby, M.A.; Mountain, R.E.; Murray, J.A.M. Repair of the Facial Nerve Using Freeze-Thawed Muscle Autografts A Surgical Model in the Sheep. *Arch. Otolaryngol. Head Neck Surg.* 1993, 119, 461–465.

28. Hems, T.E.J.; Glasby, M.A. Repair of cervical nerve roots proximal to the root ganglia an experimental study in sheep. *J. Bone Jt. Surg. Br.* 1992, 74, 918–922.

29. Turner, A.S. Experiences with Sheep as an Animal Model for Shoulder Surgery: Strengths and Shortcomings. *J. Shoulder Elb. Surg.* 2007, 16, S158–S163.

30. Ozturk, C.; Uygur, S.; Lukaszuk, M. Sheep as a Large Animal Model for Nerve Regeneration Studies. In *Plastic and Reconstructive Surgery: Experimental Models and Research Designs*; Springer-Verlag Ltd.: London, UK, 2015; pp. 507–511, ISBN 9781447163350.
31. Costa, D.; Diogo, C.C.; da Costa, L.M.; Pereira, J.E.; Filipe, V.; Couto, P.A.; Geuna, S.; Armada-Da-Silva, P.A.; Maurício, A.C.; Varejão, A.S.P. Kinematic Patterns for Hindlimb Obstacle Avoidance during Sheep Locomotion. *Neurol. Res.* 2018, 40, 963–971. <https://doi.org/10.1080/01616412.2018.1505068>.
32. Strasberg, S.R.; Mackinnon, S.E.; Genden, E.M.; Bain, J.R.; Purcell, C.M.; Hunter, D.A.; Hay, J.B. Long-segment nerve allograft regeneration in the sheep model experimental study and review of the literature. *J. Reconstr. Microsurg.* 1996, 12, 529–537.
33. Lawson, G.M.; Glasby, M.A. A comparison of immediate and delayed nerve repair using autologous freeze-thawed muscle grafts in a large animal model. The simple injury. *J. Hand Surg. Br.* 1995, 20, 663–700.
34. Jeans, L.A.; Gilchrist, T.; Healy, D. Peripheral Nerve Repair by Means of a Flexible Biodegradable Glass Fibre Wrap: A Comparison with Microsurgical Epineurial Repair. *J. Plast. Reconstr. Aesthet. Surg.* 2007, 60, 1302–1308.
35. Kim, D.H.; Kline, D.G. Management and results of peroneal nerve lesions. *Neurosurgery* 1996, 39, 319–320.
36. Nath, R.K.; Lyons, A.B.; Paizi, M. Successful Management of Foot Drop by Nerve Transfers to the Deep Peroneal Nerve. *J. Reconstr. Microsurg.* 2008, 24, 419–427.
37. Roballo, K.C.S.; Burns, D.T.; Ghnenis, A.B.; Osimanjiang, W.; Bushman, J.S. Long-Term Neural Regeneration Following Injury to the Peroneal Branch of the Sciatic Nerve in Sheep. *Eur. J. Neurosci.* 2020, 52, 4385–4394. <https://doi.org/10.1111/ejn.14835>.
38. Lezak, B.; Massel, D.H.; Varacallo, M. Peroneal Nerve Injury. In *StatPearls* [Internet]; StatPearls Publishing: Treasure Island, FL, USA, 2022. Available online: <https://www.ncbi.nlm.nih.gov/books/NBK549859/> (accessed on 4 September 2022).

CHAPTER I

39. Marciniak, C. Fibular (Peroneal) Neuropathy. Electrodiagnostic Features and Clinical Correlates. *Phys. Med. Rehabil. Clin. N. Am.* 2013, 24, 121–137.

40. Baima, J.; Krivickas, L. Evaluation and Treatment of Peroneal Neuropathy. *Curr. Rev. Musculoskelet. Med.* 2008, 1, 147–153.

41. Matsuyama, T.; Midha, R.; Mackinnon, S.E.; Munro, C.A.; Wong, P.-Y.; Ang, L.C. Long nerve allografts in sheep with cyclosporin a immunosuppression. *J. Reconstr. Microsurg.* 2000, 16, 219–225.

42. Siemionow, M.; Cwykiel, J.; Uygur, S.; Kwiecien, G.; Oztürk, C.; Szopinski, J.; Madajka, M. Application of Epineural Sheath Conduit for Restoration of 6-Cm Long Nerve Defects in a Sheep Median Nerve Model. *Microsurgery* 2019, 39, 332–339.

43. Gilchrist, T.; Glasby, M.A.; Healy, D.M.; Kelly, G.; van Lenihan, D.; Mcdowall, K.L.; Millert, I.A.; Myles, L.M. In Vitro Nerve Repair-in Vivo. The Reconstruction of Peripheral Nerves by Entubulation with Biodegradable Glass Tubes-a Preliminary Report. *Br. J. Plast. Surg.* 1998, 51, 231–237.

44. Casañas, J.; de la Torre, J.; Soler, F.; García, F.; Rodellar, C.; Pumarola, M.; Climent, J.; Soler, R.; Orozco, L. Peripheral nerve regeneration after experimental section in ovine radial and tibial nerves using synthetic nerve grafts, including expanded bone marrow mesenchymal cells: Morphological and neurophysiological results. *Injury* 2014, 45 (Suppl. 4), S2–S6.

45. Radtke, C.; Allmeling, C.; Waldmann, K.H.; Reimers, K.; Thies, K.; Schenk, H.C.; Hillmer, A.; Guggenheim, M.; Brandes, G.; Vogt, P.M. Spider Silk Constructs Enhance Axonal Regeneration and Remyelination in Long Nerve Defects in Sheep. *PLoS ONE* 2011, 25, e16990. <https://doi.org/10.1371/journal.pone.0016990>.

46. Kornfeld, T.; Borger, A.; Radtke, C. Reconstruction of Critical Nerve Defects Using Allogenic Nerve Tissue: A Review of Current Approaches. *Int. J. Mol. Sci.* 2021, 22, 3515.

47. Pedroza-Montoya, F.E.; Tamez-Mata, Y.A.; Simental-Mendía, M.; Soto-Domínguez, A.; García-Pérez, M.M.; Said-Fernández, S.; Montes-de-Oca-Luna, R.; González-Flores, J.R.; Martínez-Rodríguez, H.G.; Vilchez-Cavazos, F. Repair of Ovine Peripheral Nerve Injuries with Xenogeneic Human Acellular Sciatic Nerves Prerecellularized with

Allogeneic Schwann-like Cells—An Innovative and Promising Approach. *Regen. Ther.* 2022, 19, 131–143. <https://doi.org/10.1016/j.reth.2022.01.009>.

48. Tamez-Mata, Y.; Pedroza-Montoya, F.E.; Martínez-Rodríguez, H.G.; García-Pérez, M.M.; Ríos-Cantú, A.A.; González-Flores, J.R.; Soto-Domínguez, A.; Montes-de-Oca-Luna, R.; Simental-Mendía, M.; Peña-Martínez, V.M.; et al. Nerve Gaps Repaired with Acellular Nerve Allografts Recellularized with Schwann-like Cells: Preclinical Trial. *J. Plast. Reconstr. Aesthet. Surg.* 2022, 75, 296–306. <https://doi.org/10.1016/j.bjps.2021.05.066>.

49. Parry, G.J. Electrodiagnostic Studies in the Evaluation of Peripheral Nerve and Brachial Plexus Injuries. *Neurol. Clin.* 1992, 10, 921–934.

50. Navarro, X. Functional Evaluation of Peripheral Nerve Regeneration and Target Reinnervation in Animal Models: A Critical Overview. *Eur. J. Neurosci.* 2016, 43, 271–286.

51. Burrell, J.C.; Browne, K.D.; Dutton, J.L.; Laimo, F.A.; Das, S.; Brown, D.P.; Roberts, S.; Petrov, D.; Ali, Z.; Ledebur, H.C.; et al. A Porcine Model of Peripheral Nerve Injury Enabling Ultra-Long Regenerative Distances: Surgical Approach, Recovery Kinetics, and Clinical Relevance. *Neurosurgery* 2020, 87, 833–846. <https://doi.org/10.1093/neuros/nyaa106>.

52. Valero-Cabré, A.; Navarro, X. Functional Impact of Axonal Misdirection after Peripheral Nerve Injuries Followed by Graft or Tube Repair. *J. Neurotrauma* 2002, 19, 1475–1485.

53. de Ruitter, G.C.W.; Malessy, M.J.A.; Alaid, A.O.; Spinner, R.J.; Engelstad, J.N.K.; Sorenson, E.J.; Kaufman, K.R.; Dyck, P.J.; Windebank, A.J. Misdirection of Regenerating Motor Axons after Nerve Injury and Repair in the Rat Sciatic Nerve Model. *Exp. Neurol.* 2008, 211, 339–350. <https://doi.org/10.1016/j.expneurol.2007.12.023>.

54. Witzel, C.; Rohde, C.; Brushart, T.M. Pathway Sampling by Regenerating Peripheral Axons. *J. Comp. Neurol.* 2005, 485, 183–190. <https://doi.org/10.1002/cne.20436>.

55. Mackinnon, S.E.; Dellon, A.L.; O'Brien, J.P. Changes in nerve fiber numbers distal to a nerve repair in the rat sciatic nerve model. *Muscle Nerve* 1991, 14, 1116–1122.

Chapter II

Evaluation of a decellularized nerve graft optimized by the BST to repair severe peripheral nerve injuries in rats and in sheep

- A novel decellularized nerve graft for repairing peripheral nerve long gap injury in the rat
- Decellularized graft for repairing severe peripheral nerve injuries in sheep

A novel decellularized nerve graft for repairing peripheral nerve long gap injury in the rat

Estefanía Contreras¹, Sara Bolívar¹, Núria Nieto-Nicolau^{2,3}, Oscar Fariñas^{2,3},
Patrícia López-Chicón^{2,3}, Xavier Navarro¹, Esther Udina¹

¹ Department of Cell Biology, Physiology and Immunology, Institute of Neuroscience, Universitat Autònoma de Barcelona, and CIBERNED, ISCIII, 08913 Bellaterra, Spain

² Barcelona Tissue Bank, Banc de Sang I Teixits (BST), Barcelona, Spain

³ Biomedical Research Institute (IIB-Sant Pau; SGR1113), Barcelona, Spain

Cell and Tissue Research **2022**, 390:355-366

Abstract

Decellularized nerve allografts are an alternative to autograft for repairing severe nerve injuries, since they have higher availability and do not induce rejection. In this study, we have assessed the regenerative potential of a novel decellularization protocol for human and rat nerves for repairing nerve resections, compared to the gold standard autograft. A 15-mm gap in the sciatic nerve was repaired with decellularized rat allograft (DC-RA), decellularized human xenograft (DC-HX), or fresh autograft (AG). Electrophysiology tests were performed monthly to evaluate muscle reinnervation, whereas histological and immunohistochemical analyses of the grafts were evaluated at 4 months. A short-term study was also performed to compare the differences between the two decellularized grafts (DC-RA and DC-HX) in early phases of regeneration. The decellularization process eliminated cellularity while preserving the ECM and endoneurial tubules of both rat and human nerves. Higher amount of reinnervation was observed in the AG group compared to the DC-RA group, while only half of the animals of the DC-HX showed distal muscle reinnervation. The density of myelinated axons was significantly higher in AG compared to both DC grafts, being this density significantly higher in DC-RA than in DC-HX. At short term, fibroblasts repopulated the DC-RA graft, supporting regenerated axons, whereas an important fibrotic reaction was observed around DC-HX grafts. In conclusion, the decellularized allograft sustained regeneration through a long gap in the rat although at a slower rate compared to the ideal autograft, whereas regeneration was limited or even failed when using a decellularized xenograft.

1. Introduction

Peripheral nerve injury results in partial or total loss of the sensory and motor functions dependent on the injured nerve(s), with important consequences for the quality of life of affected subjects (Navarro et al., 2007). It is estimated an incidence of nerve injuries of 13.9/100,000 inhabitants per year (Asplund et al., 2009) resulting in more than 300,000 such injuries in the EU per year. Although peripheral neurons have the ability to regenerate their axons and eventually reinnervate the previously denervated target organs, clinical and experimental evidence shows that regeneration is often unsatisfactory, especially following severe injuries (Pfister et al., 2011; Lovati et al., 2018).

Surgical repair is needed after nerve transections, to re-unite the two nerve stumps, with the aim to facilitate proximal axons to regenerate through the distal degenerating nerve and to finally reinnervate their target organs (Pfister et al., 2011). However, direct suture is not always possible, and long nerve gaps must be bridged. The clinical gold standard repair technic in clinics is the interposition of an autologous nerve graft between the proximal and the distal stump (Grinsell and Keating, 2014; Gaudin et al., 2016; Kornfeld et al., 2021). Although it sustains nerve regeneration across long defects, the use of an autografts has some disadvantages, such as limited availability of donor nerves, increased operating time, and morbidity at the site of extraction (e.g., pain, scars, neuroma, and sensory loss).

Although devoid of the drawbacks of autografts, allografts induce an immune rejection response by the recipient body and therefore require systemic immunosuppressive therapy. The most immunogenic elements in the allografts are Schwann cells and myelin sheaths, since their membrane present major histocompatibility complex antigens (Evans et al., 1994). Immune compatibility between donor and host is thus important to guarantee axonal regeneration, both in nerve grafts and artificial guides pre-filled with transplanted Schwann cells (Rodríguez et al., 2000). A promising alternative to autografts is a decellularized nerve allograft (Hundepool et al., 2017; Lovati et al., 2018; Philips et al., 2018). The decellularization involves several processes that guarantee immunogenic

free scaffolds from native nerves, while preserving the extracellular matrix (ECM) components and the biomechanical properties of the grafts (Szynkaruk et al., 2013; Nieto-Nicolau et al., 2021). Therefore, decellularization of human peripheral nerves is an innovative strategy in tissue engineering and it can become an alternative to autografts to repair long-gap peripheral nerve injuries. For its clinical translation, it is mandatory to evaluate the pro-regenerative potential of optimized protocols of decellularization of human cadaver nerves. However, the preclinical evaluation of human grafts in experimental models has an important limitation, since these grafts become xenografts when transplanted to experimental animals, and the immune rejection caused by donor antigens (Udina et al., 2003) or other inter-species differences (Wood et al., 2014) can interfere with their regenerative potential. Nevertheless, it is worth to further explore the potential of decellularized xenografts as a repair alternative to grafts from the same species origin. Therefore, in this study we aimed to perform a comparative assessment of the effective axonal regeneration, along a critical nerve gap of 15 mm length induced in the sciatic nerve of adult rats, repaired with a decellularized allograft, a decellularized human xenograft, or the gold standard autograft.

2. Materials and methods

2.1 Ethics Approval

This study followed the ethical precepts of the Declaration of Helsinki and was approved by local ethics committee. Human tissue was processed according to guidance for clinical use (EEC regulations 2004/23/CE and 2006/17/CE) and to the legal requirements for the use of biological samples for research in Spain (Law 14/2007 and RD 1716/2011). Ethical Committee approval was issued by CEIm Hospital Valle Hebron, Barcelona; PR (BST) 314/2019. In all cases, informed consent was obtained from the donors' relatives.

Regarding animal experiments, all the procedures were approved by the Ethics Committee of the *Universitat Autònoma de Barcelona* and *Generalitat de Catalunya* (reference #10306) and followed the European Community Council

Directive 2010/63/EU of the European Parliament on the protection of animals used for *scientific purposes*. In addition, we followed the *ARRIVE guidelines* and committed ourselves to the *3Rs of laboratory animal research*.

2.2. Preparation of acellular nerve grafts

Human sural nerves from eleven deceased donors were obtained from the Barcelona Tissue Bank - Banc de Sang i Teixits (BTB-BST, Barcelona, Spain; <https://www.bancsang.net/>) within 24 hours post-mortem. Donor screening included, but may not be limited to, the review of complete social and medical history, physical examination of the donor, complete serological and microbiological testing during retrieval, histopathological analysis, as well as any other information pertaining to risk factors for relevant communicable diseases. Sural nerve fragments were retrieved from the donor and were placed into a sterile container with Roswell Park Memorial Institute (RPMI) media without phenol (Gibco, Carlsbad, CA, USA) plus 1% antibiotics (vancomycin [Pfizer, MA, Spain], penicillin [Normon, MA, Spain], and streptomycin [Reig Jofre, BCN, Spain]) at 4°C until its decellularization in a clean room environment.

Rat sciatic nerves were harvested from Sprague-Dawley donor rats, under deep anesthesia and with sterile conditions. Samples were placed in sterile phosphate buffered solution (PBS) with antibiotic/antifungal agents (Sigma-Aldrich) and processed within 24 hours.

The decellularization protocol for human nerve samples was as described previously (Nieto-Nicolau et al., 2022). To decellularize rat nerves, that protocol was adapted, reproducing sequential incubations and using zwitterionic and non-ionic detergents for 3 days. Zwitterionic sulfobetaines 10 and 16 were purchased from Sigma-Aldrich (Munich, Germany). Non-ionic Triton X-200 was changed by Triton X-100 (Sigma-Aldrich). This protocol was optimized adding an incubation with hypertonic 1 M NaCl (Sigma-Aldrich) during 4 h and 0.1 mg/ml Pulmozyme DNASE (Roche, Barcelona, Spain) for 3 h. After DNASE treatment, the nerves were washed once in 0.5 M Tris–EDTA buffer and several times in ultrapure water. The process was carried out at room temperature for 4 days.

Histological evaluation of decellularized nerve grafts

Decellularized nerve grafts were fixed in paraformaldehyde 4% for 24 hours at 4°C, then transferred to phosphate buffered (PB) and incubated with saccharose 30% for 24-48h. Samples were cryo-embedded with Tissue Tek® OCT compound (Sakura, Fleminweg, Netherlands) and cross sections of 15 mm thickness were obtained with a cryotome. After blocking with a solution of normal goat serum or normal donkey serum (10%) containing 0.3% Triton, sections were incubated overnight at 4°C with primary antibodies against S-100 protein (S100; Schwann cells; 1:50; 22520-DiaSorin), neurofilament (NF200; myelinated axons; 1:400; AB5539-Millipore), non-collagenous connective tissue glycoprotein (laminin; 1:500; AHP420-Biorad) and collagen (Collagen IV; 1:400; 134001-Setareh Biotec). Following washes, sections were incubated with secondary antibodies bound to Alexa Fluor 488 and Alexa Fluor 594. Sections were also stained with DAPI (DAPI; nuclei; 1:100; D9564-10MG-Sigma) and myelin stain (Fluoromyelin; myelin; 1:300; F34651-Invitrogen). Immunolabeled sections were viewed under epifluorescence microscopy (Olympus BX51).

2.3. In vivo long term studies

Female Sprague-Dawley rats (12 weeks of age and weighing 296-322 g) were used. They were housed under a 12-h-light-dark cycle in a temperature-controlled animal care facility with ad libitum access to water and food.

Seventeen female Sprague-Dawley rats were randomized into three different groups: autograft (AG) (n=6), decellularized rat allograft (DC-RA) (n=5) and decellularized human xenograft (DC-HX) (n=6), and followed for 120 days. Rats were anesthetized with ketamine (75 mg/kg) and medetomidine (0.01 mg/kg) intraperitoneally. The right hindlimb was shaved and sterilized with povidone-iodine solution. A skin incision was made, and the right sciatic nerve was exposed and resected. In the autograft group, a 15 mm long nerve segment of the sciatic nerve was excised and then, sutured again in place using three 10-0 nylon epineural sutures. In the rat allograft and human xenograft, a 15 mm decellularized rat allograft or a 15 mm decellularized human xenograft were

sutured to the host nerve stumps. The muscles were sutured with 6-0 and the skin with 3-0 silk and staples. Postoperative care included amitriptyline (20mg/l) in drinking water to prevent autotomy (Navarro et al., 1994) and buprenorphine 0.03 mg/Kg subcutaneously to treat postoperative pain.

Electrophysiological tests

Reinnervation of target muscles was assessed at 30, 60, 90 and 120 days post-injury (dpi) by motor nerve conduction tests. Animals were anesthetized as indicated above and the sciatic nerve was stimulated with transcutaneous needle electrodes placed at the sciatic notch delivering single pulses of increasing intensity (Synergy Medelec, Viasys HealthCare), and the compound muscle action potential (CMAP) was recorded by placing electrodes on the tibialis anterior (TA), gastrocnemius (GA), and plantar interosseus (PL) muscles. The reference electrode was placed at the fourth toe and a ground electrode was placed at the knee. The amplitude and latency of the CMAP was measured. The contralateral intact limbs were used as control. The rat body temperature was maintained throughout the test with a thermostatic warming flat coil.

Histological evaluation

At the end of the 120 days follow-up, animals were euthanized by an intraperitoneal injection of pentobarbital, transcardially perfused with 4% paraformaldehyde in PBS for 30 min and the sciatic nerves were collected and divided in three parts.

The middle segment of the nerve graft was processed for immunofluorescence labeling as indicated above. Serial sections were incubated for staining axons (NF200), Schwann cells (S100), ionized calcium-binding adapter molecule 1 (Iba1; macrophages; 1:500; 19-19741-Rafer) and laminin. Samples were washed and incubated with secondary antibodies Alexa Fluor 488 goat anti-chicken (1:200; A11039-Invitrogen), Alexa Fluor 488 donkey anti-goat (1:200; A11055-Invitrogen) and Alexa Fluor 594 goat anti-rabbit (1:200; A21207-Invitrogen) diluted in PBS-Triton 0.3%.

The proximal and distal segments of the grafted nerve, including suture levels were post-fixed in 3% glutaraldehyde–3% paraformaldehyde in cacodylate-buffer solution (0.1 m, pH 7.4) at 4°C. These segments were post-fixed with osmium tetroxide (2%, 2 h) and dehydrated through ethanol series prior to embedding in epon resin. Semithin 0.5 µm thick sections were stained with toluidine blue and examined by light microscopy (Olympus BX40). Sets of images obtained at 1000x were chosen by systematic sampling of squares representing at least 30% of the nerve cross-sectional area (Gómez et al 1996). Measurements of cross-sectional area of the whole nerve and counts of the number of myelinated nerve fibers were carried out using ImageJ software.

2.4. In vivo short-term studies

Twelve female Sprague-Dawley rats were randomized in two experimental groups of 6 animals each, according to the repair procedure: DC-RA and DC-HX. In each group, half of the animals were assessed at 7 days and half at 14 days post-injury. Surgeries were performed as described above. However, in this case a segment of the sciatic nerve was excised and substituted by a 12 mm DC-RA or 12 mm DC-HX, therefore using a shorter graft than for the long-term study. The proximal and distal nerve stumps were sutured by 10-0 nylon epineural sutures.

Histological evaluation

At the end of the follow-up (7 or 14 dpi), animals were euthanized and perfused as described. The sciatic nerve was harvested and divided in two equal parts, stored in cryoprotective solution of PBS-sucrose 30% at 4°C for 24 hours. The proximal nerve segment at 7dpi, and the proximal and distal nerve segment at 14dpi were embedded in Tissue Tek and 15 µm thick longitudinal sections cut serially. For immunostaining, sections were incubated overnight with primary antibodies for staining axons (NF200), Schwann cells (S100), macrophages (Iba1) and fibroblasts (vimentin; 1:400; ab92547-Abcam). Samples were washed and incubated with secondary antibodies as above. Finally, sections were

washed and cover-slipped with Fluoromount containing DAPI (1:10,000, Sigma) for nuclear counterstain.

2.5. In vitro study

Dissociate culture of DRG

Nine adult C57BL/6J mice were euthanized, and DRGs were dissected. Dissociation and culture of DRG cells was performed as previously described (Alé et al., 2014). Briefly, the ganglia were cleaned under a dissecting microscope and enzymatically digested by incubation for 30 min at 37°C in 10% trypsin, 10% collagenase and 10% DNase. The enzymatic activity was halted by adding 1 ml of DF10S, and tissue suspension was centrifuged at 900 g for 3 min. Then, the pellet was resuspended in 1 mL of culture medium and mechanically dissociated.

A total of 12,000 cells were plated on coverslips coated with poly-D-lysine plus human laminin (1 µg/µl, Sigma-Aldrich) or mice laminin (1 µg/µl, Sigma-Aldrich). After 24 h in culture, cells were fixed with 4% paraformaldehyde for 20 min, and neurons were immunostained with β3-tubuline antibody (1:500, MMS-435P/801202, Biolegend), NF200 antibody (1:800) and DAPI (1:1000, D9564-10MG-Sigma). Length of the longest neurite from β3-tubuline and NF200 positive neurons was measured at 100x magnification under epifluorescence microscopy. Three different cultures using both conditions in at least three different wells each, were analyzed.

2.6. Data Analysis

Data are expressed as mean ± standard error of the mean (SEM). The results of functional tests and histology were analyzed by two-way ANOVA. The results of the longest neurites from DRG cultures were compared using unpaired t-test. Statistical analyses were made with GraphPad Prism 8 software. A p<0.05 was considered as significant.

3. Results

3.1. Effectiveness of the decellularization procedure

Cross sections of human and rat decellularized nerve grafts were processed for immunohistochemistry. Immunolabelling against laminin and collagen IV indicated that the structure of the extracellular matrix and endoneurial tubules was well preserved and comparable. Neurofilament remnants were present though their concentration was highly reduced and fragmented, compatible with degradation of axons, whereas absence of DAPI and S100 staining indicated that cell contents were completely removed (Figure 1).

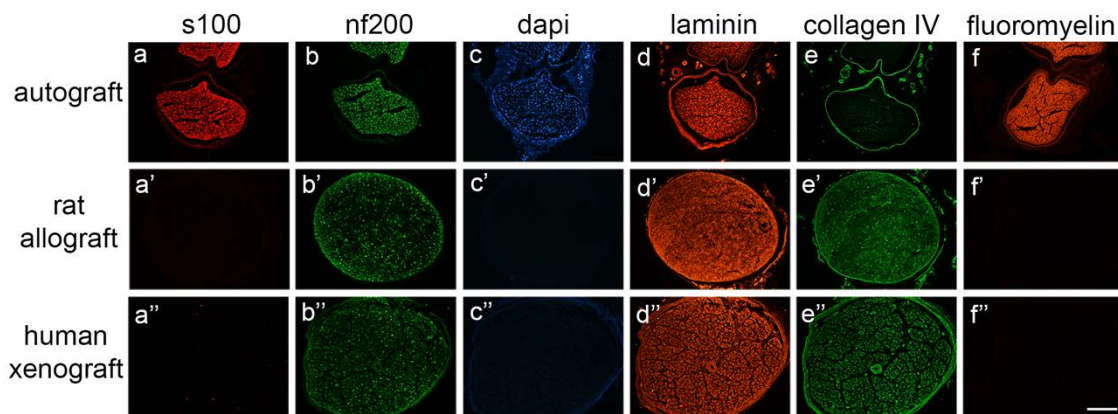


Figure 1. Decellularization efficiency. Representative micrographs showing immunolabeling of Schwann cells (s100) (a''), myelinated axons (nf200) (b''), nuclei (dapi) (c''), extracellular matrix proteins (laminin and collagen IV) (d'' and e''), respectively), and myelin (fluoromyelin) (f''), in a control nerve (native nerve) (a, b, c, d, e, f), a decellularized rat nerve allograft (a', b', c', d', e', f') and a decellularized human nerve xenograft (a'', b'', c'', d'', e'', f''). Images taken at 100 × magnification; scale bar 400 μm.

3.2. In vivo repair of a critical nerve gap with decellularized grafts

Electrophysiological test results

Nerve conduction tests were performed to assess reinnervation of TA, GM and PL muscles (Figure 2). At 60 dpi all animals from AG and DC-RA groups showed

evidence of reinnervation in the TA and GM muscles, whereas in the PL muscle CMAPs were recorded in all animals of AG group but only in 20% of DC-RA group. In the DC-HX rats only 50% of the animals showed evidence of reinnervation of the TA and GM muscles and none for the PL muscle. At 90 dpi, the amplitude of the CMAPs increased. All animals from AG and DC-RA groups had reinnervation of TA, GM and PL muscles, whereas half of the animals of the DC-HX had positive values in TA and GM muscles and only one in the PL muscle. At the end of the follow-up (120 dpi) the mean CMAP amplitude of TA (30.8 ± 1.0 mV), GM (43.0 ± 2.6 mV) and PL (2.8 ± 0.4 mV) muscles in the AG group were higher than in the DC-RA group (23.1 ± 3.7 mV, 31.4 ± 2.9 mV and 1.5 ± 0.2 mV respectively). Animals from DC-HX group showed significantly lower values compared to AG and DC-RA groups in the TA (9.7 ± 4.9 mV; $p < 0.0001$), GM (10.9 ± 5.7 mV; $p < 0.01$ vs DC-RA and $p < 0.0001$ vs AG) and PL muscles (0.05 ± 0.05 mV; $p < 0.001$ vs DC-RA and $p < 0.0001$ vs AG). Moreover, only half of the animals repaired with the human decellularized graft showed reinnervation signs in TA and GM muscles, and just 1 of the 6 animals in the PL muscle.

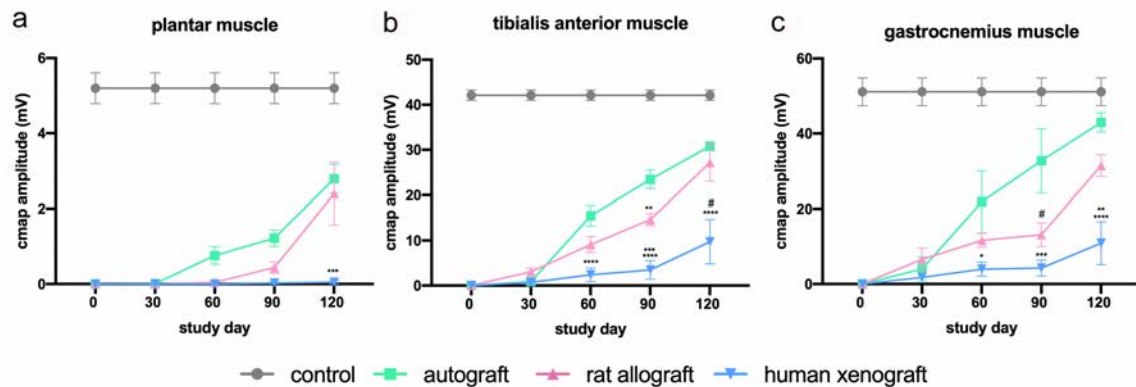


Figure 2. Electrophysiological evaluation of nerve regeneration along the 120-day follow-up after sciatic nerve section and repair. Results are presented as mean \pm SEM. Statistical analysis was performed using 2-way ANOVA. Plots show the amplitude of CMAPs of plantar ($***p < 0.001$ vs AG), tibialis anterior ($**p < 0.01$ vs AG; $***p < 0.001$ vs DC-RA; $****p < 0.0001$ vs AG; $\#p < 0.0001$ vs DC-RA) and gastrocnemius ($*p < 0.5$ vs AG; $\# < 0.5$ vs AG; $**p < 0.01$ vs DC-RA; $***p < 0.001$ vs AG; $****p < 0.0001$ vs AG) muscles.

Histological nerve assessment

At the end of follow up, at 120 dpi, nerves were harvested and processed for histological analysis. There were numerous regenerated myelinated axons and Schwann cells within the AG and DC-RA grafts, but quite limited in DC-HX grafts. The endoneurial basal lamina tubules were preserved in all the grafts, and the amount of macrophage immunolabeling was also similar (Figure 3).

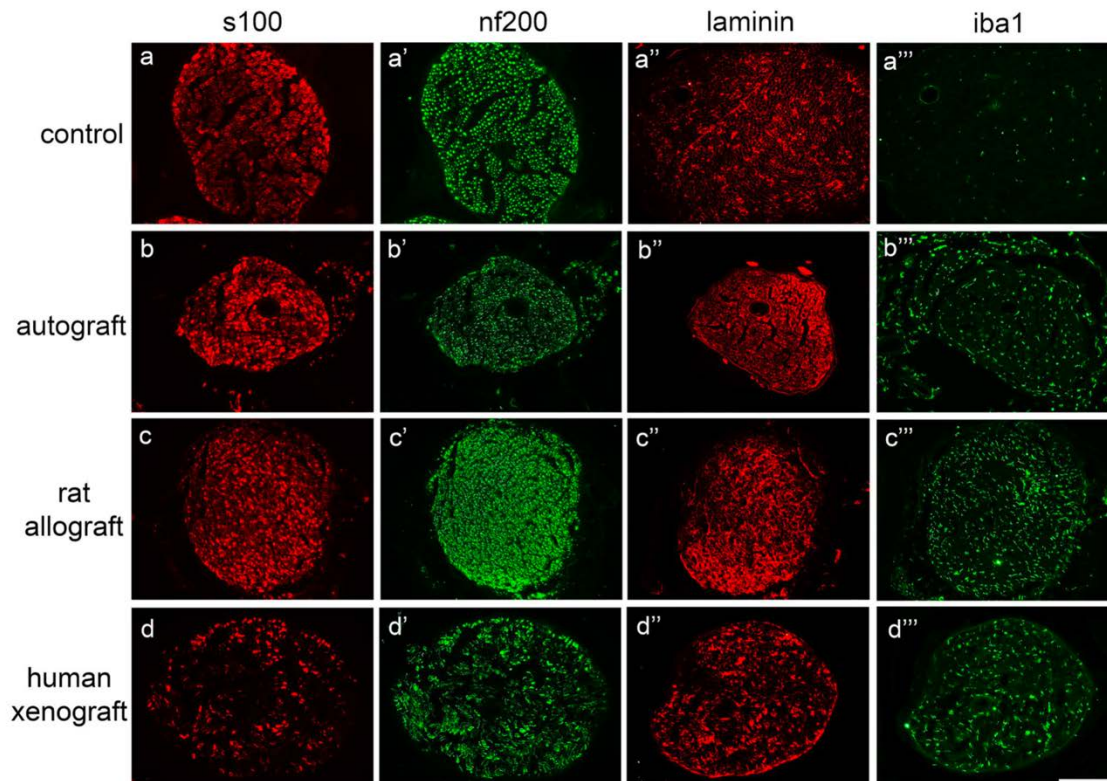


Figure 3. Immunohistochemical characterization of the grafts 120 days after implantation. Representative micrographs of nerve grafts harvested at 120 dpi showing immunofluorescence of Schwann cells labeled against S100 (a, b, c, d), myelinated axons labeled against neurofilament 200 (NF200) (a', b', c', d'), extracellular matrix proteins labeled against laminin (a'', b'', c'', d''), and macrophages labeled against Iba1 (a''', b''', c''', d''') in cross sections of the graft in a control nerve (no decellularized native nerve) (a'''), autograft (b'''), rat allograft (c'''), and human xenograft (d''') groups. Images taken at 200 × magnification; scale bar 150 μm.

Quantitative analysis demonstrated that the density of myelinated axons was statistically higher in AG (40267.78 ± 2775.7 axons/mm²) than in the DC-RA (28132.47 ± 3084.11 axons/mm², * $p < 0.5$ vs AG) and DC-HX group (18244.98 ± 3070.41 axons/mm², \$ $p < 0.5$ vs DC-RA and *** $p < 0.001$ vs AG) groups in the middle of the graft. Distal to the graft, the myelinated fiber density was also significantly higher in AG group (27293.08 ± 195.8 axons/mm²) compared to DC-RA (14337.13 ± 1324.54 axons/mm², ** $p < 0.01$) and DC-HX (2289.29 ± 513.73 axons/mm², # $p < 0.01$ vs DC-RA and **** $p < 0.0001$). All animals showed regeneration in the middle of the grafts. Distal to the nerve graft, all animals from AG and DC-RA had myelinated axons, whereas only 3/6 animals of the DC-HX showed positive results (Figure 4).

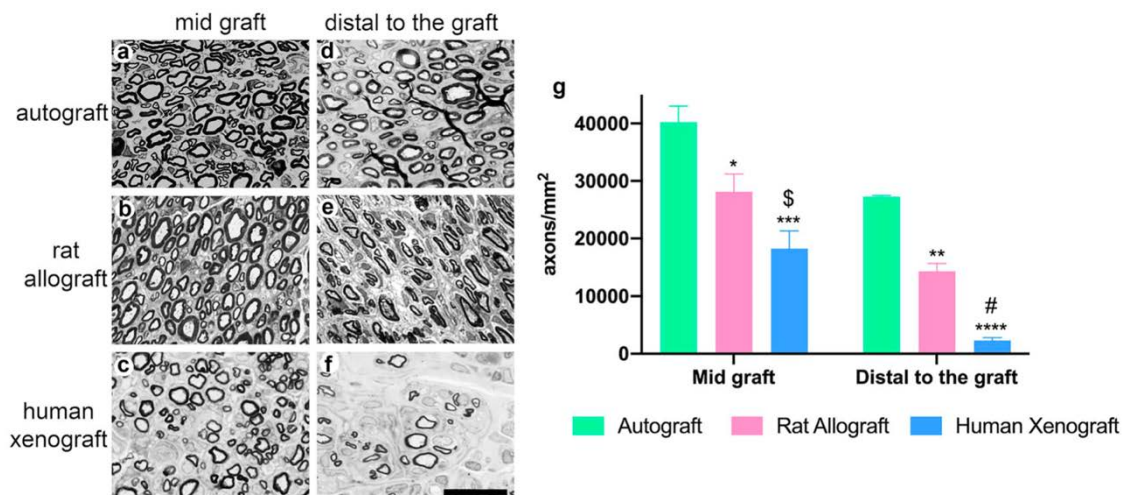


Figure 4. Histological evaluation of the regenerative potential of the grafts at 120 days. Representative transverse semithin sections of the mid graft (a, b, c) and distal to the graft (d, e, f) in autograft (a, d), decellularized rat allograft (b, e), and decellularized human xenograft (c, f) groups, stained with toluidine blue. Images were taken at $\times 1000$ magnification; scale bar 10 μ m. (g) Plots showing density of myelinated axons in the sciatic nerve at the mid graft and distal to the graft in the three groups. * $p < 0.5$ vs AG; \$ $p < 0.5$ vs DC-RA; ** $p < 0.01$ vs AG; # $p < 0.01$ vs DC-RA; *** $p < 0.001$ vs AG; **** $p < 0.0001$ vs AG

3.3. Evaluation of short-term regeneration

Considering the above results, a short-term study was performed to assess the early events of the regenerating nerves in the two types of decellularized grafts. At 7 dpi, the axonal regenerative front, labeled with NF200, reached the middle of the graft in rats of both groups, although there was higher number of axons in DC-RA than in DC-HX grafts (Figure 5a). There were relatively few Schwann cells accompanying the regenerating axons. In the DC-RA group, marked proliferation of fibroblasts was observed within the nerve, whereas in the DC-HX group, the fibroblast invasion was mainly around the nerve. The Iba1 reactivity, corresponding to macrophages, was higher in the DC-HX group (Figure 5b).

In samples taken at 14 dpi, a greater number of Schwann cells compared to 7dpi was present around regenerating axons (Figure 5c), whereas fibroblasts showed a more organized longitudinal organization. In the DC-HX group, fibroblasts were present both inside and outside the graft, indicating an important fibrotic reaction, whereas macrophages were only present around the nerve (Figure 5d). Besides, only one of the three animals presented regenerated axons along the nerve graft. In the DC-RA group, the regenerative front reached the distal segment of the graft. In the DC-HX group, regenerating axons reached the distal segment in the only animal that had already NF positive axons at the proximal segment. As expected, in the other two animals, the graft was disorganized, with infiltrating cells and marked presence of macrophages. This is in contrast to what we observed at 7 days, when all animals of the group had some regenerative axons in the proximal half of the graft. It is possible that the important fibrotic reaction developed at 14dpi overcame the regenerative response observed at early time points.

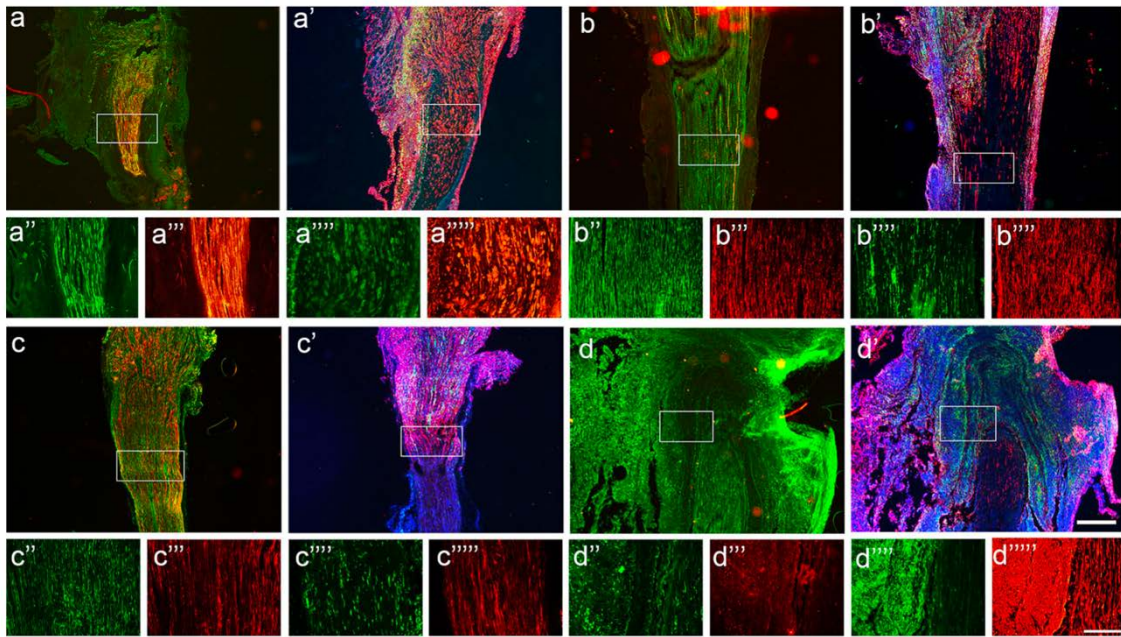


Figure 5. Immunohistochemical characterization of the grafts 1 and 2 weeks after implantation. Representative micrographs showing immunofluorescence of proximal segment of DC-RA at 7 days post injury (a'''') labeling myelinated axons and Schwann cells (a), and macrophages, fibroblasts and DAPI (a'). Proximal segment of DC-HX at 7 days post injury (b'''') labeling myelinated axons and Schwann cells (b), and macrophages, fibroblasts, and DAPI (b'). Proximal segment of DC-RA at 14 days post injury (c'''') labeling myelinated axons and Schwann cells (c), and macrophages, fibroblasts, and DAPI (c'). Proximal segment of DC-HX at 14 days post injury (d'''') labeling myelinated axons and Schwann cells (d), and macrophages, fibroblasts and DAPI (d'). Images (a, a', b, b', c, c', d, d') taken at 40×magnification; scale bar 500 μm. Below images showed myelinated axons labeled against NF200 (a'' , b'' , c'' , d''), Schwann cells labeled against S100 (a''' , b''' , c''' , d'''), macrophages labeled against Iba1 (a'''' , b'''' , c'''' , d''''), fibroblasts labeled against vimentin (a'''' , b'''' , c'''' , d''''), images taken at 200 × magnification; scale bar 200 μm

3.4. Influence of ECM origin on neurite growth of DRG neurons in culture

To evaluate if inter-species differences in ECM components, specifically in laminin, could play a role in the poorer ability of decellularized xenografts to sustain axonal regeneration, we compared neurite growth of mice DRG neurons

CHAPTER II

on slides coated with laminin either from human or from mouse origin. When mice neurons were plated on mice laminin, a higher number of neurons with neurites were observed compared to human laminin. Mean of neurite length from neurons with neurites was significantly higher in mouse laminin (175.7 ± 114.4 mm) compared to human laminin (118.9 ± 66.9 mm, $p < 0.0001$). When analyzing neurite growth of myelinated (NF positive) and non-myelinated (NF negative) neurons, similar results were found. Therefore, mean neurite length of NF positive neurons with neurites (185.7 ± 125.9 mm and 126.7 ± 66.5 mm, $p < 0.0001$) and NF negative neurons with neurites (157.9 ± 88.7 mm and 106.28 ± 66.2 mm, $p < 0.001$) (Figure 6) was significantly higher on mouse laminin compared to human laminin.

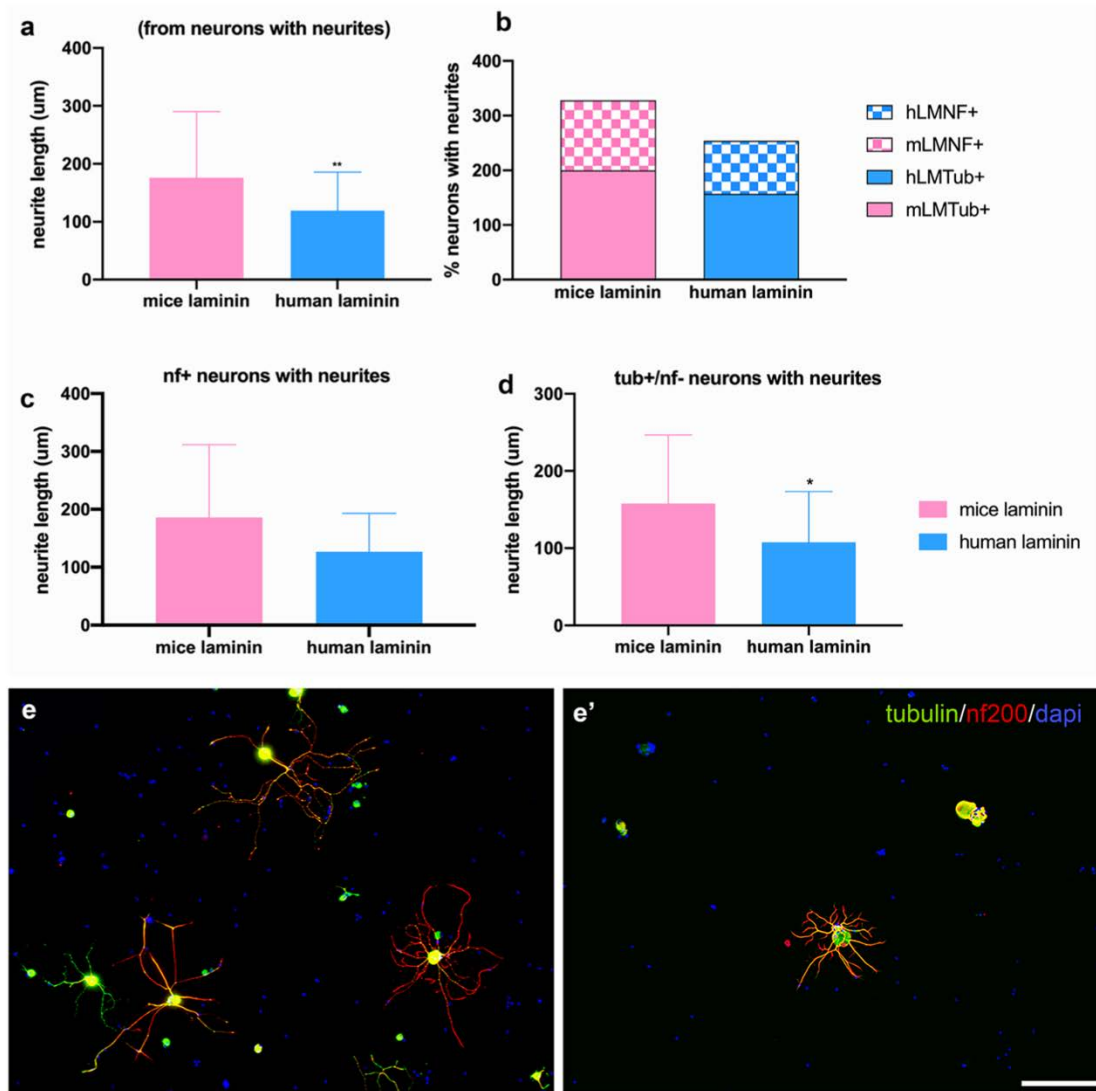


Figure 6. In vitro neural growth on laminins from different species. Plots showing the neurite length of all neurons (a), the percentage of neurons with neurites (b), the neurite length of myelinated neurons (nf200+) (c) and non-myelinated (nf200-) neurons with neurites (d). * $p < 0.5$ vs mice laminin; ** $p < 0.01$ vs mice laminin. Mouse DRG neuronal culture immunolabeled against $\beta 3$ -tubulin (green), nf200 (red) and dapi (blue), on surface coated with mouse laminin (e) or with human laminin (e'). Higher number of neurites and longer neurites can be observed on mouse laminin than on human laminin. Images taken at 100 \times magnification; scale bar 200 μ m.

4. Discussion

In this study we have performed the first in vivo assay of a novel, optimized protocol for nerve decellularization that fulfills the standardized recommendations for peripheral nerve decellularization (Nieto-Nicolau et al 2021), and demonstrated that such decellularized allograft allows for effective axonal regeneration along a very long gap in the rat, paving the way to its translation to the clinic. We have also shown that a decellularized xenograft is not adequate to ensure nerve regeneration due to interspecies differences of the ECM components to guide adequate migration of regenerating cells and axons.

Successful nerve regeneration requires an orchestrated series of events that implies a switch of neurons to a pro-regenerative state and important changes at the distal stump, that lead to Wallerian degeneration and the creation of a permissive milieu for axonal regeneration, where Schwann cells, immune cells, endothelial cells and fibroblasts play an important role supporting axonal regrowth (McDonald et al., 2006; Allodi et al., 2012; Kim et al., 2013; Dun and Parkinson, 2015; Cattin and Lloyd, 2016; Roballo and Bushman, 2019). Despite the potential of peripheral nerves to regenerate, successful functional recovery is usually limited after severe nerve lesions (Navarro et al., 2007). Thus, nerve resections that lead to long gaps between nerve stumps present poor success of regeneration and commonly limited recovery if surgically repaired (Pfister et al., 2011). This limitation is partially due to the lack of good repair alternatives to the gold standard autograft. Since it is mandatory to bridge the gap to guarantee some degree of regeneration, research has focused on a variety of graft substitutes, including decellularized graft (Nagao et al., 2011). A decellularized graft has to provide an off-the-shelf alternative to synthetic conduits while partially maintaining some of the proregenerative properties of autologous nerve grafts (Kasper et al., 2020). Currently, there is only one commercial cadaveric decellularized nerve allograft, Axogen Avance® (AxoGen Inc., Alachua, FL, USA) approved for clinical application by the FDA (Kornfeld et al., 2019; Kornfeld et al., 2021) but the limited evidence of its pro-regenerative potential has prevented its expansion to the European market. Therefore, further studies aimed to optimize

protocols to decellularize human cadaveric nerves and to evaluate its regenerative potential compared to the gold standard autografts are needed. In this sense, decellularization is a key element when using allografts since presence of cells on these grafts trigger a strong immune reaction in the recipient that limits their clinical use. The targets of rejection in peripheral nerves are mainly the Schwann cells and the myelin sheaths, because their membranes carry the antigens of the major histocompatibility complex (Evans et al., 1994). Systemic immunosuppression is effective for avoiding rejection (Udina et al., 2003), but it is not a convenient alternative for this type of non-vital graft, since it would place the patient at risk of infection, toxicity and other complications (Szynkaruk et al., 2013; Vasudevan et al., 2014). Therefore, the decellularization protocol has to guarantee elimination of donor antigens while preserving the ECM and the physical architecture of the nerve, two elements that are fundamental to sustain successful regeneration. In this sense, our protocol of decellularization (Nieto-Nicolau et al., 2021) successfully preserves the ECM and endoneurial tubules, visualized by immunolabeling against laminin and collagen IV, while removing all types of cells, as demonstrated by the lack of DAPI and the Schwann cell marker S100 in both rat and human decellularized grafts.

More importantly, this optimized decellularized allograft allows successful axonal regeneration when used to repair a critical 15mm nerve defect in the rat sciatic nerve. However, regeneration and reinnervation, evaluated both by electrophysiological tests and histological techniques, is slower in decellularized allografts compared to the native autografts. This finding is not surprising, since the decellularization eliminates all cellular components, among them Schwann cells, that are key elements orchestrating the regenerative response in the distal stump. Migration of host Schwann cells into the allograft is needed to create a permissive milieu for regeneration, a fact that explains the slower regeneration observed into a decellularized graft (Hall, 1986).

On the other hand, regeneration and reinnervation were more limited when the same gap was repaired using a decellularized xenograft, obtained from a human nerve. As previously described (Wood et al., 2014), there were appreciable

qualitative differences in the arrangement of axons (more disorganized) and in the density of myelinated axons (reduced) into the graft and distally in the decellularized xenografts compared to decellularized allografts and more with respect to the cellular autografts. A previous study also reported the higher pro-regenerative capability of allografts compared to xenografts, when repairing a smaller, 10 mm rat sciatic nerve defect (Kvist et al., 2011), whereas another found minimal differences by using the same gap to repair the rat facial nerve (Huang et al., 2015). The origin of the donor could hardly explain these differences, since Kvist et al compared xenografts from different donors and could not find a simple relation between the origin of the graft and the extent to which it supports axonal outgrowth (Kvist et al., 2011).

It remains unclear why and how interspecies differences between the host and the donor graft affect nerve regeneration (Kvist et al., 2011; Wood et al., 2014). By using a decellularized graft, no immune rejection is expected. Therefore, we decided to evaluate and compare short-term regeneration within decellularized allografts and xenografts. Consistent with the long-term study, we found that regeneration was faster in DC-RA group, whereas in the DC-HX group was limited or even failed; furthermore, this failure was accompanied with a marked cellular infiltration, evident at two weeks after grafting, not earlier, suggesting that a period of time is necessary to trigger an inflammatory/rejection response in these grafts, negatively impacting the regenerative process.

Interestingly, in the DC-RA grafts, we observed an early fibroblast proliferation, that was organized in aligned tubes inside the nerve at 14 days post grafting. It is well established that fibroblasts are key players in the formation of the initial bridge between the two nerve stumps after nerve transection (Parrinello et al., 2010). This bridge will be later invaded by migrating Schwann cells to create the adequate milieu for axons to regenerate through the graft. In fact, migration of Schwann cells is directed by fibroblasts and endothelial cells (Cattin et al., 2015), whereas Schwann cell invasion precede growth of the axons through the bridge (Chen et al., 2005; McDonald et al., 2006; Parrinello et al., 2010). In the case of a decellularized graft, both fibroblasts and Schwann cells have to migrate from

the proximal and distal nerve stumps and re-cellularize the graft. Recellularization by Schwann cells seems mandatory to guarantee regeneration, but fibroblasts are also important to facilitate attraction of Schwann cells. However, when we analyzed the decellularized grafts at 7dpi, we observed that axons preceded Schwann cells, indicating that the decellularized graft already offers a permissive milieu for axonal regeneration, thanks to the preserved architecture and the presence of ECM components. In addition, fibroblasts aligned along the endoneurial tubules, would present a pro-regenerative profile that favor axonal regeneration and contrast with the fibrotic reaction observed in other situations, that is detrimental for regeneration. In fact, in DC-HX grafts large number of fibroblasts were also observed, but mainly located around the nerve, in a reaction compatible with a foreign body response. Therefore, the different response of fibroblasts can contribute to the different regenerative potential of these two types of grafts.

On the other hand, the potential inter-species differences in ECM components can also contribute to the poorer regenerative potential of a xenograft compared to an allograft. Laminin is an important component of the ECM that interacts with axons and Schwann cells through binding with integrins (Gonzalez-Perez et al., 2013; Mckerracher et al., 1996) and that also promotes neurite growth in culture (Baron-Van Evercooren et al., 1982). We found that laminin was present in the basal lamina, inside the preserved endoneurial tubules, similarly in both types of decellularized grafts. However, when we compared the capability of mouse neurons to extend neurites in vitro, in wells coated with laminin either from mouse or from human sources, we observed that laminin from the same specie sustained stronger and longer neurite growth. This intra-specie preference can contribute to the higher potential of allografts to sustain axonal growth compared to xenografts (Kvist et al., 2011).

In conclusion, a nerve decellularization protocol that guarantees elimination of cellular contents preserving the structure and the ECM of the graft can become an alternative to autografts to repair long nerve defects, although regeneration is going to be slower in the decellularized grafts. In contrast, xenografts showed

CHAPTER II

some limitations, mainly related to inter-species immune response, fibrotic reaction and the lower capacity of ECM components to sustain axon growth of neurons from another specie. Our results demonstrate the translationality of the optimized protocol for nerve decellularization that fulfills the standardized recommendations (Nieto-Nicolau et al 2021a), and also its success as a decellularized allograft to sustain regeneration over long nerve gaps in rats.

References

- Alé A, Bruna J, Morell M, van de Velde H, Monbaliu J, Navarro X, Udina E (2014) Treatment with anti-TNF alpha protects against the neuropathy induced by the proteasome inhibitor bortezomib in a mouse model. *Exp Neurol* 253:165–173. doi.org/10.1016/j.expneurol.2013.12.020
- Allodi I, Udina E, Navarro X. Specificity of peripheral nerve regeneration: interactions at the axon level. *Progr Neurobiol* 2012, 98:16-37. doi: 10.1016/j.pneurobio.2012.05.005
- Asplund M, Nilsson M, Jacobsson A, von Holst H (2009) Incidence of traumatic peripheral nerve injuries and amputations in Sweden between 1998 and 2006. *Neuroepidemiology* 32:217–228. doi.org/10.1159/000197900
- Baron-Van Evercooren A, Kleinman HK, Ohno S, Marangos P, Schwartz JP, Dubois-Dalcq ME (1982) Nerve growth factor, laminin, and fibronectin promote neurite growth in human fetal sensory ganglia cultures. *J Neurosci Res* 8:179-93. doi:10.1002/jnr.490080208
- Cattin AL, Burden JJ, Van Emmenis L, Mackenzie FE, Hoving JJ, Garcia Calavia N, Guo Y, McLaughlin M, Rosenberg LH, Quereda V, Jamecna D, Napoli I, Parrinello S, Enver T, Ruhrberg C, Lloyd AC (2015) Macrophage-induced blood vessels guide Schwann cell-mediated regeneration of peripheral nerves. *Cell* 162:1127-1139. doi:10.1016/j.cell.2015.07.021
- Cattin AL, Lloyd AC (2016) The multicellular complexity of peripheral nerve regeneration. *Curr Opin Neurobiol* 39:38-46. doi:10.1016/j.conb.2016.04.005
- Chen YY, McDonald D, Cheng C, Magnowski B, Durand J, Zochodne DW (2005) Axon and Schwann cell partnership during nerve regrowth. *J Neuropathol Exp Neurol* 64:613-622. doi:10.1097/01.jnen.0000171650.94341.46
- Dun XP, Parkinson DB (2015) Visualizing peripheral nerve regeneration by whole mount staining. *PLoS One* 10:e0119168. doi:10.1371/journal.pone.0119168
- Evans PJ, Midha R, Mackinnon SE (1995) The peripheral nerve allograft: a comprehensive review of regeneration and neuroimmunology. *Prog Neurobiol* 43:187-233. doi:10.1016/0301-0082(94)90001-9
- Gaudin R, Knipfer C, Henningsen A, Smeets R, Heiland M, Hadlock T (2016) Approaches to peripheral nerve repair: generations of biomaterial conduits yielding to replacing autologous nerve grafts in craniomaxillofacial surgery. *Biomed Res Int* 2016:3856262. doi:10.1155/2016/3856262

CHAPTER II

- Gonzalez-Perez F, Udina E, Navarro X (2013) Extracellular matrix components in peripheral nerve regeneration. *Int Rev Neurobiol* 108:257-275. doi:10.1016/B978-0-12-410499-0.00010-1
- Grinsell D, Keating CP (2014) Peripheral nerve reconstruction after injury: a review of clinical and experimental therapies. *Biomed Res Int* 2014:698256. doi:10.1155/2014/698256
- Hall SM (1996) Regeneration in cellular and acellular autografts in the peripheral nervous system. *Neuropathol Appl Neurobiol* 12:27-46. doi:10.1111/j.1365-2990.1986.tb00679.x
- Huang H, Xiao H, Liu H, Niu Y, Yan R, Hu M (2015) A comparative study of acellular nerve xenografts and allografts in repairing rat facial nerve defects. *Mol Med Rep* 12(4):6330-6336. doi:10.3892/mmr.2015.4123
- Hundepool CA, Nijhuis TH, Kotsougiani D, Friedrich PF, Bishop AT, Shin AY (2017) Optimizing decellularization techniques to create a new nerve allograft: an in vitro study using rodent nerve segments. *Neurosurg Focus* 42(3):E4. doi:10.3171/2017.1.FOCUS16462
- Kasper M, Deister C, Beck F, Schmidt CE (2020) Bench-to-bedside lessons learned: commercialization of an acellular nerve graft. *Adv Health Mater* 9:e2000174. doi:10.1002/adhm.202000174
- Kim HA, Mindos T, Parkinson DB (2013) Plastic fantastic: Schwann cells and repair of the peripheral nervous system. *Stem Cells Transl Med* 2:553-557. doi:10.5966/sctm.2013-0011
- Kornfeld T, Borger A, Radtke C (2021) Reconstruction of critical nerve defects using allogenic nerve tissue: a review of current approaches. *Int J Mol Sci* 22:3515. doi:10.3390/ijms22073515
- Kornfeld T, Vogt PM, Radtke C (2019) Nerve grafting for peripheral nerve injuries with extended defect sizes. *Wien Med Wochenschr* 169:240-251. doi:10.1007/s10354-018-0675-6
- Kvist M, Sondell M, Kanje M, Dahlin LB (2011) Regeneration in, and properties of, extracted peripheral nerve allografts and xenografts. *J Plast Surg Hand Surg* 45:122-128. doi:10.3109/2000656X.2011.571847
- Lovati AB, D'Arrigo D, Odella S, Tos P, Geuna S, Raimondo S (2018) Nerve repair using decellularized nerve grafts in rat models. A review of the literature. *Front Cell Neurosci* 12:427. doi: 10.3389/fncel.2018.00427.

- McDonald D, Cheng C, Chen Y, Zochodne D (2006) Early events of peripheral nerve regeneration. *Neuron Glia Biol* 2:139-147. doi:10.1017/S1740925X05000347
- McKerracher L, Chamoux M, Arregui CO (1996) Role of laminin and integrin interactions in growth cone guidance. *Mol Neurobiol* 12:95-116. doi:10.1007/BF02740648
- Nagao RJ, Lundy S, Khaing ZZ, Schmidt CE (2011) Functional characterization of optimized acellular peripheral nerve graft in a rat sciatic nerve injury model. *Neurol Res* 33:600-608. doi:10.1179/1743132810Y.0000000023
- Navarro X, Butí M, Verdú E (1994) Autotomy prevention by amytriptiline after peripheral nerve section in different strains of mice. *Restor Neurol Neurosci* 1994, 6:151-157. doi: 10.3233/RNN-1994-6209
- Navarro X, Vivó M, Valero-Cabré A (2007) Neural plasticity after peripheral nerve injury and regeneration. *Prog Neurobiol* 82:163-201. doi:10.1016/j.pneurobio.2007.06.005
- Nieto-Nicolau N, López-Chicón P, Fariñas O, Bolívar S, Udina E, Navarro X, Casaroli-Marano R, Vilarrodona A (2021) Effective decellularization of human nerve matrix for regenerative medicine with a novel protocol. *Cell Tissue Res* 384:167-177. doi:10.1007/s00441-020-03317-3
- Nieto-Nicolau N, López-Chicón P, Torrico C, Bolívar S, Contreras-Carreton E, Udina E, Navarro X, Casaroli-Marano RP, Fariñas O, Vilarrodona A (2022) "Off-the-Shelf" nerve matrix preservation. *Biopreserv Biobank* 20:48-58. doi: 10.1089/bio.2020.0158. Epub 2021 Sep 20. PMID: 34542324
- Parrinello S, Napoli I, Ribeiro S, Wingfield Digby P, Fedorova M, Parkinson DB, Doddrell RD, Nakayama M, Adams RH, Lloyd AC (2010) EphB signaling directs peripheral nerve regeneration through Sox2-dependent Schwann cell sorting. *Cell* 143:145-55. doi: 10.1016/j.cell.2010.08.039. PMID: 20869108; PMCID: PMC3826531.
- Pfister BJ, Gordon T, Loverde JR, Kochar AS, Mackinnon SE, Cullen DK. (2011) Biomedical engineering strategies for peripheral nerve repair: surgical applications, state of the art, and future challenges. *Crit Rev Biomed Eng* 39:81-124. doi:10.1615/critrevbiomedeng.v39.i2.20
- Philips C, Campos F, Roosens A, Sánchez-Quevedo MDC, Declercq H, Carriel V (2018) Qualitative and quantitative evaluation of a novel detergent-based method for decellularization of peripheral nerves. *Ann Biomed Eng* 46:1921-1937. doi: 10.1007/s10439-018-2082-y
- Roballo KCS, Bushman J (2019) Evaluation of the host immune response and functional recovery in peripheral nerve autografts and allografts. *Transpl Immunol* 53:61-71. doi: 10.1016/j.trim.2019.01.003

CHAPTER II

- Rodríguez FJ, Verdú E, Ceballos D, Navarro X (2000) Nerve guides seeded with autologous schwann cells improve nerve regeneration. *Exp Neurol* 161:571-84. doi: 10.1006/exnr.1999.7315
- Szynkaruk M, Kemp SW, Wood MD, Gordon T, Borschel GH (2013) Experimental and clinical evidence for use of decellularized nerve allografts in peripheral nerve gap reconstruction. *Tissue Eng Part B Rev* 19:83-96. doi: 10.1089/ten.TEB.2012.0275
- Vasudevan S, Huang J, Botterman B, Matloub HS, Keefer E, Cheng J (2014) Detergent-free decellularized nerve grafts for long-gap peripheral nerve reconstruction. *Plast Reconstr Surg Glob Open* 2:e201. doi: 10.1097/GOX.0000000000000118
- Wood MD, Kemp SW, Liu EH, Szynkaruk M, Gordon T, Borschel GH (2014) Rat-derived processed nerve allografts support more axon regeneration in rat than human-derived processed nerve xenografts. *J Biomed Mater Res A* 102:1085-91. doi:10.1002/jbm.a.34773

Decellularized graft for repairing severe peripheral nerve injuries in sheep

Estefanía Contreras^{1,2}, Sara Traserra^{1,2}, Sara Bolívar^{1,3}, Núria Nieto-Nicolau⁴, Jessica Jaramillo¹, Joaquim Forés^{1,5}, Eduard Jose-Cunilleras⁶, Xavier Moll⁶, Félix García⁶, Ignacio Delgado-Martínez¹, Oscar Fariñas^{4,7}, Patrícia López-Chicón^{4,7}, Anna Vilarrodona^{4,8}, Esther Udina^{1,3}, Xavier Navarro^{1,3}

¹ Department of Cell Biology, Physiology and Immunology, and Institute of Neuroscience, Universitat Autònoma de Barcelona, Bellaterra, Spain

² Integral Service for Laboratory Animals (SIAL), Faculty of Veterinary, Universitat Autònoma de Barcelona, Bellaterra, Spain

³ Centro de Investigación Biomédica en Red sobre Enfermedades Neurodegenerativas, Instituto de Salud Carlos III, Bellaterra, Spain

⁴ Barcelona Tissue Bank, Banc de Sang i Teixits, Barcelona, Spain

⁵ Hand and Peripheral Nerve Unit, Hospital Clínic i Provincial, Universitat de Barcelona, Barcelona, Spain

⁶ Department of Animal Medicine and Surgery, Universitat Autònoma de Barcelona, Bellaterra, Spain;

⁷ Biomedical Research Institute Sant Pau (IIB-Sant Pau), Barcelona, Spain

⁸ Vall Hebron Institute of Research (VHIR), Barcelona, Spain

Accepted for publication in Neurosurgery

Abstract

Background and Objectives: Peripheral nerve injuries resulting in a nerve defect require surgical repair. The gold standard, the autograft, has several limitations and, therefore, new alternatives must be developed. The main objective of this study is to assess nerve regeneration through a long gap nerve injury (5 cm) in the peroneal nerve of sheep with a decellularized nerve allograft.

Methods: A nerve gap 5 cm long was made in the peroneal nerve of sheep and repaired by an autograft (AG) or by a decellularized allograft (DCA). Functional tests were performed once a month, and electrophysiology and echography evaluations at 6.5 and 9 months post-surgery. Nerve grafts were harvested at 9 months for immunohistochemical and morphological analyses.

Results: The decellularization protocol completely eliminated the cells while preserving the extracellular matrix of the nerve. No significant differences were observed in functional tests of locomotion and pain response. Reinnervation of the tibialis anterior (TA) muscles occurred in all animals, with some delay in DCA compared to AG groups. Histology showed a preserved fascicular structure in both AG and DCA, however, the number of axons distal to the nerve graft was higher in AG than in DCA.

Conclusion: The decellularized graft assayed supported effective axonal regeneration when used to repair a 5 cm long gap in the sheep. As expected, a delay in functional recovery was observed compared to the autograft due to the lack of Schwann cells.

1. Introduction

Severe peripheral nerve injuries result in loss of sensory, autonomic, and motor functions of the body segment innervated by the injured nerve.¹ Despite the regenerative potential of peripheral neurons, functional recovery after severe nerve injury is generally limited. Surgical repair by direct suturing the two nerve stumps is mandatory in nerve transections. Injuries that produce long defects (>2 cm) require graft implantation to bridge proximal and distal nerve stumps providing a path for regeneration. The gold standard for the repair of nerve defects is the autologous graft, since it provides the extracellular matrix (ECM) and cellular components of normal nerves and is not subject to immune rejection.^{2,3} Unfortunately, the autograft requires sacrificing a healthy donor nerve from the patient and its sources are limited, results in longer intraoperative time, and may produce site morbidity.⁴

A promising replacement of the nerve autograft is the decellularized nerve allograft.^{5,6,7} Decellularization provides immunogenic free scaffolds, preserving the ECM components and the biomechanical properties of the native nerve.^{8,9} Allografts offer several advantages over autografts, such as off-the-shelf availability, easy handling, and shorter surgical time.¹⁰ Since these grafts have been decellularized to avoid immune rejection, the lack of glial and other supporting cells limits the regenerative capability of allografts compared to autografts, especially when used to repair long gaps. From a translational perspective, the efficacy of new reparative grafts should be evaluated in models that closely resemble size and length of human nerves.^{2,11} Rodents, extensively used for preclinical studies, present faster axonal regeneration than humans, besides the small length of nerve gaps that can be produced, limiting their adequacy to evaluate long grafts.¹² Large animal models allow to investigate larger gaps and longer regeneration distances, simulating nerve injuries and regeneration seen in humans. Sheep are an adequate model to study nerve regeneration because their nerves are more similar to humans than rat nerves,¹³ and long gap injuries can be induced and repaired similar to humans.^{14,15}

In this study we assessed a novel decellularized nerve graft for repairing a 5 cm long gap in the peroneal nerve of sheep, compared to the gold standard autograft.

2. METHODS

2.1. Nerve decellularization

Peroneal nerves were harvested from four donor *Lacaune* sheep under aseptic conditions. Samples were stored in phosphate buffered saline (PBS) with antibiotic-antifungal agents (Sigma-Aldrich) and processed within 24 hours. Decellularization was made as described previously.^{9,16} Nerve samples longer than 5 cm were sequentially incubated in zwitterionic sulfobetaines 10 and 16, and non-ionic Triton X-100 detergent for 10 days, and then incubated in hypertonic 1M NaCl during 4 h and 0.1 mg/ml Pulmozyme DNASE (Roche, Barcelona, Spain) for 3 h.

For assessing the effectiveness of the decellularization procedure, small segments of each nerve were fixed in paraformaldehyde 4% and cryoprotected in PBS with saccharose 30%. Then, 15 µm thick transverse sections were obtained with a cryotome (Leica), and processed for immunohistochemistry with primary antibodies anti-rabbit S100 protein (Schwann cells; 1:50; 22520-DiaSorin), anti-goat neurofilament (NF200; myelinated axons; 1:400; AB5539-Millipore), and anti-rabbit laminin (1:500; AHP420-Biorad), and with myelin stain (Fluoromyelin; 1:300; F34651-Invitrogen). Following washes, sections were incubated with appropriate secondary antibodies conjugated to AlexaFluor 488 and AlexaFluor 594 (Invitrogen). The samples were viewed under fluorescence microscopy for detection of cell remnants and ECM scaffold.

Assessment of DNA content was made as described previously.⁹ Briefly, nerve tissue was digested with 0.5 mg/mL papain (Sigma-Aldrich) at 60°C for 3 h. DNA was isolated from the lysate with the DNeasy Blood and Tissue Kit (Qiagen), and quantified with the Picogreen DNA Quantification Kit (Invitrogen).

2.2. Animals and surgical procedure

All the procedures were approved by the Ethics Committee of our institution, and followed the European Community Council Directive 2010/63/EU on protection of animals used for scientific purposes. The study did not involve human subjects.

Ten adult female *ripollisa* sheep (*Ovis aries*), aged 3-5 years and weighing 54-78 kg, were used. They were from a different strain than the donor sheep. Sheep were randomized in two experimental groups: autograft (AG) (n=4) and decellularized allograft (DCA) (n=6). The surgical procedure was performed under sterile conditions by an expert nerve surgeon. Briefly, a skin incision along the thigh followed by splitting of semitendinous and biceps femoris muscles allowed to expose the peroneal nerve. A 5 cm gap was made and repaired with the same fragment of the peroneal nerve resected, maintaining the original orientation, as an ideal autograft, or with a decellularized allograft (Figure 1). In both cases, the two nerve stumps were sutured to each end of the graft with 8/0 epineural sutures.

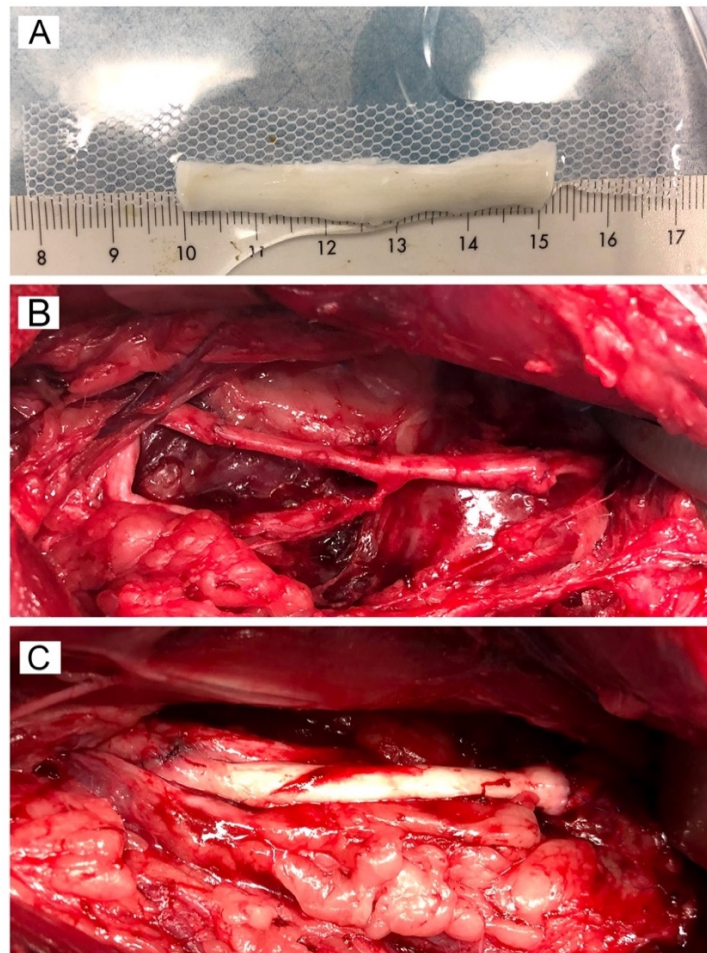


Figure 1. The decellularized peroneal nerve of sheep (A) was trimmed into 5-cm long segments. The same nerve segment resected was used as autograft (B) or the decellularized nerve allograft (C) was used to bridge the gap.

2.3. Functional evaluation

At monthly intervals until 9 months post-surgery (mps), sheep were tested for motor and sensory functional deficits of the operated hindlimb as previously described in detail.¹⁵ Parameters assessed focused on locomotion and footdrop during walking, and withdrawal reflex to pinching the skin of the dorsum of the hoof. Each test was scored in a scale from 0 (normal), -1 (partial loss), to -2 (complete loss).

Reinnervation of the tibialis anterior (TA) muscle was electrophysiologically assessed at 6.5 and 9 mps under general anesthesia with an electromyography (EMG) apparatus (Sapphyre 4ME, Vickers Healthcare, UK). The sciatic nerve was stimulated with transcutaneous needle electrodes placed at the sciatic notch, and the compound muscle action potential (CMAP) was recorded with monopolar needle electrodes.

Ultrasound examination of the TA muscle was performed at the same session, with a MyLab Gamma (Esaote, Genova, Italy) apparatus and a linear ultrasound probe. The size of the TA muscle was measured by determining cross-sectional area and perimeter using B-mode ultrasound, employing a 15 MHz linear transducer, and optimizing the image at a depth of 3 cm and focal point at 1.5 cm. The contralateral hindlimb was used as control in all the tests.

2.4. Histological evaluation

At the end of the follow-up, set up at 9 mps, animals were euthanized with an overdose of pentobarbital (400 mg/kg intravenously). Samples of the nerve graft, including at least 2 cm from proximal and distal sutures, were harvested, and fixed in paraformaldehyde 4% for 5 days at 4°C. Control samples were from the contralateral nerve. A 0.5 cm segment from the middle of the graft and from the distal end were embedded in paraffin and 5 µm thick cross-sections obtained with a microtome. Samples were deparaffinated and stained with hematoxylin/eosin to visualize the general structure of the nerve, or were processed for immunohistochemistry against Schwann cells (S100) and myelinated axons (NF200) as described above. Histological samples were viewed under light microscopy and immunolabeled sections under epifluorescence microscopy

(Olympus BX51). Quantitative analysis was performed by measuring the cross-sectional area of nerve grafts and distal nerve, and counting the number of NF200-labeled axons in systematically selected fields; the total number of regenerated myelinated axons was then calculated.

Segments of 0.5 cm from the middle of the graft and from the distal nerve were postfixed in 3% paraformaldehyde and 3% glutaraldehyde in PBS. Then, the segments were postfixed in osmium tetroxide, dehydrated in series of ethanol, and embedded in Epon resin. Semithin 0.5 μ m sections were stained with toluidine blue, and representative images taken by light microscopy.

2.5. Data analysis

Data are expressed as mean \pm standard error of the mean (SEM). Results of electrophysiological and echography tests and histology were analyzed by Student's t test and two-way ANOVA after checking for normal distribution, using GraphPad Prism 9 (GraphPad Software). The analysis for longitudinal functional evaluation tests was performed using a rank-transformation to obtain a non-parametrical approach prior to applying a Generalized Estimating Equations (GEE) model with an estimation of within-subject correlation from AR(1) approach, using SPSS version 26. These models included group of treatment, time and their interaction as factors. The significance level was set at 0.05 two-tailed.

3. Results

3.1. Effectiveness of the decellularization procedure

Immunolabeling against NF200 (myelinated axons), S100 (Schwann cells) and DAPI (marker of nucleus) indicated that cell contents were completely removed in the decellularized nerves, while the structure of the ECM and endoneurial tubules was preserved as shown by laminin and collagen IV labeling (Figure 2). The DNA content was below the 50 ng/mg threshold in the decellularized nerves (5.56 ± 2.78 ng/mg), significantly lower than in native nerves (476.13 ± 43.50 ng/mg).

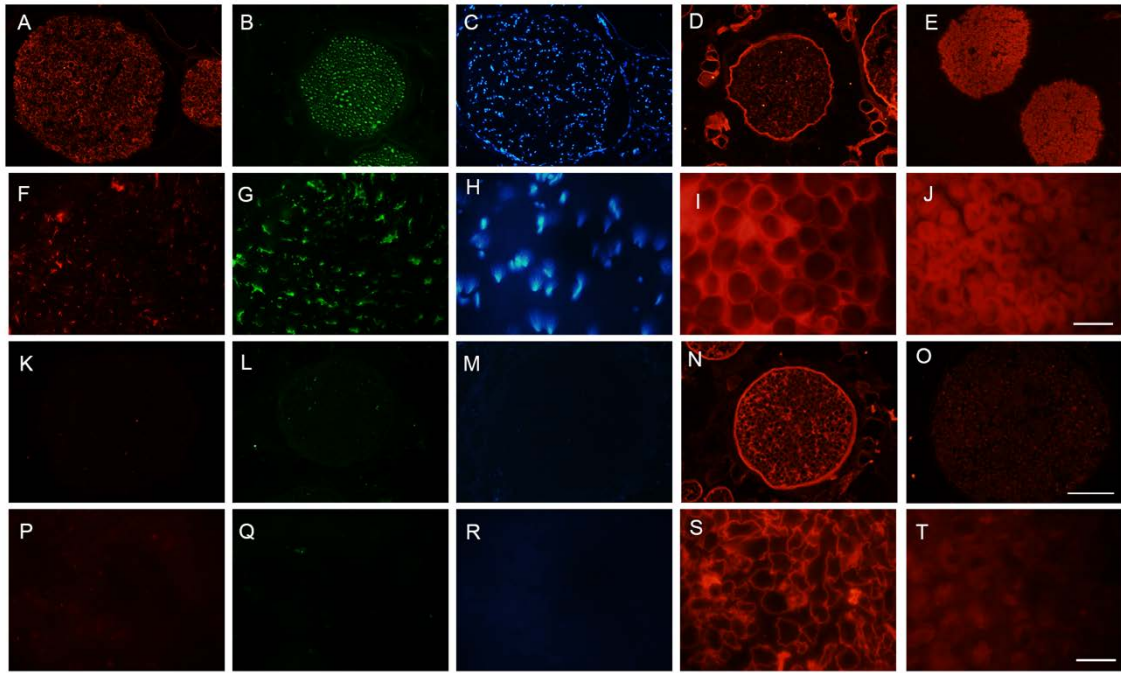


Figure 2. Representative micrographs showing immunofluorescence of Schwann cells (A, F, K, P), myelinated axons (B, G, L, Q), nuclei (C, H, M, R), extracellular matrix proteins (D, I, N, S) and myelin (E, J, O, T), in a control sheep peroneal nerve (A-J) and in a decellularized sheep peroneal nerve (K-T). A-E and K-O scale bar 150 μm , F-J and P-T scale bar 25 μm . Images F-J correspond to higher magnification of a field in images A-E, respectively, and images P-T correspond to higher magnification of a field in images K-O, respectively.

3.2. Functional results

After the surgery, all the sheep, except two animals of group DCA, were able to correctly maintain plantar support in orthostatic position. One DCA sheep required a splint during all the follow-up and was excluded from functional analyses. During fast walking, foot drop gait was evident in all sheep after surgery, as they failed to make plantar stepping in some steps. Significant improvement ($p > 0.05$) was observed from 150 days in the AG group and from 6 mps in the DCA group with respect to values at 1 mps (Figure 3A), but there were no significant differences between the two groups. The paw withdrawal response to pinching the skin of the dorsum of the hoof was completely abolished after the surgery. It reappeared at 5 mps, and improved in score, reaching significant

improvement ($p < 0.05$) from 6 mps compared to values at 1 mps in both groups (Figure 3B).

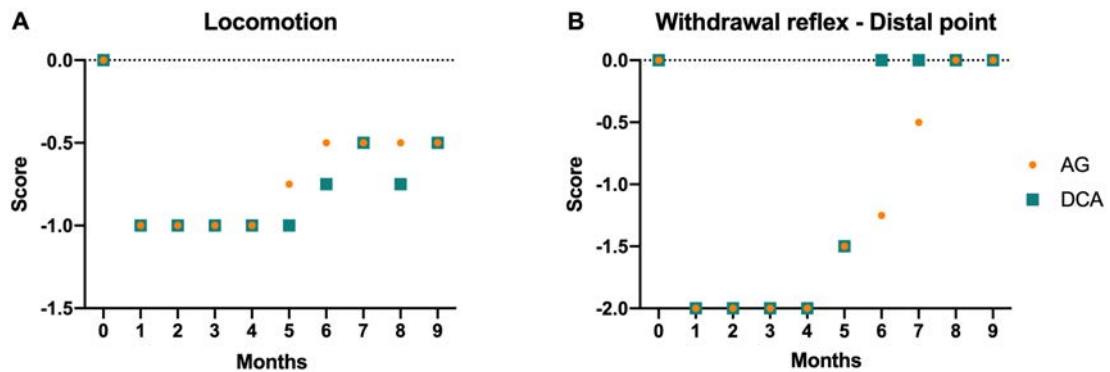


Figure 3. Plots of functional tests scoring during the 9 months follow-up. Both AG and DCA groups showed a similar evolution in locomotion (A) and in withdrawal reflex tests (B). Values are shown as the median. There were no significant differences between the two groups at any of the time points tested.

In the left control hindlimb, TA CMAP evoked by sciatic nerve stimulation had an onset latency of 3.7-4.8 msec and a peak amplitude of 17-25 mV. In the right operated hindlimb, at 6.5 mps, CMAPs of late latency and small amplitude were recorded in 3 of 4 animals from AG group (1.53 ± 0.67 mV) and in 2 of 5 from DCA group (0.09 ± 0.06 mV) (Figure 4). At 9 mps, CMAPs were recorded in all animals, with increased amplitude and without significant differences between groups (AG 5.0 ± 1.3 mV; DCA 3.3 ± 0.6 mV) (Figure 4B).

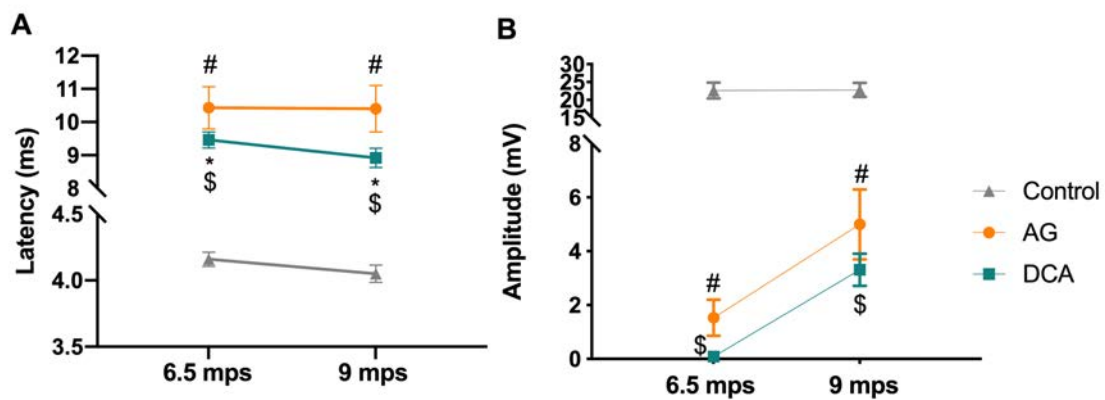


Figure 4. Plots of the latency (A) and the amplitude (B) of the TA CMAP recorded at 6.5 and 9 mps in AG (n=4) and DCA (n=6) groups, compared to the control

contralateral hindlimb (n=10). The CMAP amplitudes increased at 9 mps, without statistical differences between the AG and the DCA groups. In both groups, the amplitude was significantly lower than in control hindlimbs. * $p < 0.05$ vs DCA; # $p < 0.05$ vs control; \$ $p < 0.05$ vs control.

At 6.5 mps, the area and the perimeter of the TA muscle, assessed by echography, were lower in AG (area 2.61 ± 0.35 cm²; perimeter 7.92 ± 5.26 mm) and DCA groups (area 1.88 ± 0.09 cm²; perimeter 7.55 ± 1.61 mm) compared to the control muscle (area 6.13 ± 0.16 cm²; perimeter 11.16 ± 0.09 mm; $p < 0.0001$). At 9 mps, the size of the TA muscle increased in AG (area 3.43 ± 0.23 cm²; perimeter 8.79 ± 2.18 mm) and DCA groups (area 2.56 ± 0.26 cm²; perimeter 8.49 ± 2.67 mm) but was still significantly smaller than the control values ($p < 0.001$) (Figure 5).

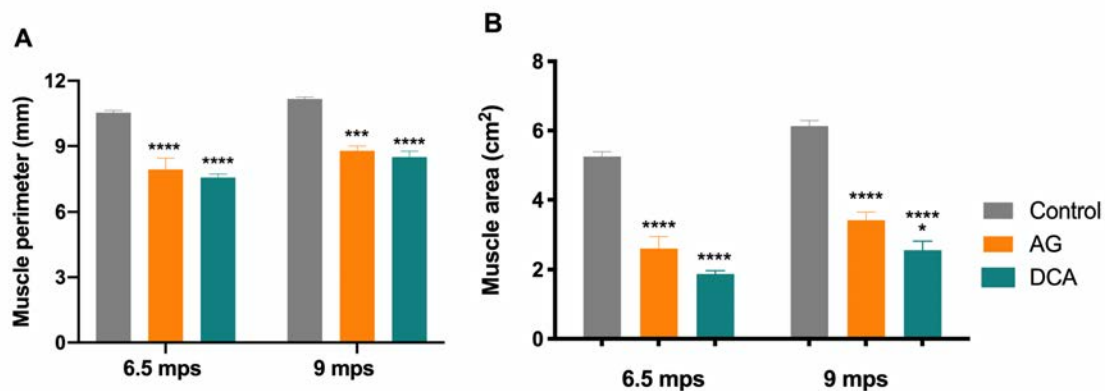


Figure 5. Histograms of the perimeter (A) and area (B) of the TA muscle obtained by ultrasound imaging. The size of the TA muscle was decreased in AG and DCA groups compared to the contralateral hindlimb (**** $p < 0.0001$ vs control). The TA muscle area was significantly higher in the AG group compared to DCA group (* $p < 0.05$) at the end of the follow-up.

The TA muscle was weighed fresh after extraction. The mean values were 40.0 ± 2.1 g and 33.8 ± 3.7 g in AG and DCA groups, respectively, both lower ($p < 0.05$) than the weight of control muscles (74.8 ± 4.5 g).

3.3. Histological results

The grafted nerves showed a well-preserved fascicular structure. Regenerating axons were observed both inside and outside the fascicles in the AG, but only inside the fascicles in DCA (Figure 6). Semithin sections stained with toluidine blue showed numerous myelinated and unmyelinated axons regenerating within the preserved fascicles, but also small clusters of axons regenerated outside the fascicles in the AG group (see Figure 6E and K). In the DCA group, the structure of the fascicles was preserved and contained regenerating axons, although axons were smaller than in the AG group.

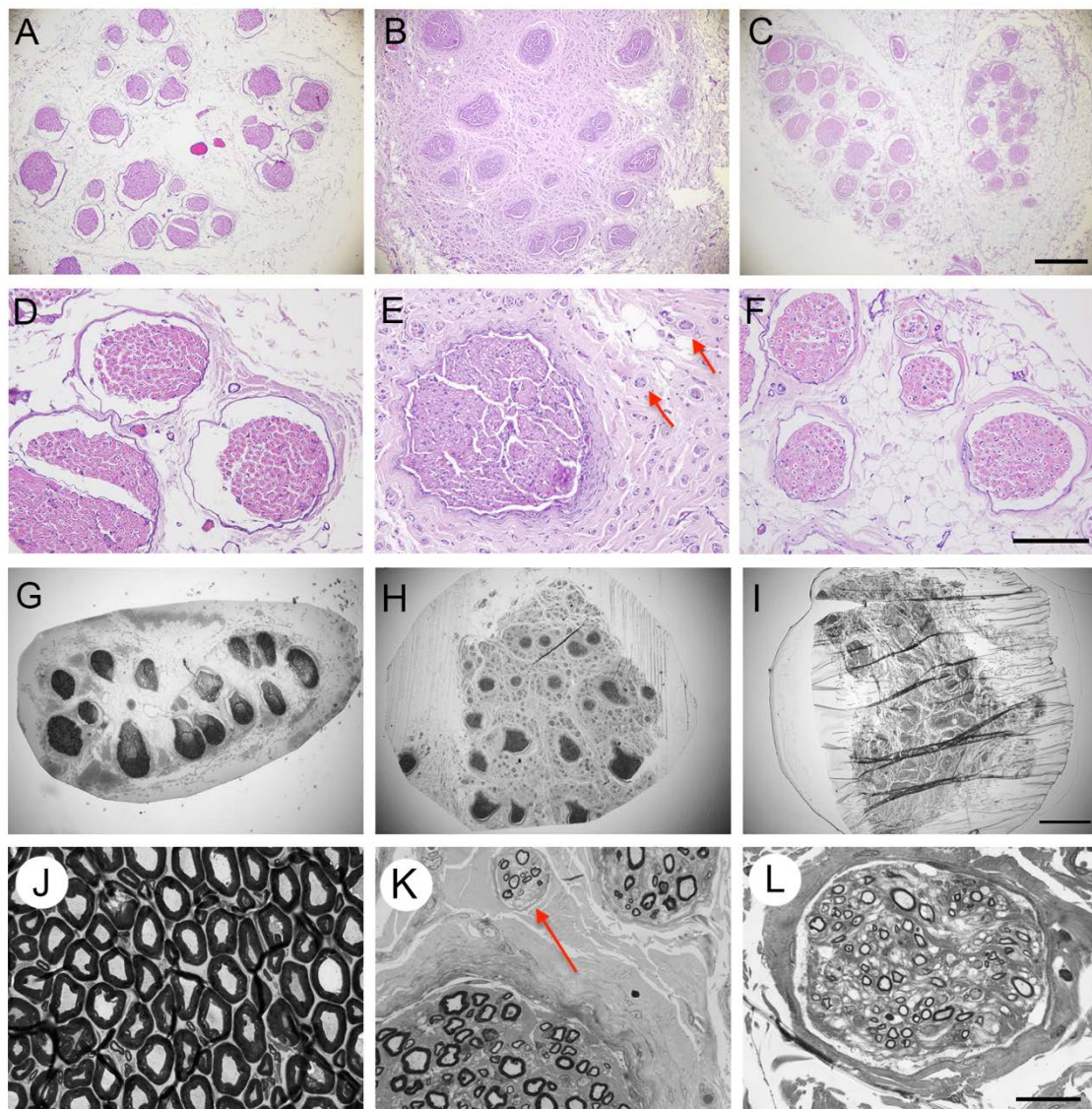


Figure 6. Representative micrographs of cross sections at the middle of the nerve graft of the sheep stained with hematoxylin and eosin. (A, D) control nerve, (B,

CHAPTER II

E) autograft and (C, F) decellularized nerve allograft; A, B, C scale bar 500 μ m, and D, E, F scale bar 150 μ m. Representative semithin transverse sections of the nerve graft stained with toluidine blue. (G, J) control nerve, (H, K) autograft, and (I, L) decellularized nerve allograft; G, H, I scale bar 500 μ m, and J, K, L scale bar 25 μ m. Red arrows in E and K point to the small regenerative clusters outside the defined fascicles in the AG group.

Distal to the nerve grafts, regenerating axons and Schwann cells grew inside the fascicles in both experimental groups (Figure 7). The mean number of NF200-labeled myelinated axons was $21,676 \pm 3,716$ axons in the control peroneal nerve, while in the middle segment of the grafts there were $26,213 \pm 2,798$ axons in the AG group, and $18,724 \pm 3,410$ axons in the DC group. The mean values in the distal nerve were $20,600 \pm 6,082$ axons in AG group and $7,780 \pm 1,871$ axons ($p < 0.05$ vs AG) in DCA group.

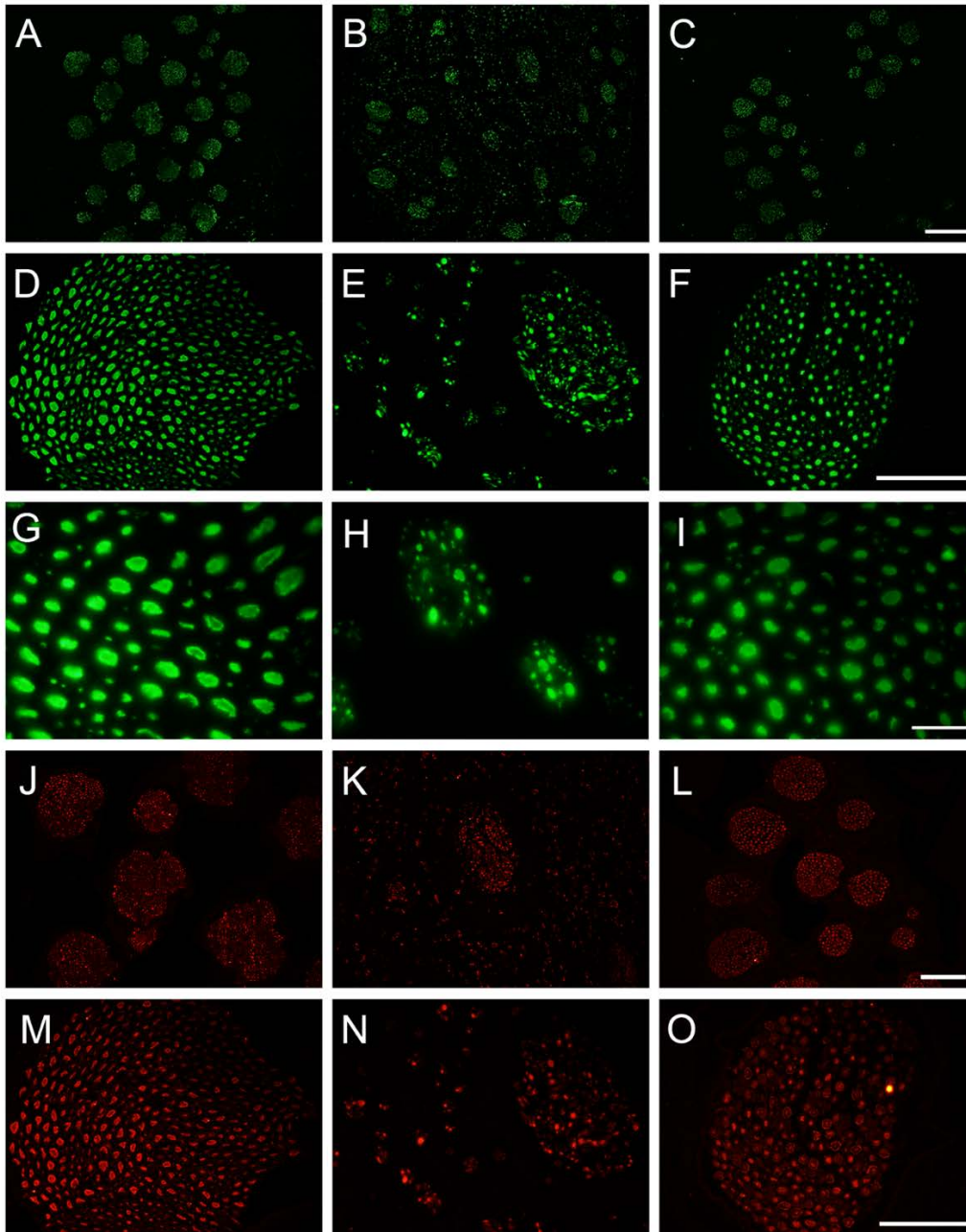


Figure 7. Representative micrographs of cross sections at the middle of the nerve graft showing immunofluorescence of myelinated axons labeled against Neurofilament 200 of a control nerve (A, D, G), an autograft (B, E, H) and a decellularized allograft (C, F, I). Note that image H is focused on some small regenerating clusters outside the main graft fascicles. A, B, C scale bar 500 μm ; D, E, F scale bar 100 μm ; G, H, I scale bar 25 μm . Representative micrographs of cross sections of the nerve graft labeled against S100 protein of control (J, M), AG (K, N) and DCA (L, O) sheep. J, K, L scale bar 200 μm and M, N, O scale bar 100 μm .

4. Discussion

In a previous study, we demonstrated that a rat allograft, decellularized following a new protocol, effectively promoted axonal regeneration in the rat sciatic model along a critical gap of 15 mm length.¹⁶ In this study, we have evaluated the regenerative potential of this decellularized nerve allograft in a large animal such as the sheep. The sheep hindlimb nerves are adequate for investigating new repair procedures with potential clinical translation, since they have similar size and length to human limb nerves.^{17,18} Moreover, they are mixed nerves, causing both motor and sensory deficits after injury that can be assessed over time with techniques commonly used in humans.^{14,15}

Our results indicate that the decellularization protocol used is highly efficient to eliminate cells, including Schwann cells, and DNA content from the nerve of sheep, while preserving the ECM and endoneurial tubules, similar to what was proved with rat and human nerves.^{9,16} Therefore, no immune rejection was observed using such decellularized nerve grafts in our studies.

Repair was carried out with 5 cm long decellularized allografts or autografts. This is a nerve defect of clinical relevance, since available nerve conduits approved for clinical use have a maximal gap length limited to 2-3 cm.¹⁷ Besides, when repairing digital nerve injuries with a short gap, autograft and allograft performed comparably and were superior to conduit repair.¹⁹ The only marketed acellular nerve allograft, Avance[®] Nerve Graft (Axogen, Alachua, FL) is indicated for repairing human nerve defects up to 5 cm, but it provides meaningful recovery only in a third of repairs of gaps 5 to 7 cm in lower limb nerves.²⁰ Previous studies in sheep peroneal nerve assaying decellularized allografts in gaps of 3 cm²¹ and 7 cm²² showed effective regeneration, whereas cold-preserved nerve allografts failed to support regeneration along an 8 cm gap.²³ Other assays in sheep used sciatic and tibial nerves repaired with nerve conduits leaving 6 cm gap,^{24,25} and with recellularized allografts in a 2 cm gap,²⁶ with results that were lower but approached those obtained with autologous nerve grafts.

Reinnervation and regeneration were evaluated by functional, electrophysiological, and echographic evaluations and with final histological

analyses. Animals of both experimental groups showed functional recovery in locomotion and in sensory responses to a similar level. Electrophysiological tests showed reinnervation of the TA muscle in all the animals at the end of the follow-up, although with slightly lower CMAP amplitude in group DCA. Besides, the size and weight of the TA muscle were lower in group DCA than in group AG. These results suggest that axonal regeneration was slower in the decellularized nerve graft compared to autograft, as expected due to the lack of Schwann cells that give support to regenerating axons.^{4,27} However, the levels of recovery may become similar with more time, considering that the slope of the CMAP amplitude along time was parallel in AG and DCA groups. Moreover, it is worth noting that the autograft we used was an “ideal” graft, i.e., the same segment of nerve resected and resutured, that allows higher regeneration than smaller caliber nerve grafts,²⁸ commonly used in the clinic.

The number of regenerated axons at the mid portion of the graft was similar in AG and DCA groups, and in the range of the control peroneal nerve. However, distal to the graft regenerated axons were significantly less in the DCA group compared to the AG group, a fact indicative of a slower regeneration rate in decellularized grafts. Interestingly, growth of myelinated axons in the decellularized graft was circumscribed to the endoneurium of the preserved fascicles, whereas in the autograft some axons regenerated extra-fascicularly. Other studies, using different types of allografts,^{2,23,29,30} found considerable regenerated axons following an extrafascicular route, indicating that the ECM was not so consistent. Therefore, the histological findings of our study suggest that the decellularization protocol used maintains the structural properties of the nerve and favors regeneration within the preserved fascicular paths.

5. Conclusion

Our results prove the translational potential of this new decellularization protocol that guarantees elimination of the cellular contents while preserving the ECM of the nerve graft. This decellularized graft may become an alternative to the autograft for repairing defects of at least 5 cm in large nerves. Moreover, it may

CHAPTER II

constitute the basis for an enhanced graft if re-cellularized with mesenchymal stem cells or Schwann cells from the same or compatible individuals.

References

1. Kasper M, Deister C, Beck F, Schmidt CE. Bench-to-bedside lessons learned: commercialization of an acellular nerve graft. *Adv Healthc Mater* 2020; 9(16):e2000174. doi:10.1002/adhm.202000174
2. Forden J, Xu QG, Khu KJ, Midha R. A long peripheral nerve autograft model in the sheep forelimb. *Neurosurgery* 2011; 68(5):1354-1362. doi:10.1227/NEU.0b013e31820c08de
3. Cai J, Peng X, Nelson KD, Eberhart R, Smith GM. Synergistic improvements in cell and axonal migration across sciatic nerve lesion gaps using bioresorbable filaments and heregulin-beta1. *J Biomed Mater Res A* 2004; 69(2):247-258. doi:10.1002/jbm.a.20119
4. Moore AM, MacEwan M, Santosa KB, et al. Acellular nerve allografts in peripheral nerve regeneration: a comparative study. *Muscle Nerve* 2011; 44(2):221-234. doi:10.1002/mus.22033
5. Hundepool CA, Nijhuis TH, Kotsougiani D, Friedrich PF, Bishop AT, Shin AY. Optimizing decellularization techniques to create a new nerve allograft: an in vitro study using rodent nerve segments. *Neurosurg Focus* 2017; 42(3):E4. doi:10.3171/2017.1.FOCUS16462
6. Lovati AB, D'Arrigo D, Odella S, Tos P, Geuna S, Raimondo S. Nerve repair using decellularized nerve grafts in rat models. A review of the literature. *Front Cell Neurosci* 2018; 12:427. doi:10.3389/fncel.2018.00427
7. Philips C, Campos F, Roosens A, Sánchez-Quevedo MDC, Declercq H, Carriel V. Qualitative and quantitative evaluation of a novel detergent-based method for decellularization of peripheral nerves. *Ann Biomed Eng* 2018; 46(11):1921-1937. doi:10.1007/s10439-018-2082-y
8. Szykaruk M, Kemp SW, Wood MD, Gordon T, Borschel GH. Experimental and clinical evidence for use of decellularized nerve allografts in peripheral nerve gap reconstruction. *Tissue Eng Part B Rev* 2013; 19(1):83-96. doi:10.1089/ten.TEB.2012.0275
9. Nieto-Nicolau N, López-Chicón P, Fariñas O, et al. Effective decellularization of human nerve matrix for regenerative medicine with a novel protocol. *Cell Tissue Res* 2021; 384(1):167-177. doi:10.1007/s00441-020-03317-3
10. Immerman I. Allograft nerve reconstruction: the new gold standard?: Commentary on an article by Peter Tang et al.: "No difference in outcomes detected between decellular nerve allograft and cable autograft in rat sciatic

- nerve defects". *J Bone Joint Surg Am* 2019; 101(10):e48. doi:10.2106/JBJS.19.00168
11. Atchabahian A, Genden EM, MacKinnon SE, Doolabh VB, Hunter DA. Regeneration through long nerve grafts in the swine model. *Microsurgery* 1998; 18(6):379-382. doi:10.1002/(sici)1098-2752(1998)18:6<379::aid-micr7>3.0.co;2-5
 12. Tos P, Ronchi G, Papalia I, et al. Chapter 4: Methods and protocols in peripheral nerve regeneration experimental research: part I-experimental models. *Int Rev Neurobiol* 2009; 87:47-79. doi:10.1016/S0074-7742(09)87004-9
 13. Matsuyama T, Midha R, Mackinnon SE, Munro CA, Wong PY, Ang LC. Long nerve allografts in sheep with Cyclosporin A immunosuppression. *J Reconstr Microsurg* 2000; 16(3):219-225. doi:10.1055/s-2000-7556
 14. Alvites, R.D.; Branquinho, M.V.; Sousa, A.C.; Zen, F.; Maurina, M.; Raimondo, S.; Mendonça, C.; Atayde, L.; Geuna, S.; Varejão, A.S.P.; et al. Establishment of a sheep model for hind limb peripheral nerve injury: common peroneal nerve. *Int J Mol Sci* 2021; 22(3):1401. doi:10.3390/ijms22031401
 15. Contreras E, Traserra S, Bolívar S, et al. Repair of long peripheral nerve defects in sheep: a translational model for nerve regeneration. *Int J Mol Sci* 2023; 24(2):1333. doi:10.3390/ijms24021333
 16. Contreras E, Bolívar S, Nieto-Nicolau N, et al. A novel decellularized nerve graft for repairing peripheral nerve long gap injury in the rat. *Cell Tissue Res* 2022a; 390(3):355-366. doi:10.1007/s00441-022-03682-1
 17. Kornfeld T, Vogt PM, Radtke C. Nerve grafting for peripheral nerve injuries with extended defect sizes. *Wien Med Wochenschr* 2019; 169(9-10):240-251. doi:10.1007/s10354-018-0675-6
 18. Roballo KCS, Burns DT, Ghnenis AB, Osimanjiang W, Bushman JS. Long-term neural regeneration following injury to the peroneal branch of the sciatic nerve in sheep. *Eur J Neurosci* 2020; 52(10):4385-4394. doi:10.1111/ejn.14835
 19. Herman ZJ, Ilyas AM. Sensory outcomes in digital nerve repair techniques: an updated meta-analysis and systematic review. *Hand (N Y)* 2020; 15(2):157-164. doi: 10.1177/1558944719844346
 20. Safa B, Jain S, Desai MJ, et al. Peripheral nerve repair throughout the body with processed nerve allografts: Results from a large multicenter study. *Microsurgery* 2020; 40(5):527–537. doi.org/10.1002/micr.30574

21. Tamez-Mata Y, Pedroza-Montoya FE, Martínez-Rodríguez HG, et al. Nerve gaps repaired with acellular nerve allografts recellularized with Schwann-like cells: preclinical trial. *J Plast Reconstr Aesthet Surg* 2022; 75(1):296–306. doi.org/10.1016/j.bjps.2021.05.066.
22. Contreras E, Traserra S, Bolívar S, et al. Repair of long nerve defects with a new decellularized nerve graft in rats and in sheep. *Cells* 2022b; 11(24):4074. doi:10.3390/cells11244074
23. Strasberg SR, Mackinnon SE, Genden EM, et al. Long-segment nerve allograft regeneration in the sheep model: experimental study and review of the literature. *J Reconstr Microsurg* 1996; 12(8):529-37. doi:10.1055/s-2007-1006625.
24. Radtke C, Allmelting C, Waldmann KH, et al. Spider silk constructs enhance axonal regeneration and remyelination in long nerve defects in sheep. *PLoS One* 2011; 25: e16990. doi:10.1371/journal.pone.0016990.
25. Kornfeld T, Nessler J, Helmer C, et al. Spider silk nerve graft promotes axonal regeneration on long distance nerve defect in a sheep model. *Biomaterials* 2021; 271:120692. doi: 10.1016/j.biomaterials.2021.120692.
26. Pedroza-Montoya FE, Tamez-Mata YA, Simental-Mendía M, et al. Repair of ovine peripheral nerve injuries with xenogeneic human acellular sciatic nerves prerecellularized with allogeneic Schwann-like cells – an innovative and promising approach. *Regen Ther* 2022; 19:131–43. doi:10.1016/j.reth.2022.01.009.
27. Hall SM. Regeneration in cellular and acellular autografts in the peripheral nervous system. *Neuropathol Appl Neurobiol* 1986; 12(1):27-46. doi:10.1111/j.1365-2990.1986.tb00679.x
28. Rodríguez FJ, Verdú E, Ceballos D, Navarro X. Nerve guides seeded with autologous Schwann cells improve nerve regeneration. *Exp Neurol* 2000; 161(2):571-84. doi: 10.1006/exnr.1999.7315.
29. Gómez N, Cuadras J, Butí M, Navarro X. Histologic assessment of sciatic nerve regeneration following resection and graft or tube repair in the mouse. *Restor Neurol Neurosci* 1996; 10(4):187-196. doi:10.3233/RNN-1996-10401
30. Evans PJ, MacKinnon SE, Midha R, Wade JA, Hunter DA, Nakao Y, Hare GM. Regeneration across cold preserved peripheral nerve allografts. *Microsurgery* 1999;19(3):115-27. doi: 10.1002/(sici)1098-2752(1999)19:3<115::aid-micr1>3.0.co;2-9.

Chapter III

Evaluation of a decellularized allograft optimized by Verigrift to repair severe peripheral nerve injuries in rats and in sheep

Repair of Long Nerve Defects with a New Decellularized Nerve Graft in Rats and in Sheep

Estefanía Contreras^{1,2}, Sara Traserra^{1,2}, Sara Bolívar^{1,3}, Joaquím Forés^{1,4}, Eduard Jose-Cunilleras⁵, Ignacio Delgado-Martínez^{1,3}, Félix García⁵, Esther Udina^{1,3} and Xavier Navarro^{1,3}

1. Institute of Neurosciences, Department Cell Biology, Physiology and Immunology, Universitat Autònoma de Barcelona, 08193 Bellaterra, Spain

2. Integral Service for Laboratory Animals (SIAL), Faculty of Veterinary, Universitat Autònoma de Barcelona, 08193 Bellaterra, Spain

3. Centro de Investigación Biomédica en Red Sobre Enfermedades Neurodegenerativas (CIBERNED), 28031 Madrid, Spain

4. Hand and Peripheral Nerve Unit, Hospital Clínic i Provincial, Universitat de Barcelona, 08036 Barcelona, Spain

5. Department of Animal Medicine and Surgery, Universitat Autònoma de Barcelona, 08193 Bellaterra, Spain

6. VERIGRAFT AB, Arvid Wallgrens Backe 20, 41346 Göteborg, Sweden

Cells **2022**, *11*, 4074

Abstract: Decellularized nerve allografts (DC) are an alternative to autografts (AG) for repairing severe peripheral nerve injuries. We have assessed a new DC provided by VERIGRAFT. The decellularization procedure completely removed cellularity while preserving the extracellular matrix. We first assessed the DC in a 15 mm gap in the sciatic nerve of rats, showing slightly delayed but effective regeneration. Then, we assayed the DC in a 70 mm gap in the peroneal nerve of sheep compared with AG. Evaluation of nerve regeneration and functional recovery was performed by clinical, electrophysiology and ultrasound tests. No significant differences were found in functional recovery between groups of sheep. Histology showed a preserved fascicular structure in the AG while in the DC grafts regenerated axons were grouped in small units. In conclusion, the DC was permissive for axonal regeneration and allowed to repair a 70 mm long gap in the sheep nerve.

1. Introduction

Peripheral nerve injuries results in partial or total loss of the sensory, autonomic and motor functions dependent on the injured nerve, with important consequences for the quality of life of affected patients [1]. It is estimated that more than 300,000 persons are affected by traumatic nerve injury every year in North America and Europe [2,3]. Although peripheral neurons are able to regenerate after axotomy, and eventually reinnervate target organs, functional recovery is often unsatisfactory, especially following severe injuries [4,5]. Poor functional outcomes generally stem from long regenerative distances coupled with a relatively slow rate of axonal regeneration (~1–2 mm/day), creating prolonged periods of denervation that ultimately limit the regenerative capacity of the distal nerve structure [6,7]. Therefore, a special challenge regarding recovery after peripheral nerve injury are long distance nerve defects and proximal injuries in long limbs.

When the length of the gap created by a nerve injury is too long to allow apposition and direct suture without tension, nerve grafts are usually employed for repairing. The graft between the stumps of a transected nerve offers mechanical guidance, and the Schwann cells of the graft and their basal lamina play an essential role in promoting axonal growth [8]. The autologous nerve graft represents the “gold standard” surgical treatment for complex peripheral nerve injuries in the clinic; however, autografts present a number of limitations. Apart from the paucity of expendable nerve tissue, harvesting autologous nerves results in significant donor site morbidity, increased risk of infection, and longer intraoperative times [9]. The alternative use of allografts has been discouraging, since the immune rejection directed against Schwann cells and myelin sheaths of the graft impedes axonal regeneration [10]. Processed acellular nerve allograft has been promoted as a potential replacement [9,11]. If adequately decellularized, such grafts do not induce immune response, whereas the internal nerve structure, including endoneurial tubules, basal lamina and extracellular matrix (ECM) components, remains supporting axonal regeneration, despite the absence of the activated Schwann cells [8].

Allograft and autograft repair of nerve defect injury in small animals have indicated that regeneration is possible on critical length nerve gaps [12,13]. Even though the anatomy of rodent nerves has been well studied and is similar to that of humans [14], the important difference in size between these species compared to humans limits the translation of the results obtained, since axonal regeneration is faster in smaller animals and relatively short gaps can be produced in them [15,16]. Indeed, it is not clear if the mechanisms involved in peripheral nerve trauma, repair and regeneration are closely conserved across species [6,16,17]. In order to achieve results that may be applicable to humans, a translational large animal model for peripheral nerve surgery is important [6,17,18]. A valid animal model for nerve regeneration studies should have similar anatomy and length of the nerves to humans and follow a similar regeneration rate after nerve injury. Sheep have emerged as one of the most adequate large animals for pre-clinical studies on a variety of peripheral nerves [18–23]. Thus, experimental studies in small and large animal models are fundamental to optimize the decellularization process and to evaluate the regenerative capacity of novel allografts. In this study, we assessed a newly prepared decellularized nerve graft used for repairing a critical gap of 15 mm of the sciatic nerve in rats, and given the obtained success, we extended to a comparative assessment of nerve regeneration along a nerve gap of 70 mm length in the peroneal nerve of adult sheep repaired with the new decellularized nerve graft, provided by VERIGRAFT AB, or with an autograft as the gold standard method of repair.

2. Materials and Methods

2.1. Nerve Decellularization

Rat sciatic nerves were harvested from five euthanized Sprague Dawley rats under aseptic conditions. Specimens of sheep nerves for the decellularized allografts were obtained from four donor sheep from the colony of Servei de Granges i Camps Experimentals (SGiCE) of the Universitat Autònoma de Barcelona (UAB). Peroneal nerves were harvested from euthanized sheep under aseptic conditions. The harvested nerves were stored in phosphate buffered

saline (PBS) plus antibiotic-antimycotic agents, maintained at 4 °C and shipped to VERIGRAFT AB.

For decellularization, the nerves were thawed and agitated in NaCl (Fisher Scientific, Göteborg, Sweden) for 24 h, PBS (Medicago, Uppsala, Sweden) for 6 h and Deoxyribonuclease (DNase; VWR, Stockholm, Sweden) overnight. The nerves were washed 3 × 5 min in H₂O after NaCl and DNase. This process was repeated three times. Then the nerves were washed in PBS for 24 h. After decellularization, samples were taken for DNA quantification and histology before peracetic acid sterilization and final washes in PBS under sterile conditions. The sterilized decellularized nerves were shipped in PBS at 2–4 °C. One nerve segment was decellularized for each animal to be transplanted. DNA was extracted from 10–25 mg wet tissue with the DNeasy Blood & Tissue kit (Qiagen, Mettmann, Germany) and quantified with the Qubit dsDNA HS assay kit (Invitrogen, Waltham, MA, USA), according to the manufacturer's instructions. DNA concentration was calculated using the DNA standard supplied with the Qubit dsDNA HS assay kit.

After decellularization, a small segment of each decellularized nerve was fixed in paraformaldehyde 4% for 4 h at room temperature (RT) and then transferred to PBS with sucrose 30% for 24 h. Samples were cryo-embedded with OCT and serially cut in 15 µm thick transverse sections with a cryotome. The sections were blocked and permeabilized with 0.3% Triton-X100 and 10% normal donkey serum and/or goat donkey serum for 1 h. Then, slides were incubated overnight at 4 °C with primary antibodies against anti-rabbit S-100 protein (S100; to label Schwann cells; 1:50; 22520-DiaSorin), anti-chicken neurofilament (NF200; myelinated axons; 1:400; AB5539-Millipore), anti-rabbit non-collagenous connective tissue glycoprotein (laminin; 1:500; AHP420-Biorad), and with myelin stain (Fluoromyelin; 1:300; F34651-Invitrogen), all diluted in 0.1% Triton-PBS. Following three washes in PBS, the sections were incubated with secondary antibodies conjugated to Alexa Fluor 488 goat anti-chicken (1:200; A11039-Invitrogen) and Alexa Fluor 594 goat anti-rabbit (1:200; A21207-Invitrogen) for 1 h. After two washes with PBS, samples were incubated with DAPI stain for nuclei (1:100; D9564-10MG-Sigma) diluted in PBS for 2 min. After three more washes

in PBS, immunolabeled sections were cover-slipped with Fluoromount (Sigma-Aldrich, St. Louis, MI, USA) and viewed under epifluorescence microscopy (Olympus BX51).

All the procedures were approved by the Ethics Committees of the UAB and Generalitat de Catalunya, and followed the European Community Council Directive 2010/63/EU of the European Parliament on the protection of animals used for scientific purposes.

2.2. Rat Study

For the implantation, ten female Sprague Dawley rats (12 weeks of age) were randomly assigned into two different experimental groups: autograft (AG) (n=5) or decellularized rat allograft (DRA) (n=5). Animals were anesthetized with ketamine (75 mg/kg) and medetomidine (0.01 mg/kg) intraperitoneally. A skin incision was made on the right hindlimb and the biceps femoris muscle was incised to expose the sciatic nerve. A 15 mm in length was removed and then, in the AG group, the same nerve was sutured again maintaining the same orientation. In the DRA group, the nerve removed was substituted by a 15 mm length decellularized rat allograft. In both cases, the proximal and distal nerve stumps were sutured by 10-0 nylon epineural sutures. Postoperative care included amitriptyline (20 mL/L) in drinking water to prevent autotomy [24] and buprenorphine (0.03 mg/kg subcutaneously) to treat postoperative pain.

Reinnervation of target muscles were assessed by monthly noninvasive nerve conduction tests until the end time, set at 120 days post injury (dpi). Under general anesthesia, the rat was placed on a warm plate, and the sciatic nerve was stimulated with transcutaneous needle electrodes placed at the sciatic notch using a Sapphire 4M electromyograph (EMG) (Medelec, Vickers, Surrey, U.K.), by delivering single pulses of 0.1 ms of increasing intensity. The compound muscle action potential (CMAP) was recorded from the tibialis anterior (TA), gastrocnemius (GM) and plantar interosseus (PL) muscles with small needle electrodes transcutaneously placed on the active muscle belly and the reference in the fourth toe [25,26]. The ground electrode was placed at the knee. The contralateral hindlimb was used as a control since there are not significant

changes in electrophysiological properties of the contralateral limb after a unilateral nerve lesion [25].

At the end of the study, animals were euthanized by an overdose of pentobarbital (200 mg/kg i.p.) and samples from the sciatic nerve were harvested. Samples were fixed in paraformaldehyde 4% and then, divided in three different parts. The proximal and distal segments, including suture levels were post-fixed in 3% glutaraldehyde-3% paraformaldehyde in cacodylate-buffer solution (0.1 M, pH 7.4) at 4 °C for 48 h. To evaluate the microstructure of the nerve, samples were embedded in epon resin. Semithin 0.5 µm sections were stained with 1% toluidine blue and visualized with a light microscope (Olympus BX40). The cross-sectional area of the whole nerve was measured at 40X. Images were obtained at 1000X from fields chosen by systematic sampling of squares, representing at least 30% of the transverse area of the nerve [27,28]. Counts of the number of myelinated nerve fibers were conducted using ImageJ software (version 1.52d). Only myelinated fibers whose contour was completely within each field photograph or cut at two borders of the square were counted. The total number of myelinated fibers per nerve was obtained from the fiber density of the sampled fields and the total transverse endoneurial area. The middle segment of the sciatic nerve was processed for immunolabeling as explained above for axons (NF200), Schwann cells (S100), laminin and macrophages (anti-goat iba 1; ionized calcium-binding adapter molecule 1; 1:500; 19-19741-Rafer). Samples were washed and incubated with secondary antibodies Alexa Fluor 488 goat anti-chicken (1:200; A11039-Invitrogen), Alexa Fluor 488 donkey anti-goat (1:200; A11055-Invitrogen) and Alexa Fluor 594 goat anti-rabbit (1:200; A21207-Invitrogen) diluted in PBS-Triton 0.3%. Finally, sections were cover-slipped with Fluoromount containing DAPI (1:10,000; Sigma-Aldrich). Sections were visualized with an epifluorescence microscope (Olympus BX51) for qualitative assessment of the regeneration process. Observations were focused on the relationship between axons and Schwann cells and the number of infiltrating macrophages.

2.3. Sheep Study

Ten female ripollesa sheep (*Ovis aries*), weighing 55–75 Kg, from the animal facility of SGiCE of the UAB were used. The sheep were divided in two experimental groups of 5 animals each, according to the repair procedure performed: autograft and decellularized allograft. A blood sample was taken before the surgery and at the end of the study to perform hematological and biochemical standard analyses, to ensure that the sheep were in good health state. A general clinical assessment was performed once a week until the end of the study.

2.4. Surgical Procedure

The animals were fasted 16 h prior to the surgery to reduce the ruminal content and prevent deviant swallowing. Animals were sedated by midazolam (0.2 mg/Kg) and morphine (0.4 mg/Kg i.m.). Anesthesia was induced by propofol (4 mg/Kg i.v.) and maintained by isoflurane 2% in 2 L/min oxygen administered with a pressure-controlled ventilator. Analgesia was provided by diazepam (0.5 mg/Kg i.v.), and an antibiotic dose of cefazoline (20 mg/Kg i.v.). Fluid therapy was applied with Ringer solution infusion (10 mL/Kg/h).

The operative procedure was conducted using a sterile technique with the sheep in a left lateral decubitus position on an operating table. On the right hindlimb, the peroneal nerve was exposed using a longitudinal lateral skin incision along the thigh followed by splitting of the semitendinous and biceps femoris muscles. Under the operating microscope, the common peroneal nerve was resected 1 cm above the iliac vein to create a 7 cm gap. The repair was conducted by bridging the two nerve stumps with a decellularized nerve allograft or with an autograft (Figure 1). The resected nerve segment was used as autograft maintaining the original orientation. The decellularized nerve graft was easy to handle and suture, without notable difference compared with the nerve autograft. The nerve stumps were sutured to each end of the graft by means of 8/0 epineural sutures. The suture resistance was tested against light stretching. The incision was closed in layers and disinfected with chlorhexidine and Aluspray®. After the surgery, the animals were allowed to recover in couples in the animal's facility. During the

post-operative period, analgesia was provided twice a day with buprenorphine (0.01 mg/Kg s.c.) for 2 days and once a day with meloxicam (0.2 mg/Kg s.c.) for 3 days.

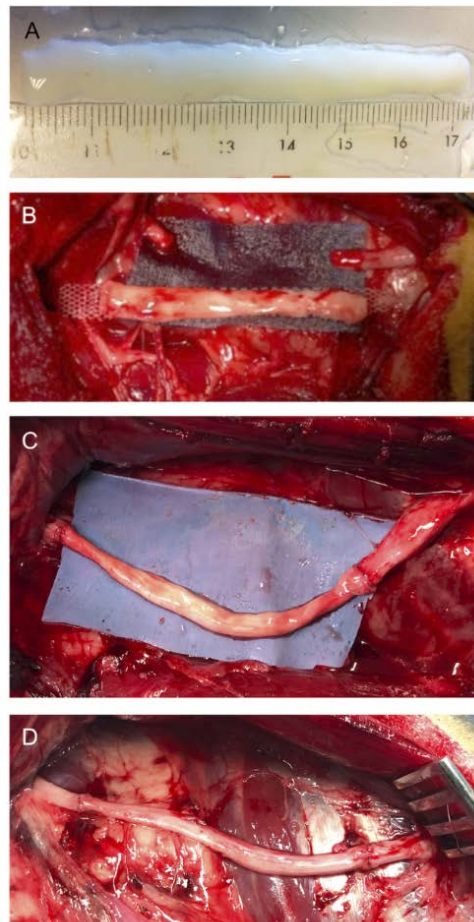


Figure 1. Decellularized nerve allograft (A) was trimmed into 7-cm nerve long and then it was placed into the gap created in the common peroneal nerve (B). The decellularized nerve allograft (C) or the same nerve segment resected used as autograft (D) were sutured bridging the gap.

2.5. Functional Tests

At monthly intervals, animals were tested for evidence of hindlimb functional recovery. Each parameter was assessed in a semiquantitative arbitrary scale from 0 (no deficit), -1 (partial deficit or functional loss) to -2 (complete loss of response in the maneuver tested). Locomotion was assessed qualitatively while freely walking in the stable, paying particular attention to the foot-drop position of the operated hindlimb (0 = normal walking; -1 = a few failures; -2 = foot drop in most steps). The TA muscle mass was assessed by manual palpation comparing

both the denervated and control side (0 = similar mass; -1 = slight reduction; -2 = marked reduction). The proprioceptive response was tested by the capability of replacing the hoof from a plantarflexion position forced by the experimenter to a plantar support position (0 = consistent response; -1 = one failure; -2 = two or 3 failures). The withdrawal reflex of the limb was evaluated by pinching with a hemostat the skin of the dorsum of the paw at three sites between the ankle and the hoof (Figure S1), proximal, middle and distal. Each site was tested twice in the same session and separately scored as: 0 = fast and strong withdrawal response of the limb; -1 = weak response or not consistent in the 2 trials; -2 = no response in 2 trials.

2.6. Electrophysiological Tests

Motor nerve conduction tests were performed at 5, 6.5 and 9 months post surgery (mps) under general anesthesia (diazepam 0.25 mg/Kg and ketamine 5 mg/Kg i.v.). An EMG apparatus (Sapphire 4ME, Vickers, Surrey, U.K.) was used for these tests. The sciatic nerve was stimulated, at supramaximal intensity, at the sciatic notch with a pair of percutaneous needle electrodes, and the compound muscle action potential (CMAP) was recorded from the TA muscle with monopolar needle electrodes, the active electrode on the muscle belly, and the reference at the distal tendon. Moreover, free-running EMG recordings were made to detect fibrillation potentials, as a sign of muscle denervation. The contralateral hindlimb was tested at the same session and its values used as control.

2.7. Ecographic Evaluation of Hindlimb Muscles

Ultrasound examinations were performed at 6.5 and 9 mps, after the electrophysiological tests, while animals were anesthetized, using a MyLab® Gamma (Esaote, Genova, Italy) device and a linear ultrasound probe. The cross-sectional area and perimeter of the TA muscle was determined using a B-mode ultrasound, employing a 15 MHz linear transducer, and optimizing the image at a depth of 3 cm and focal point at 1.5 cm. To optimize image acquisition and good skin contact, the hair over the area of interest was clipped and the skin cleaned with water and mild soap, and acoustic gel was used. In preliminary studies, we

established that the point of interest to standardize image acquisition was the cranial aspect of the crus at a midpoint between the tibial crest and the tuber calcanei (Figure S2).

2.8. Histological Evaluation

After performing the functional test 9 months after injury and when still anesthetized, animals were euthanized using an intravenous injection of Euthasol (400 mg/Kg i.v.). Nerve segments extending at least 1 cm from the proximal suture and 2 cm from the distal suture of the graft were harvested and fixed in paraformaldehyde 4% for 7 days at 4 °C. TA muscles were taken and weighed, and samples of TA muscles and of the skin of the dorsum of the paw were obtained and fixed in paraformaldehyde 4% for 7 days at room temperature.

After fixation, the peroneal nerves were divided into 5 different sections (see Results 3.3.4), and each section was further divided in two halves. The first half of Section 2 from the middle of the graft and Section 4 from the distal end were embedded in paraffin and 5 µm thick cross sections were obtained with a microtome. Samples from the midpoint of the graft were deparaffinized and stained with hematoxylin at 10% in absolute ethanol (Hematoxylin cryst. 1.04302.0100, Sigma Aldrich) and eosin at 0.5% in distilled water (Eosin Y, 1.15935.0100, Sigma Aldrich) to visualize the general structure of the nerve. Briefly, the samples were hydrated in H₂O for 10 min, then, stained for 5 min in hematoxylin. After two washes in H₂O, samples were introduced in 70% ethanol with 1% of hydrochloric acid for 30 s. Samples were washed again and stained with eosin for 5 min. Finally, samples were dehydrated, and mounted in gelatinized glass slides. Other sections were dewaxed and processed for immunohistochemistry against S-100 protein to label Schwann cells, and neurofilament NF200 to label myelinated axons, as explained above. Following washes, the sections were incubated with secondary antibodies bound to Alexa Fluor 488 and Alexa Fluor 594, mounted on gelatinized slides and viewed under epifluorescence microscopy. Quantitative analysis was performed with sets of images obtained at 1000X by measuring the cross-section area of the nerves and grafts, and then counting the number of NF200 labeled axons in systematically

selected fields, with at least 8 representative fields comprising more than 30% of the transverse area, under epifluorescence microscopy (Olympus BX51) using ImageJ software.

The second half of Section 2 from the middle of the graft and Section 4 from the distal nerve were postfixed in 3% paraformaldehyde and 3% glutaraldehyde in phosphate-buffered saline. The nerve segments were postfixed in osmium tetroxide, dehydrated in a series of ethanol, and embedded in epon resin. Semithin 0.5 μm thick sections were stained with toluidine blue, and representative images were taken by light microscopy.

TA muscle and skin samples were also processed for paraffin embedding. Samples were stained with hematoxylin and eosin, as explained above for the nerve samples, to visualize the general structure and to evaluate qualitatively the areas showing denervation atrophy.

2.9. Data Analysis

Data are expressed as mean \pm standard error of the mean (SEM). The results of functional tests and histology were analyzed by the Student's t test and a two-way ANOVA after checking for normal distribution, using GraphPad Prism 8 software. A $p < 0.05$ was considered as significant.

3. Results

3.1. Effectiveness of the Decellularization Procedure

The decellularization procedure developed removed all donor cells and DNA from the nerve segments, while the ECM as well as structural layers of the graft remained intact. In this way, the nerve grafts can provide guidance to the regenerating axons upon implantation. DNA content averaged 159.7 ± 18.7 ng/mg tissue in the native nerves of sheep, and 0.35 ± 0.02 ng/mg tissue in the decellularized nerves. Cross sections of decellularized nerve grafts were processed for immunohistochemistry before implantation. Immunolabeling against laminin showed that the structure of the ECM was well preserved. Faint staining against NF200, S100 and Fluoromyelin in the decellularized nerve grafts, of both rats and sheep, was compatible with lack of axons (NF200) and Schwann

cells (S100), and good decellularization (absence of DAPI, general marker of nucleus), thus indicating that cell contents were completely removed (Figure 2).

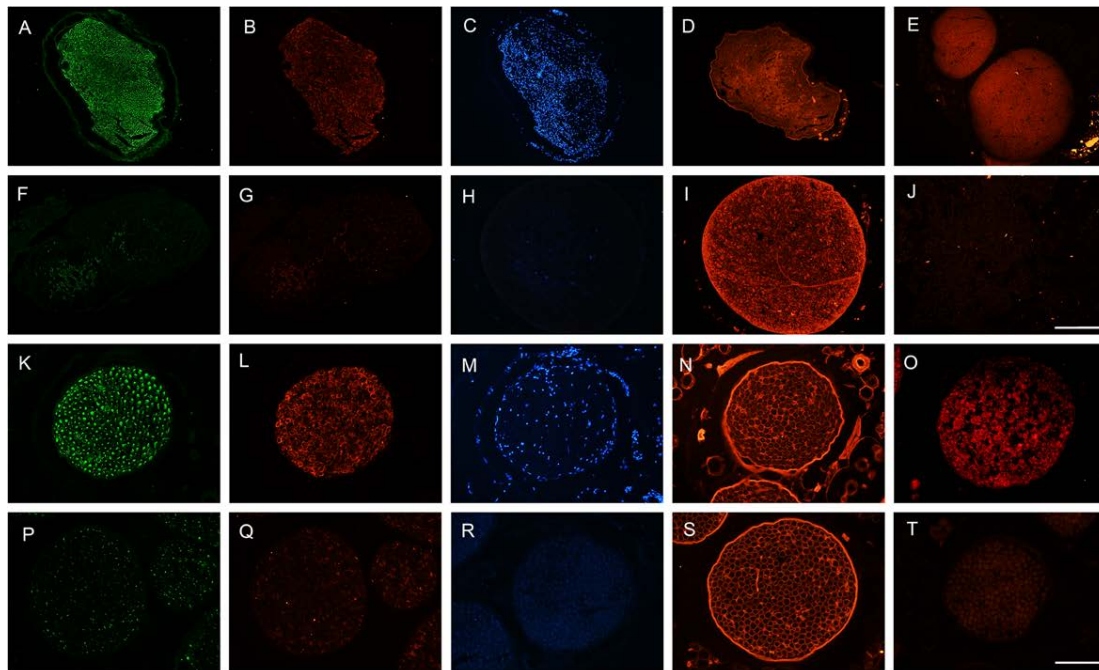


Figure 2. Representative micrographs showing immunofluorescence of myelinated axons (A,F,K,G), Schwann cells (B,G,L,Q), nuclei (C,H,M,R), extracellular matrix proteins (D,I,N,S) and myelin (E,J,O,T), in a control rat sciatic nerve (A,B,C,D,E), in a decellularized rat nerve (F,G,H,I,J), in a control sheep peroneal nerve (K,L,M,N,O) and in a decellularized sheep nerve (P,Q,R,S,T). Scale bar 150 μ m.

3.2. Rat Study

Denervation of the GM, TA and PL muscles was observed in both experimental groups at 30 dpi. At 60 dpi, all animals from the AG and DRA groups showed electrophysiological evidence of starting reinnervation in the GM and TA muscles. Three of the animals of the AG group had recorded CMAPs of small amplitude evoked by electrical stimulation, whereas none of the animals of the DRA group showed evidence of reinnervation in the PL muscle. At 90 dpi, the amplitude of the CMAPs increased for TA and GM muscles in both groups. All the rats of the AG group but only two thirds of the rats of the DRA group showed positive values for PL muscle. At the end of the follow-up, set up at 120 dpi, group AG had significantly higher mean CMAP amplitude values than the DRA group in TA (28.8

± 1.8 mV vs. 19.3 ± 2.8 mV; $p < 0.05$), GM (41.3 ± 3.9 mV vs. 23.7 ± 1.5 mV; $p < 0.05$) and PL (2.3 ± 0.4 mV vs. 0.5 ± 0.1 mV; $p < 0.05$) muscles (Figure 3A).

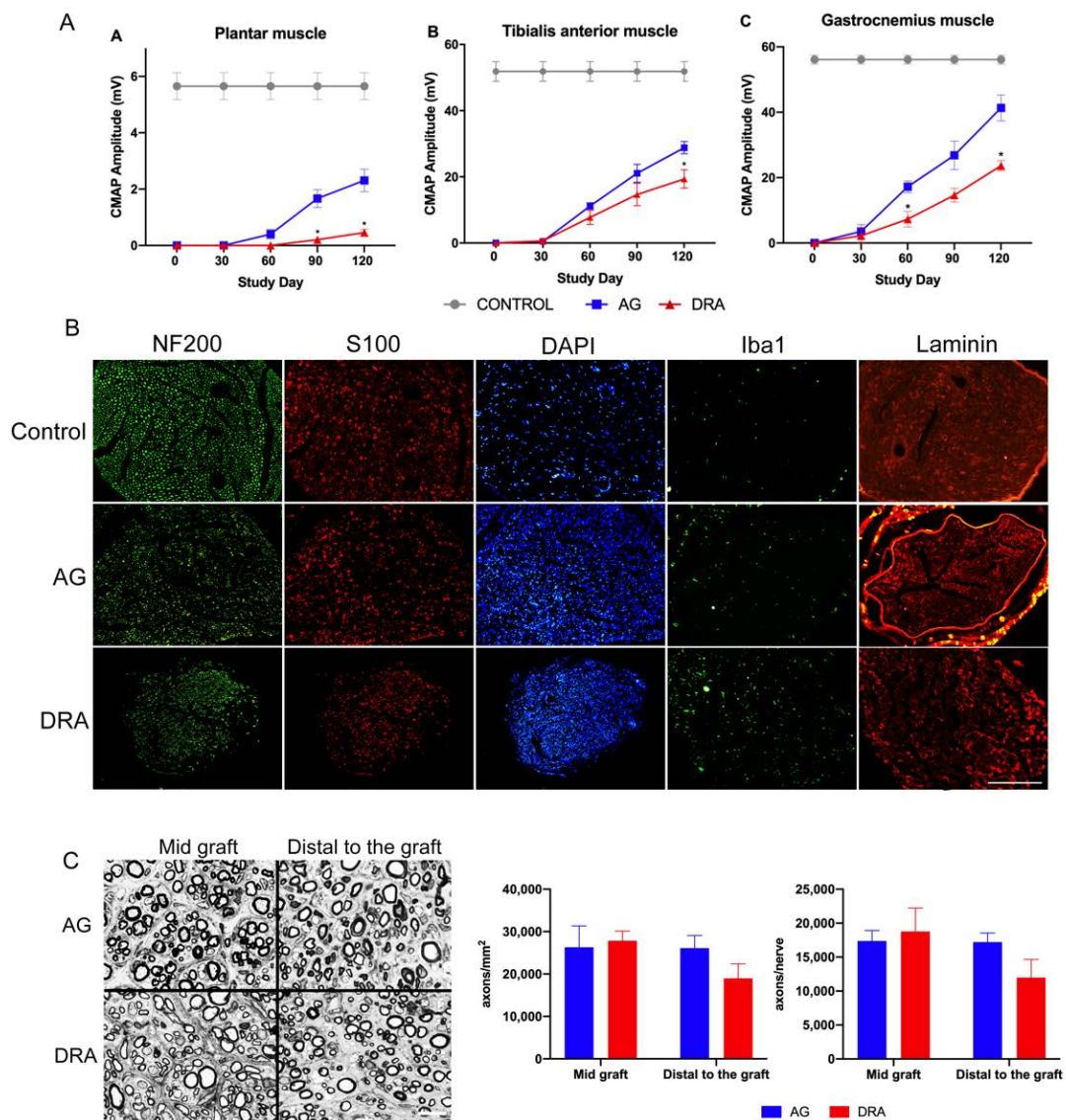


Figure 3. Results of the electrophysiological tests and histological evaluation after repair of a 15 mm long gap in the rat sciatic nerve. (A) Electrophysiological evaluation of nerve regeneration along 120 days follow-up after sciatic nerve section and repair with an autograft (AG, n = 5) or with a decellularized allograft (DRA, n = 5). Results are presented as mean \pm SEM. Statistical analysis was performed using 2way ANOVA. Plots show the amplitude of CAMP of plantar ($*p < 0.05$ vs. AG), tibialis anterior ($*p < 0.05$ vs. AG) and gastrocnemius ($*p < 0.05$ vs. AG) muscles. (B) Representative micrographs showing immunofluorescence of myelinated axons labeled against Neurofilament 200, Schwann cells labeled

against S100, nuclei labeled with DAPI, macrophages labeled with IBA1 and extracellular matrix labeled with laminin in cross sections of nerve graft in control, AG and DRA groups; scale bar 200 μm . (C) Representative transverse semithin sections of the mid graft and distal to the graft in AG and DRA groups, stained with toluidine blue. Scale bar 10 μm . Plots show the density and the number of myelinated axons in the sciatic nerve at mid graft and distal to the graft. Normal values in our laboratory for the sciatic nerve in rats average $8,076 \pm 215$ myelinated axons, with a density of $11,336 \pm 698$ per mm^2 .

The histological observations of transverse nerve sections showed the typical appearance of regenerated nerves, with numerous small size myelinated and unmyelinated axons inside the endoneurial compartments of the nerve graft and in the distal nerve. Immunohistochemical labeling showed numerous axons accompanied by Schwann cells along the grafts, but at lower density than in control nerves (Figure 3B). Quantitative analysis of the myelinated axons under light microscopy showed similar density in the middle of the graft in the AG group ($26,320 \pm 5013$ axons/ mm^2) compared to the DRA group ($27,858 \pm 2257$ axons/ mm^2), and similar total number of axons ($17,395 \pm 1525$ axons/nerve) in the AG group and DRA group ($18,773 \pm 3464$ axons/nerve). Distally to the graft, all animals from the AG and DRA groups had regenerated myelinated axons, but the density was higher in the AG group ($26,105 \pm 2991$ axons/ mm^2) than in the DRA group ($18,992 \pm 3358$ axons/ mm^2); similarly, the total number of axons distal to the graft was also higher in the AG group ($17,224 \pm 1329$ axons/nerve) compared to the DRA group ($11,983 \pm 2664$ axons/nerve) (Figure 3C), but without significant differences between the two groups.

3.3. Sheep Study

All sheep from both groups recovered well from the surgical procedure without any side effect and survived until the end of the study. No significant clinical signs, except for the right hindlimb dysfunction, were observed in the animals during the experimental follow-up. The sheep were able to stand and walk and have good mobility. Due to the peroneal nerve injury, two animals, one of each group, had a marked foot-drop posture that produced pressure ulcers on the dorsal skin of the

paw. A splint was placed 30 days post-operation to prevent further foot lesions, and ulcers were treated with chlorhexidine and antibiotic cream and covered. Only one of the sheep, in group DC, did not recover and continued with the foot-drop posture until the end of the study.

3.3.1. Functional Test Results

All the sheep showed close to normal locomotion activity after the surgery. In the resting orthostatic position, all the sheep, except one from the AG group, were able to correctly position the right hind hoof, maintaining the plantar support. When tested during fast walking, a foot-drop gait was evidenced in all sheep, as they failed to make plantar stepping in some steps (scored -1 or -2). A significant improvement ($p < 0.05$) in dorsiflexion was observed at the end of the follow-up in the AG group with respect to values at 30 days (Figure 4). The right TA muscle showed a reduction in size from one month after the surgery. There was a significant improvement appreciated in the last two months of the follow-up in the AG group. The reposition of the injured hindlimb when displaced to the dorsum, indicating proprioceptive inputs, was partially reduced after the surgery and the score significantly recovered to normal value at the end of the follow-up. The withdrawal reflex response was induced in 3 different sites: proximal, mid and distal in the dorsum of the paw. The response was suppressed after the surgery and slowly recovered with time. At the distal site, the test was more sensitive, without full recovery in all the sheep at 9 months post-operation (Figure 4). The AG group showed significant recovery from 4 months post-operation while the DC group had significant improvement from 5 months post-operation with respect to values at 30 days.

Overall, the functional tests showed the expected failure due to a peroneal nerve injury, and partial recovery of sensory-mediated functions, whereas motor recovery and muscle mass remained relatively steady until the last month of follow-up.

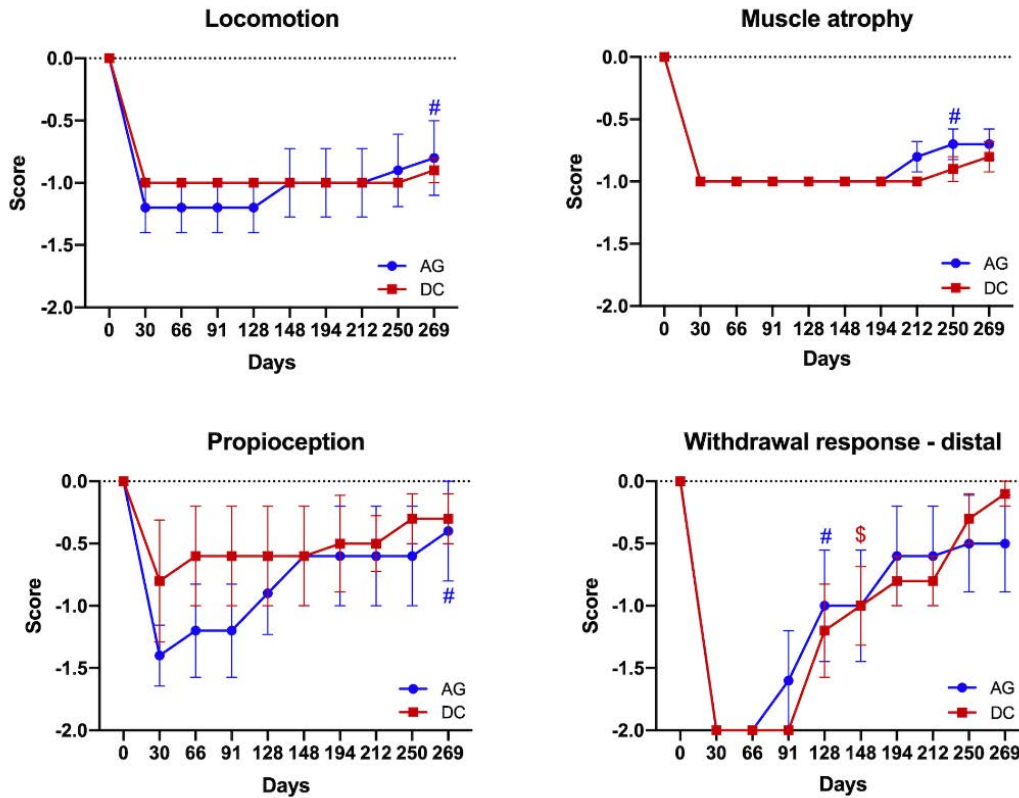


Figure 4. Plots of the functional evaluation along the 9 months follow-up in the two groups of sheep. Similar evolution was observed for all the tests applied, without significant differences between the groups AG and DC. Regarding the time evolution, AG group ($n = 5$) showed a significant recovery in all the tests applied ($\# p < 0.05$) vs. baseline at 30 days post-operation, while animals of DC group ($n = 5$) only showed a significant recovery in the withdrawal response-distal ($\$ p < 0.05$) vs. baseline at 30 days post-operation.

3.3.2. Electrophysiological Test Results

In the left, control hindlimb, the TA CMAP evoked by stimulation at the sciatic notch appeared at an onset latency of 4.2–4.4 msec and had a maximal amplitude of 20–22 mV, with small variations between sheep (Figure 5A). In the right, operated side, at 5 months none of the animals showed evidence of TA muscle reinnervation. Fibrillation potentials, signs of existing muscle denervation, were detected. At 6.5 months, CMAPs of late latency, small amplitude and disperse shape were recorded in 3 sheep of group AG and in 3 sheep of group DC. Fibrillation potentials were also recorded in TA muscles without CMAP response (Figure S3). At 9 months, CMAPs, recorded in 4 sheep of each group,

were of slightly higher amplitude and still of long latency, compatible with early reinnervation of the TA muscle. No significant differences were found between groups AG and DC in any parameter of the nerve conduction tests, although CMAP amplitude was comparatively higher in group AG than in group DC (Table 1).

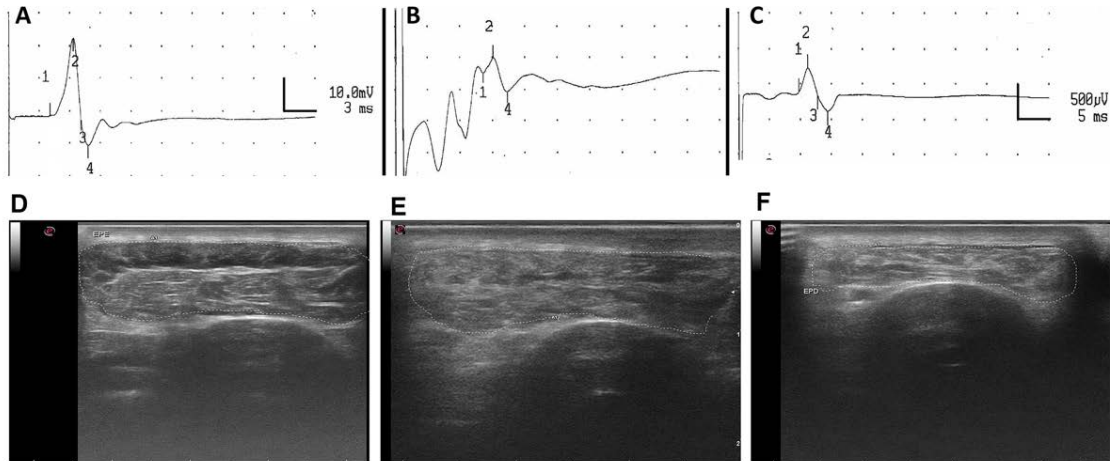


Figure 5. Representative EMG recordings of the CMAP recorded in the TA muscle evoked by stimulation of the sciatic nerve in the intact left hindlimb (A), and in the operated right hindlimb of a sheep at 6.5 (B) and 9 (C) months after operation. Labels: “1” at the onset, “2” at the peak, “4” at the end of the CMAP. Scale in A: amplitude 10 mV/square and time 3 ms per square; in B and C: amplitude 500 μ V/square and time 5 ms per square. Representative echographic images of the TA muscle recorded in the intact left hindlimb (D) and in the operated right hindlimb of a sheep repaired with an autograft (E) or with a decellularized nerve allograft (F).

Table 1. Values of the nerve conduction tests in the peroneal nerve and of the echography tests in the peroneal innervated muscles, in the control left limb and in the operated right limb (n=5 each) at 6.5 and 9 months postoperation. *p<0.05 vs. AG; **p<0.01 vs. AG. Results were analyzed by unpaired t test using GraphPad Prism 8 software.

Nerve Conduction.	Group	Latency (msec)	CMAP	
			Amplitude (mV)	n + Response
Control (L)	AG	4.38 ± 0.16	21.26 ± 1.54	5/5
Control (L)	DC	4.24 ± 0.09	22.84 ± 1.02	5/5
6.5 mo	AG	11.05 ± 1.52	0.97 ± 0.48	3/5
6.5 mo	DC	16.87 ± 4.54	0.21 ± 0.11	3/5
9 mo	AG	11.58 ± 1.06	1.87 ± 0.72	4/5
9 mo	DC	13.16 ± 1.50	0.46 ± 0.16	4/5
Echography		TA area (cm ²)	TA perimeter (cm)	
Control (L)	AG	5.30 ± 0.29	10.30 ± 0.24	
Control (L)	DC	5.31 ± 0.48	10.30 ± 0.44	
6.5 mo	AG	1.90 ± 0.07	7.34 ± 0.23	
6.5 mo	DC	1.48 ± 0.03 **	6.87 ± 0.08	
9 mo	AG	2.44 ± 0.21	7.95 ± 0.17	
9 mo	DC	1.85 ± 0.09 *	7.45 ± 0.11	

3.3.3. Echographic Evaluation of TA Muscles

In denervated muscles, the density of the muscle imaging changed, and the size (measured both as area and perimeter) was decreased, evidencing muscle atrophy and increased connective tissue secondary to denervation (see Figure 5D–F). At 6.5 months post-surgery, the TA muscle area in the DC group was significantly lower than in the AG group (** $p < 0.01$). At the end of the follow-up, there was a tendency to recover muscle size, although it was still significantly lower in the DC group than in the AG group (* $p < 0.05$) (Table 1). The size of the TA muscles in the two sheep without electrophysiological responses, one from each experimental group, was the smallest (1.85 cm² in area and 7.41 cm in perimeter in the AG group and 1.56 cm² and 7.36 cm in the DC group), pointing to a relationship between muscle size and degree of reinnervation.

3.3.4. Histological Assessment

Most of the animals from AG and DC groups presented grafted nerves with a well-preserved structure and neuroma visible at proximal and distal ends corresponding with the suture lines (Figure 6A–C). The control peroneal nerve was composed of multiple small fascicles, usually more than 30, each containing numerous nerve fibers densely packed in the endoneurium. In the AG group, the structure of the fascicles was preserved in the graft, but regenerating axons were detected both inside and outside of the perineurium delimiting the fascicles. In contrast, no clear fascicles were observed in the decellularized grafts, where regenerating axons were seen grouped in small regenerative units, disperse within the graft structure (Figure 6E–M).

Semithin sections stained with toluidine blue showed, in the AG group, a preserved structure of the fascicles with many myelinated axons of different sizes. In addition, there were small new regenerative units that contained a small number of myelinated axons. In the DC group, the structure of the fascicles was not conserved, although new regenerative units were observed throughout the nerve with a large number of myelinated axons (Figure 6M; marked with red arrows).

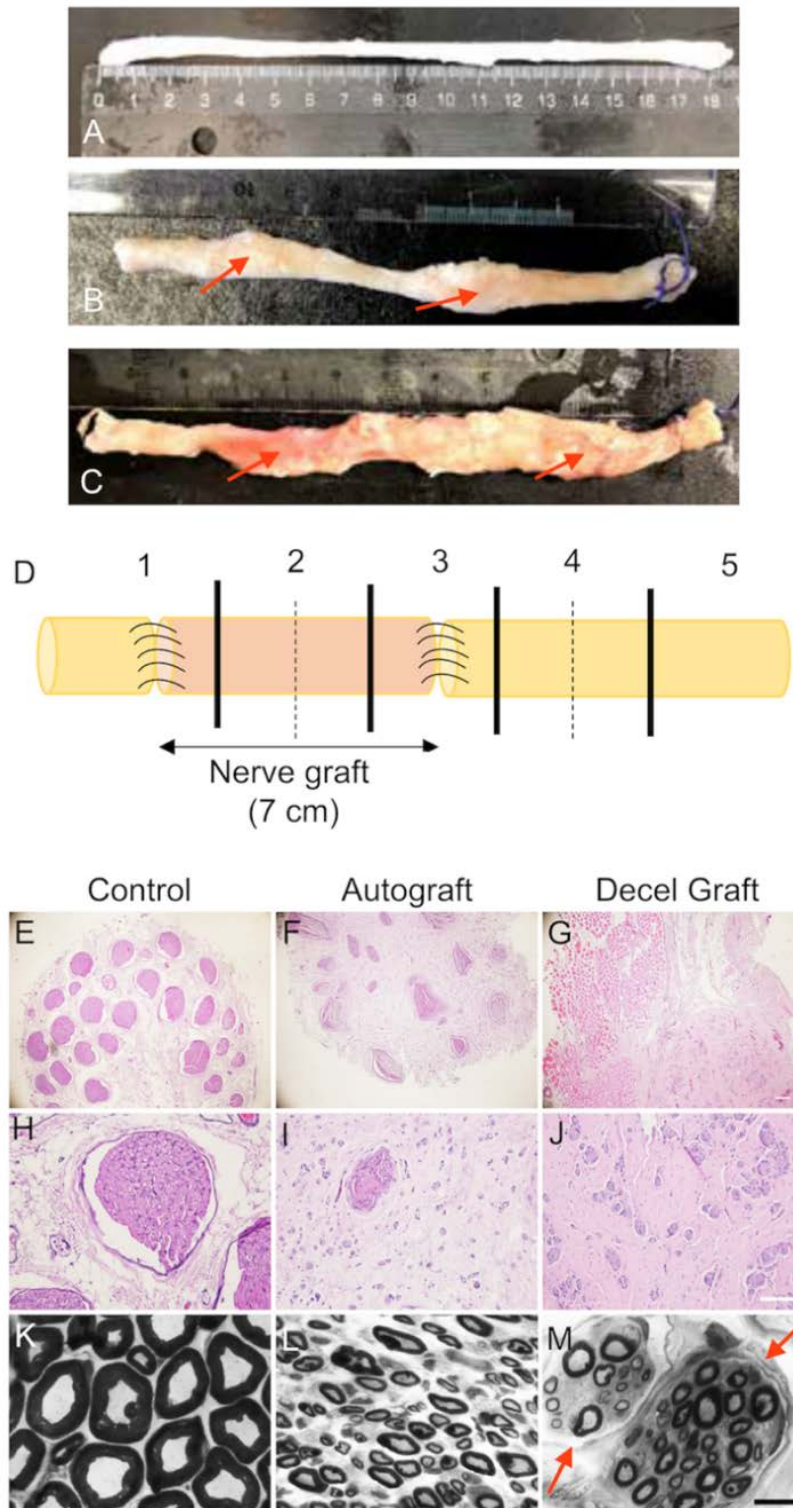


Figure 6. Macroscopic representative pictures of a control sheep peroneal nerve (A), a peroneal nerve autograft (B), and a decellularized nerve allograft (C), both with a neuroma visible (marked with red arrows) at proximal and distal sutures, harvested at the end of the study. (D) Schema of the division in sections of nerves harvested. Section 1 includes the proximal suture and Section 3 includes the

distal suture of the graft. Sections 2 and 4 were divided into two different segments (dotted line). Micrographs of cross sections of the proximal segment of the graft of sheep stained with hematoxylin and eosin. (E,H) control nerve, (F,I) autograft and (G, J) decellularized nerve graft; E, F, G scale bar 200 μm , and H, I, J scale bar 100 μm . Representative semithin transverse sections of the graft of sheep in AG and DC groups, stained with toluidine blue. (K) control nerve, (L) autograft and (M) decellularized nerve graft, scale bar 10 μm . Red arrows in M point to the newly formed regenerative small fascicles.

Distal to the graft, the multifascicular structure of the peroneal nerve was maintained and most regenerating axons grew within the distal nerve fascicles. Immunohistochemical labeling at the middle part of the grafts (noted with dotted line in Figure 6D) from AG animals showed axons and Schwann cells (Figure 7) present within both fascicular and extrafascicular areas, whereas in the decellularized grafts of the DC group, axons and glial cells were dispersed in small regenerative clusters. Regarding the analysis of NF200 labeled axons, group AG had 1 animal with a very low number of regenerating axons while 2 animals had higher than control values. One animal did not show regenerated axons, likely attributable to suture dehiscence early after the operation. Group DC also had 1 animal without regenerating axons.

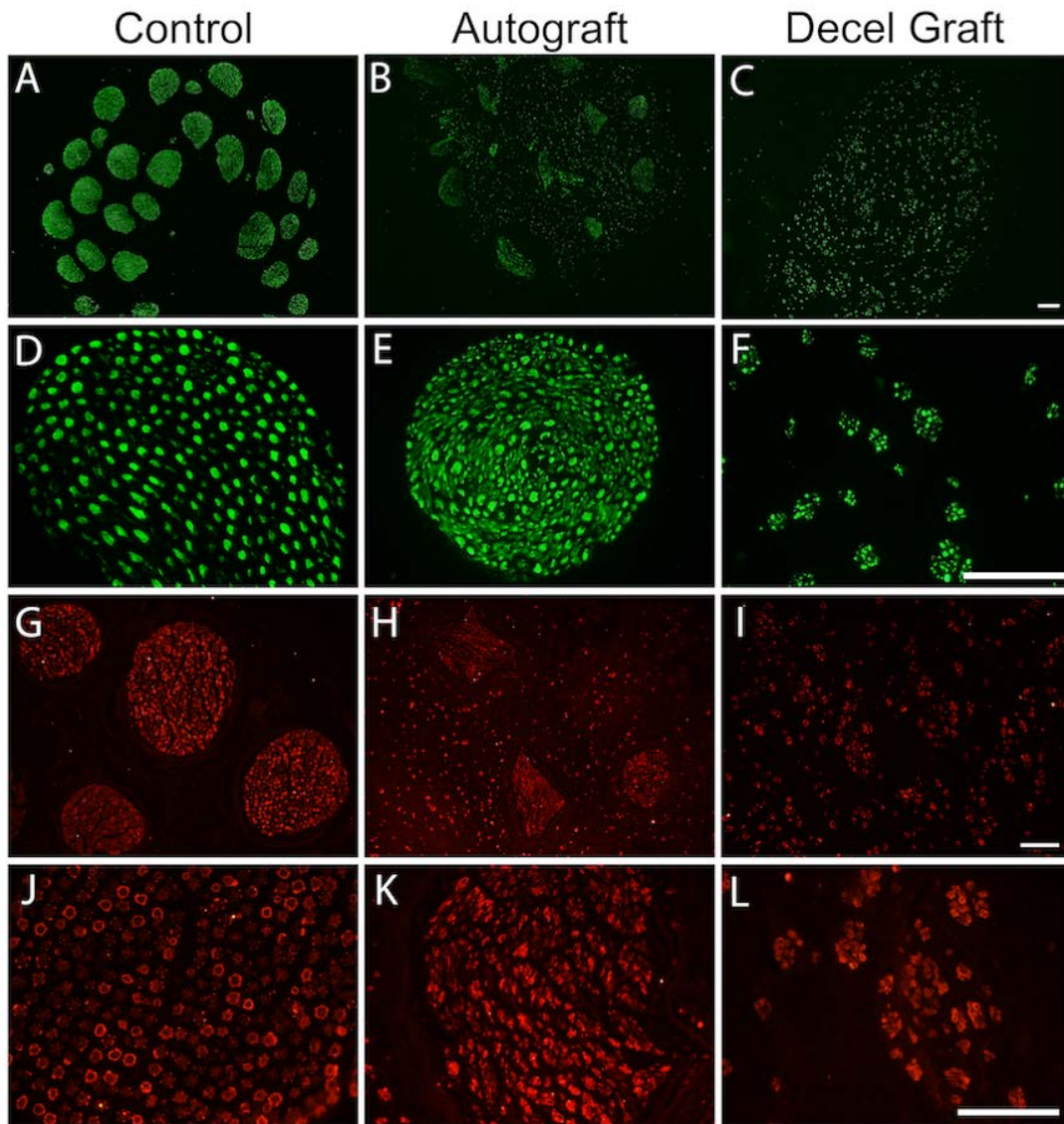


Figure 7. Representative micrographs showing immunofluorescence of myelinated axons labeled against Neurofilament 200 in cross sections of the proximal graft in AG and DC groups. (A,D) control nerve, (B,E) autograft and (C,F) decellularized nerve graft. A, B, C scale bar 200 μm , and D, E, F scale bar 100 μm . Representative micrographs showing immunofluorescence labeling of Schwann cells with an antibody against the S100 protein in cross sections of the proximal graft in AG and DC groups. (G,J) control nerve, (H,K) autograft and (I,L) decellularized nerve graft. G, H, I scale bar 100 μm , and J, K, L scale bar 100 μm .

The estimated mean number of myelinated axons was $21,676 \pm 3716$ in the control peroneal nerve, whereas in the mid segment of the grafts (Figure 6

Section 2 dotted line) there were $26,213 \pm 2798$ axons in the four regenerated sheep of the AG group, and $18,724 \pm 3410$ in the four sheep of the DC group at 9 months post-surgery. The corresponding values at the nerve distal to the graft were $20,600 \pm 6082$ for the AG group and 7780 ± 1871 ($p < 0.05$) for the DC group (Figure 6 Section 4 dotted line). The higher number of regrowing axons in the graft is indicative of some excessive regenerative sprouting that was remodeled at the distal nerve.

3.3.5. Histological Evaluation of Reinnervated Targets

In the operated hindlimb, the TA muscle showed a heterogeneous structure in both groups, AG and DC (Figure 8A–F). Some areas appeared normal, although muscle fibers had a smaller diameter than normal, likely corresponding to reinnervated areas of the muscle. Other areas showed signs of atrophy and inflammatory infiltration. The skin samples, processed in sagittal sections, showed distinct organization in three layers: epidermis, dermis and subcutaneous tissue. The skin of the dorsum of the paw had a similar aspect to the skin from the contralateral side, without signs of cell infiltration or atrophy (Figure 8G–L).

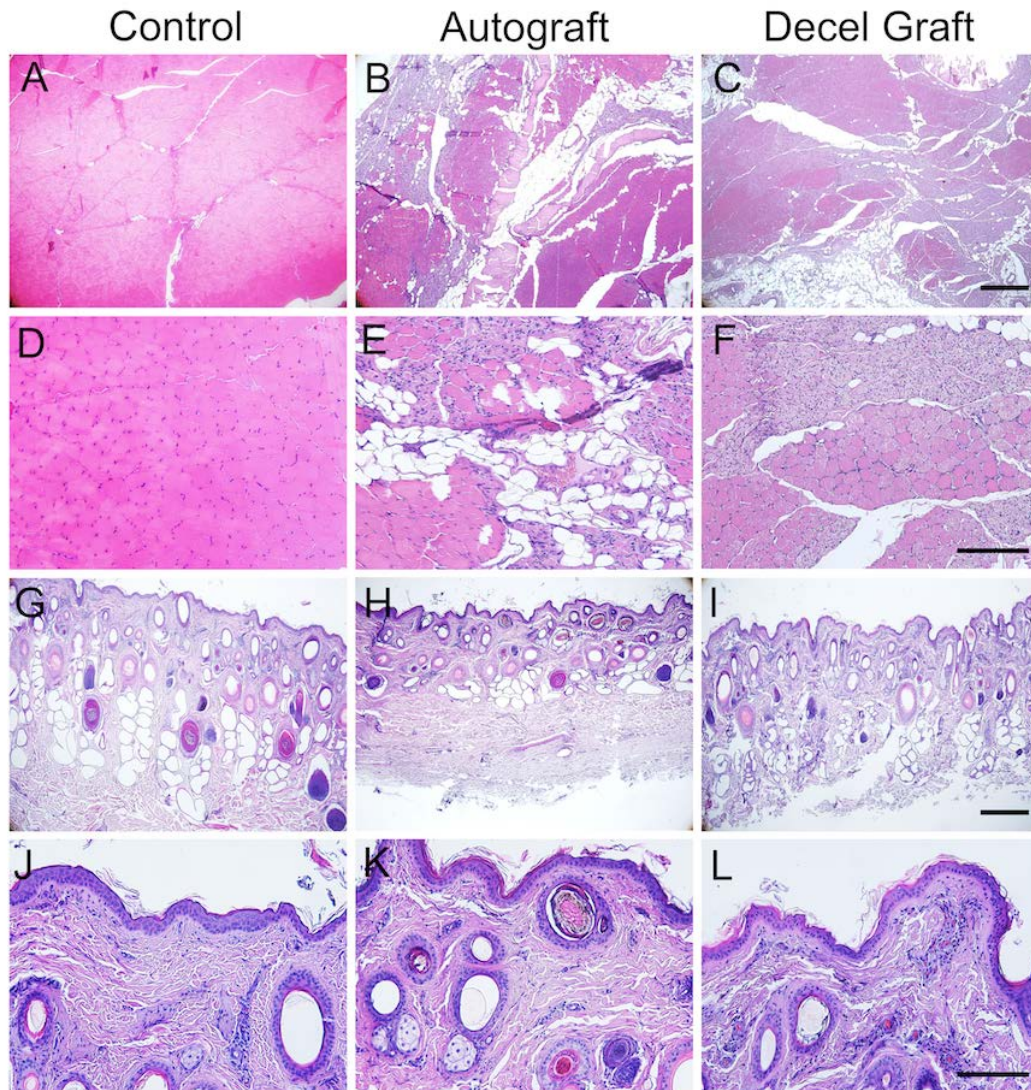


Figure 8. Representative micrographs of cross sections of the Tibialis Anterior muscle stained with hematoxylin and eosin from (A,D) the contralateral side (control), (B,E) an animal from AG group, (C,F) an animal from DC group. A, B, C scale bar 200 μm , and D, E, F scale bar 100 μm . Representative micrographs of perpendicular sections of the skin of the dorsum of the foot stained with hematoxylin and eosin from (G, J) the contralateral side (control), (H, K) an animal from AG group, (I, L) an animal from DC group. G, H, I scale bar 200 μm , and J, K, L scale bar 100 μm .

4. Discussion

The gold standard repair technique for long gap peripheral nerve injuries is grafting an autologous nerve. However, sources for autologous nerve grafts are limited, so it is not possible to use this method to treat extended or multiple nerve

lesions [29]. Acellular nerve allografts appear as a good alternative for autografts, considering that they come from a natural and abundant source, are not overtly immunogenic, and may keep a normal-like ECM structure which helps guiding regenerating axons [8,30]. Moreover, an allograft may offer several technical advantages over the autograft, such as off-the-shelf availability, easy handling, shorter surgical time, and no donor graft site morbidity [31]. Nevertheless, acellular allografts also have some limitations, mainly related to the lack of cell support for axonal regeneration, since it is important to eliminate cellularity in order to avoid immune rejection.

The results of our studies indicate that the used, novel procedure for tissue decellularization is highly efficient, eliminating all cells and DNA from the nerve segment, while preserving a normal-like structure of the perineurium and endoneurial tubules. Consequently, the decellularized graft did not induce an immune rejection response after in vivo implantation and proved to be a good substrate for axon growth and migration of host cells into the graft, allowing effective regeneration and functional recovery. The results of the two studies made in rats and in sheep showed promising results in terms of functional reinnervation and axonal regeneration, although the outcomes of the DC allograft were comparatively lower than those achieved with an ideal AG (i.e., the same nerve segment resected and re-sutured in place). The DC allograft allowed effective regeneration across a critical 15 mm long nerve gap in the rat sciatic nerve, and a 7 cm long gap in the sheep peroneal nerve, in both cases a length that cannot be effectively bridged with synthetic nerve conduits and represents a challenge for surgical nerve repair. The limiting gap size depends on the nerve and the animal species. Seminal experimental reports showed that regenerating axons are able to bridge synthetic conduits such as silicone, up to 4 mm in the mouse and 10 mm in the rat [15,32], and less than 30 mm in primates [33,34], but failed through longer gaps.

4.1. Nerve Regeneration in the Sheep Peroneal Nerve Model

Small animal models are commonly used to replicate challenging clinical scenarios [6,26,35,36]. In contrast to small-animal models, large-animal models

allow investigation of longer and more clinically relevant nerve defects and harvesting long segments of donor nerves. This reflects the actual situation in most human nerve injuries in which damage to the nerve often extends over several centimeters [22]. Hence, standardized models of long nerve gap injury in large animals are necessary to evaluate tolerability and efficacy of new treatment strategies for severe nerve injuries [6]. In this sense, sheep are proposed as an optimal large animal model, since they have similarities in general body and neural structures to humans [37,38], and particularly peripheral nerve dimensions and structure similar to humans [20,39–41]. Moreover, their calm nature, compared to other large animals used as experimental models, such as pigs, enables easier postoperative management and clinical testing [18,42].

In the present study, the regenerative potential of a novel decellularized nerve allograft was evaluated and compared to autograft repair of a 70 mm long resection of the peroneal nerve in sheep. This nerve is the most commonly affected in injuries involving the lower limb in humans [41,43]. Moreover, it is adequate because it is similar in size and plurifascicular, as is the human peroneal nerve, and induces a limited motor deficit that still allows the animals to stand and walk [20,44]. Since the common peroneal nerve is a mixed nerve, both motor and sensory functional loss in the denervated targets is expected [45]. Therefore, paralysis of dorsiflexion muscles and lack of sensitivity of the dorsum of the foot was observed, although all the sheep showed close to normal locomotion after recovery from the surgery, and most of them were able to position the hind hoof in a normal resting position. Similar to motor function, proprioceptive sensibility of the denervated muscles was also affected, and complete recovery was achieved with time in all the animals. We hypothesize that this recovery could be accounted by the normal processing of information by the intact tibial and sural nerves, also innervating the hind limb, so that the contribution of the peroneal nerve is limited. The response observed as a withdrawal flexion of the hind limb at early times, when no axons of the injured peroneal nerve could have regenerated to the ankle level, can be attributed to collateral reinnervation by sprouts from nearby cutaneous nerve tributaries of tibial and sural nerves, a phenomenon that has been well studied in other smaller mammals [46,47] as well

as in human subjects [48]. Therefore, results obtained in the functional sensory tests can be confounded by collateral reinnervation and are not completely useful to report nerve regeneration and cutaneous reinnervation. In contrast, electrophysiological assessment of the recovery of the CMAP of the TA muscle was the most sensitive test. Although the electrophysiological parameters rarely return to normal levels after nerve injury, they are frequently used to evaluate nerve regeneration and muscle reinnervation in humans and animal models [6,49–51]. Electrophysiological tests evidenced reinnervation of the TA muscle in a 3/5 sheep of both AG and DC groups at 6.5 months, and in 4/5 at 9 months. The time needed for axonal regeneration to distal targets in the sheep hindlimb is considerably long, taking into consideration that the distance between the proximal section of the peroneal nerve and the entrance of the nerve into the TA muscle is about 34 to 36 cm. Since we found early electrophysiological evidence of reinnervation of the TA muscle at 6.5 months, a regeneration rate between 1.7 and 2 mm/day can be estimated. The lower amplitude of the recorded CMAPs in the DG group than in the AG group, may suggest a slightly slower regeneration along the decellularized graft.

At the end of follow up, histological assessment of the graft and the distal regenerated nerve was performed. The extent of axonal regeneration in the grafts was evaluated by using neurofilament immunolabeling [22,52]. Schwann cells were observed within the decellularized nerve graft 9 months after the repair, indicating that the host cells migrated from proximal and distal stumps into the graft. Neurofilament labeling was present in most of the grafts, corroborating successful axonal regeneration in these animals and confirming the functional results. However, the incomplete functional recovery observed, as evidenced by the low amplitude of TA CMAPs recorded at 9 months (about 8% and 2% of control values in AG and DC groups, respectively), compared with the extensive amount of regeneration into the grafts suggests that many regenerating axons need more time to reach target organs and therefore, longer follow up periods are needed in this model to assess maximal functional outcomes, as reported also in humans [53].

4.2. Regenerative Potential of the Acellular Nerve Graft

The only available and FDA approved processed nerve allograft to repair human nerve defects of a length up to 5 cm is the marketed allograft Axogen Avance®. This product provides an off-the-shelf alternative to synthetic conduits while maintaining some proregenerative properties of autologous nerve grafts [54], providing overall 82% meaningful recovery in repairs of nerve gaps up to 70 mm [55]. No adverse events have been observed, despite some failures reported pointed to a careful consideration of acellular nerve allografts in long, large diameter injured nerves [56]. In this study, we have evaluated a novel decellularized nerve graft that allowed axonal regeneration across not only a 15 mm long gap in rats, but also a 70 mm gap in sheep, offering good perspectives for marketing applications. Electrophysiological and functional test results indicated a similar course, although with some delay, of muscle reinnervation than with the ideal autograft used.

However, the organization of the regenerating axons was different in the decellularized graft compared to the autograft. In the decellularized grafts, regenerated axons were found in an extrafascicular location, and only in the distal nerve sections the fascicles were consistently well defined, with very few extrafascicular axons visible, as described in previous studies [22,57]. This indicates that the matrix of the decellularized nerve is not so consistent as in a fresh nerve autograft, that has not been previously manipulated, even when the macroscopic observation indicates a well-preserved structure of the connective tissue, ECM molecules and fascicles in the decellularized grafts before implantation. Although further optimization of the decellularization protocol can be performed, there is a delicate equilibrium between preserving nerve architecture and completely decellularizing the graft to avoid immune rejection.

Finally, the number of regenerated axons distal to the graft was lower in the DC group compared to the AG group, indicative of a slower regeneration along the decellularized graft. Therefore, although the decellularized graft is permissive for regeneration, the lack of a cellular component causes slower regeneration into the graft compared to the ideal cellular autografts. This is expected, mainly due

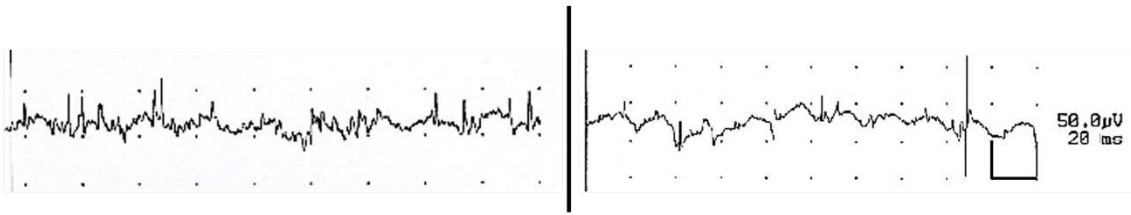
to the important role of Schwann cells in axonal regeneration [8]. Interestingly, this slower regeneration into the graft implies a delayed onset but does not have to translate in a significantly poorer functional recovery, according to previous observations [9]. In fact, electrophysiological recovery was quite limited in the two groups of rats followed for 4 months (see Figure 3A), and in the two groups of sheep evaluated up to 9 months after injury (Table 1), comparing to control values obtained in the contralateral hind limb. These results point out the long gap bridged by the graft and the long distance that axons had to grow to reinnervate target organs as determinants for the functional outcome. In this sense, the optimization of acellular grafts and recellularization methods to improve their regenerative capability offers a window of opportunity to improve recovery in this type of injuries, when the gold standard technique has already limited potential.



Supplementary Figure 1: Flexor withdrawal reflex test. Photograph of the maneuver used to pinching the dorsum of the foot with a hemostat for assessing the withdrawal reflex response in a proximal, middle and distal point (A).



Supplementary Figure 2: Performance of the echography of the TA muscle. Photograph of the hindlimb with the handheld ultrasound probe placed at a midpoint between the tibial crest (marked with a red *) and the tuber calcanei to obtain a cross-sectional image of the TA muscle. Before image acquisition, the skin was shaved, and cleaned with mild soap and water. Ultrasound gel was placed on the probe contact surface.



Supplementary Figure 3: Fibrillation potentials. Recordings of fibrillation potentials in the denervated TA muscle of the operated right hindlimb of sheep at 6.5 months after operation, repaired with an autograft (left trace) or with a decellularized nerve allograft (right trace).

References

1. Navarro, X.; Vivó, M.; Valero-Cabré, A. Neural Plasticity after Peripheral Nerve Injury and Regeneration. *Prog. Neurobiol.* **2007**, *82*, 163–201. <https://doi.org/10.1016/j.pneurobio.2007.06.005>.
2. Noble, J.; Munro, C.A.; Prasad, V.S.; Midha, R. Analysis of upper and lower extremity peripheral nerve injuries in a population of patients with multiple injuries. *J. Trauma.* **1998**, *45*, 116–122. <https://doi.org/10.1097/00005373-199807000-00025>.
3. Robinson, L.R. Traumatic Injury to peripheral nerves. *Muscle Nerve.* **2000**, *23*, 863–873. [https://doi.org/10.1002/\(sici\)1097-4598\(200006\)23:6<863::aid-mus4>3.0.co;2-0](https://doi.org/10.1002/(sici)1097-4598(200006)23:6<863::aid-mus4>3.0.co;2-0).
4. Allodi, I.; Guzmán-Lenis, M.S.; Hernández, J.; Navarro, X.; Udina, E. In Vitro Comparison of Motor and Sensory Neuron Outgrowth in a 3D Collagen Matrix. *J. Neurosci. Methods* **2011**, *198*, 53–61. <https://doi.org/10.1016/j.jneumeth.2011.03.006>.
5. Pfister, B.J.; Gordon, T.; Loverde, J.R.; Kochar, A.S.; Mackinnon, S.E.; Cullen, D.K.. Biomedical Engineering Strategies for Peripheral Nerve Repair: Surgical Applications, State of the Art, and Future Challenges. *Crit. Rev. Biomed. Eng.* **2011**, *39*, 81–124. <https://doi.org/10.1615/critrevbiomedeng.v39.i2.20>.
6. Burrell, J.C.; Browne, K.D.; Dutton, J.L.; Laimo, F.A.; Das, S.; Brown, D.P.; Roberts, S.; Petrov, D.; Ali, Z.; Ledebur, H.C.; et al. A Porcine Model of Peripheral Nerve Injury Enabling Ultra-Long Regenerative Distances: Surgical Approach, Recovery Kinetics, and Clinical Relevance. *Neurosurgery* **2020**, *87*, 833–846. <https://doi.org/10.1093/neuros/nyaa106>.
7. Gordon, T.; Tyreman, N.; Raji, M.A. The Basis for Diminished Functional Recovery after Delayed Peripheral Nerve Repair. *J. Neurosci.* **2011**, *31*, 5325–5334. <https://doi.org/10.1523/JNEUROSCI.6156-10.2011>.
8. Hall, S.M. Regeneration in Cellular and Acellular Autografts in the Peripheral Nervous System. *Neuropathol. Appl. Neurobiol.* **1986**, *12*, 27–46. <https://doi.org/10.1111/j.1365-2990.1986.tb00679.x>.
9. Moore, A.M.; MacEwan, M.; Santosa, K.B.; Chenard, K.E.; Ray, W.Z.; Hunter, D.A.; Mackinnon, S.E.; Johnson, P.J. Acellular Nerve Allografts in Peripheral Nerve Regeneration: A Comparative Study. *Muscle Nerve.* **2011**, *44*, 221–234. <https://doi.org/10.1002/mus.22033>.

10. Evans, P.J.; Midhat, R.; Mackinnon, S.E. The peripheral nerve allograft: A comprehensive review of regeneration and neuroimmunology. *Prog. Neurobiol.* **1994**, *43*, 187–233. [https://doi.org/10.1016/0301-0082\(94\)90001-9](https://doi.org/10.1016/0301-0082(94)90001-9).
11. Isaacs, J.; Safa, B. A Preliminary Assessment of the Utility of Large-Caliber Processed Nerve Allografts for the Repair of Upper Extremity Nerve Injuries. *Hand* **2017**, *12*, 55–59. <https://doi.org/10.1177/1558944716646782>.
12. Lovati, A.B.; D'Arrigo, D.; Odella, S.; Tos, P.; Geuna, S.; Raimondo, S. Nerve Repair Using Decellularized Nerve Grafts in Rat Models. A Review of the Literature. *Front. Cell Neurosci.* **2018**, *12*, 427. <https://doi.org/10.3389/fncel.2018.00427>.
13. Kornfeld, T.; Vogt, P.M.; Radtke, C. Nerve Grafting for Peripheral Nerve Injuries with Extended Defect Sizes. *Wien. Med. Wochenschr.* **2019**, *169*, 240–251. <https://doi.org/10.1007/s10354-018-0675-6>.
14. Tos, P.; Ronchi, G.; Papalia, I.; Sallen, V.; Legagneux, J.; Geuna, S.; Giacobini-Robecchi, M.G. Chapter 4 Methods and Protocols in Peripheral Nerve Regeneration Experimental Research: Part I-Experimental Models. *Int. Rev. Neurobiol.* **2009**, *87*, 47–79. [https://doi.org/10.1016/S0074-7742\(09\)87004-9](https://doi.org/10.1016/S0074-7742(09)87004-9).
15. Yannas, I.v.; Hill, B.J. Selection of Biomaterials for Peripheral Nerve Regeneration Using Data from the Nerve Chamber Model. *Biomaterials* **2004**, *25*, 1593–1600. [https://doi.org/10.1016/S0142-9612\(03\)00505-2](https://doi.org/10.1016/S0142-9612(03)00505-2).
16. Kaplan, H.M.; Mishra, P.; Kohn, J. The Overwhelming Use of Rat Models in Nerve Regeneration Research May Compromise Designs of Nerve Guidance Conduits for Humans. *J. Mater. Sci. Mater. Med.* **2015**, *26*, 226. <https://doi.org/10.1007/s10856-015-5558-4>.
17. Angius, D.; Wang, H.; Spinner, R.J.; Gutierrez-Cotto, Y.; Yaszemski, M.J.; Windebank, A.J. A Systematic Review of Animal Models Used to Study Nerve Regeneration in Tissue-Engineered Scaffolds. *Biomaterials* **2012**, *33*, 8034–8039. <https://doi.org/10.1016/j.biomaterials.2012.07.056>.
18. Diogo, C.C.; Camassa, J.A.; Pereira, J.E.; da Costa, L.M.; Filipe, V.; Couto, P.A.; Geuna, S.; Maurício, A.C.; Varejão, A.S. The Use of Sheep as a Model for Studying Peripheral Nerve Regeneration Following Nerve Injury: Review of the Literature. *Neurol. Res.* **2017**, *39*, 926–939. <https://doi.org/10.1080/01616412.2017.1331873>.
19. Hems, T.E.; Glasby, M.A. Repair of cervical nerve roots proximal to the root ganglia. An experimental study in sheep. *J. Bone Jt. Surg. Br.* **1992**, *74*, 918–922. <https://doi.org/10.1302/0301-620X.74B6.1447258>.

20. Strasberg, S.R.; Mackinnon, S.E.; Genden, E.M.; Bain, J.R.; Purcell, C.M.; Hunter, D.A.; Hay, J.B. Long-segment nerve allograft regeneration in the sheep model: Experimental study and review of the literature. *J. Reconstr. Microsurg.* **1996**, *12*, 529–547. <https://doi.org/10.1055/s-2007-1006625>.
21. Matsuyama, T.; Midha, R.; Mackinnon, S.E.; Munro, C.A.; Wong, P.-Y.; Ang, L.C. Long nerve allografts in sheep with Cyclosporin A immunosuppression. *J. Reconstr. Microsurg.* **2000**, *16*, 219–225. <https://doi.org/10.1055/s-2000-7556>.
22. Forden, J.; Xu, Q.G.; Khu, K.J.; Midha, R. A Long Peripheral Nerve Autograft Model in the Sheep Forelimb. *Neurosurgery* **2011**, *68*, 1354–1362. <https://doi.org/10.1227/NEU.0b013e31820c08de>.
23. Radtke, C.; Allmeling, C.; Waldmann, K.H.; Reimers, K.; Thies, K.; Schenk, H.C.; Hillmer, A.; Guggenheim, M.; Brandes, G.; Vogt, P.M. Spider Silk Constructs Enhance Axonal Regeneration and Remyelination in Long Nerve Defects in Sheep. *PLoS ONE* **2011**, *6*, e16990. <https://doi.org/10.1371/journal.pone.0016990>.
24. Navarro, X.; Butí, M.; Verdú, E. Autotomy Prevention by Amitriptyline after Peripheral Section in Different Strains of Mice. *Restor. Neurol. Neurosci.* **1994**, *6*, 151–157. <https://doi.org/10.3233/RNN-1994-6209>.
25. Valero-Cabré, A.; Navarro, X. Functional Impact of Axonal Misdirection after Peripheral Nerve Injuries Followed by Graft or Tube Repair. *J. Neurotrauma.* **2002**, *19*, 1475–1485. <https://doi.org/10.1089/089771502320914705>.
26. Gonzalez-Perez, F.; Cobianchi, S.; Heimann, C.; Phillips, J.B.; Udina, E.; Navarro, X. Stabilization, Rolling, and Addition of Other Extracellular Matrix Proteins to Collagen Hydrogels Improve Regeneration in Chitosan Guides for Long Peripheral Nerve Gaps in Rats. *Neurosurgery* **2017**, *80*, 465–474. <https://doi.org/10.1093/neuros/nyw068>.
27. Gomez, N.; Cuadras, J.; Butí, M.; Navarro, X. Histologic assessment of sciatic nerve regeneration following resection and graft or tube repair in the mouse. *Restor. Neurol. Neurosci.* **1996**, *10*, 187–196. <https://doi.org/10.3233/RNN-1996-10401>.
28. Ceballos, D.; Cuadras, J.; Verdú, E.; Navarro, X. Morphometric and ultrastructural changes with ageing in mouse peripheral nerve. *J. Anat.* **1999**, *195*, 563–576. <https://doi.org/10.1046/j.1469-7580.1999.19540563.x>.
29. Raimondo, S.; Fornaro, M.; Tos, P.; Battiston, B.; Giacobini-Robecchi, M.G.; Geuna, S. Perspectives in Regeneration and Tissue Engineering of Peripheral Nerves. *Ann. Anat.* **2011**, *193*, 334–340. <https://doi.org/10.1016/j.aanat.2011.03.001>.

30. Ide, C.; Tohyama, K.; Yokota, R.; Nitatori, T.; Onodera, S. Schwann Cell Basal Lamina and Nerve Regeneration. *Brain Res.* **1983**, *288*, 61–75. [https://doi.org/10.1016/0006-8993\(83\)90081-1](https://doi.org/10.1016/0006-8993(83)90081-1).
31. Immerman, I. Allograft Nerve Reconstruction: The New Gold Standard?: Commentary on an Article by Peter Tang, MD MPH, FAOA; et al. No Difference in Outcomes Detected Between Decellular Nerve Allograft and Cable Autograft in Rat Sciatic Nerve Defects. *J. Bone. Jt. Surg. Am.* **2019**, *101*, e48. <https://doi.org/10.2106/JBJS.19.00168>.
32. Butí, M.; Verdú, E.; Labrador, R.O.; Vilches, J.J.; Forés, J.; Navarro, X. Influence of Physical Parameters of Nerve Chambers on Peripheral Nerve Regeneration and Reinnervation. *Exp. Neurol.* **1996**, *137*, 26–33. <https://doi.org/10.1006/exnr.1996.0003>.
33. Mackinnon, S.E.; Dellon, A.L. Clinical nerve reconstruction with a bioabsorbable polyglycolic acid tube. *Plast. Reconstr. Surg.* **1990**, *85*, 419–429. <https://doi.org/10.1097/00006534-199003000-00015>.
34. Archibald, S.J.; Shefner, J.; Krarup, C.; Madison, R.D. Monkey Median Nerve Repaired by Nerve Graft or Collagen Nerve Guide Tube. *J. Neurosci.* **1995**, *15*, 4109–4123. <https://doi.org/10.1523/JNEUROSCI.15-05-04109.1995>.
35. Hoben, G.M.; Ee, X.; Schellhardt, L.; Yan, Y.; Hunter, D.A.; Moore, A.M.; Snyder-Warwick, A.K.; Stewart, S.; Mackinnon, S.E.; Wood, M.D. Increasing Nerve Autograft Length Increases Senescence and Reduces Regeneration. *Plast. Reconstr. Surg.* **2018**, *142*, 952–961. <https://doi.org/10.1097/PRS.00000000000004759>.
36. Matsumine, H.; Niimi, Y.; Matsumine, H. An Electrophysiological Evaluation Method for the Ovine Facial Nerve. *Regen. Ther.* **2021**, *18*, 76–81. <https://doi.org/10.1016/j.reth.2021.03.008>.
37. Ribitsch, I.; Baptista, P.M.; Lange-Consiglio, A.; Melotti, L.; Patruno, M.; Jenner, F.; Schnabl-Feichter, E.; Dutton, L.C.; Connolly, D.J.; van Steenbeek, F.G.; et al. Large Animal Models in Regenerative Medicine and Tissue Engineering: To Do or Not to Do. *Front. Bioeng. Biotechnol.* **2020**, *8*, 972. <https://doi.org/10.3389/fbioe.2020.00972>.
38. Banstola, A.; Reynolds, J.N.J. The Sheep as a Large Animal Model for the Investigation and Treatment of Human Disorders. *Biology* **2022**, *11*, 1251. <https://doi.org/10.3390/biology11091251>.

39. Lawson, G.M.; Glasby, M.A. A Comparison of Immediate and Delayed Nerve Repair Using Autologous Freeze-Thawed Muscle Grafts in a Large Animal Model. The Simple Injury. *J. Hand Surg. Br.* **1995**, *20*, 663–700.
40. Jeans, L.A.; Gilchrist, T.; Healy, D. Peripheral Nerve Repair by Means of a Flexible Biodegradable Glass Fibre Wrap: A Comparison with Microsurgical Epineurial Repair. *J. Plast. Reconstr. Aesthet. Surg.* **2007**, *60*, 1302–1308. <https://doi.org/10.1016/j.bjps.2006.06.014>.
41. Alvites, R.D.; Branquinho, M.v.; Sousa, A.C.; Zen, F.; Maurina, M.; Raimondo, S.; Mendonça, C.; Atayde, L.; Geuna, S.; Varejão, A.S.P.; et al. Establishment of a Sheep Model for Hind Limb Peripheral Nerve Injury: Common Peroneal Nerve. *Int. J. Mol. Sci.* **2021**, *22*, 1401. <https://doi.org/10.3390/ijms22031401>.
42. Vasudevan, S.; Yan, J.G.; Zhang, L.L.; Matloub, H.S.; Cheng, J.J. A Rat Model for Long-Gap Peripheral Nerve Reconstruction. *Plast. Reconstr. Surg.* **2013**, *132*, 871–876. <https://doi.org/10.1097/PRS.0b013e31829fe515>.
43. Lezak, B.; Massel, D.H. Peroneal Nerve Injury [Updated 2022 Sep 4]. In *StatPearls*; StatPearls Publishing: Treasure Island, FL, USA; 2022 January. Available online: <https://www.ncbi.nlm.nih.gov/books/NBK549859/> (accessed on 7 September 2022).
44. Roballo, K.C.S.; Burns, D.T.; Ghnenis, A.B.; Osimanjiang, W.; Bushman, J.S. Long-Term Neural Regeneration Following Injury to the Peroneal Branch of the Sciatic Nerve in Sheep. *Eur. J. Neurosci.* **2020**, *52*, 4385–4394. <https://doi.org/10.1111/ejn.14835>.
45. Marciniak, C. Fibular (Peroneal) Neuropathy. Electrodiagnostic Features and Clinical Correlates. *Phys. Med. Rehabil. Clin. N. Am.* **2013**, *24*, 121–137. <https://doi.org/10.1016/j.pmr.2012.08.016>.
46. Ma, W.; Bisby, M.A. Calcitonin Gene-Related Peptide, Substance P and Protein Gene Product 9.5 Immunoreactive Axonal Fibers in the Rat Footpad Skin Following Partial Sciatic Nerve Injuries. *J. Neurocytol.* **2000**, *29*, 249–262. <https://doi.org/10.1023/a:1026519720352>.
47. Cobianchi, S.; de Cruz, J.; Navarro, X. Assessment of Sensory Thresholds and Nociceptive Fiber Growth after Sciatic Nerve Injury Reveals the Differential Contribution of Collateral Reinnervation and Nerve Regeneration to Neuropathic Pain. *Exp. Neurol.* **2014**, *255*, 1–11. <https://doi.org/10.1016/j.expneurol.2014.02.008>.
48. Theriault, M.; Dort, J.; Sutherland, G.; Zochodne, D.W. A Prospective Quantitative Study of Sensory Deficits after Whole Sural Nerve Biopsies in Diabetic and

- Nondiabetic Patients Surgical Approach and the Role of Collateral Sprouting. *Neurology* **1998**, *50*, 480–484. <https://doi.org/10.1212/wnl.50.2.480>.
49. Kemp, S.W.P.; Cederna, P.S.; Midha, R. Comparative Outcome Measures in Peripheral Regeneration Studies. *Exp. Neurol.* **2017**, *287*, 348–357. <https://doi.org/10.1016/j.expneurol.2016.04.011>.
50. Krarup, C. Nerve Conduction Studies in Selected Peripheral Nerve Disorders. *Curr. Opin. Neurol.* **2002**, *15*, 579–593. <https://doi.org/10.1097/00019052-200210000-00009>.
51. Navarro, X. Functional Evaluation of Peripheral Nerve Regeneration and Target Reinnervation in Animal Models: A Critical Overview. *Eur. Neurosci.* **2016**, *43*, 271–286. <https://doi.org/10.1111/ejn.13033>.
52. Neubauer, D.; Graham, J.B.; Muir, D. Chondroitinase Treatment Increases the Effective Length of Acellular Nerve Grafts. *Exp. Neurol.* **2007**, *207*, 163–170. <https://doi.org/10.1016/j.expneurol.2007.06.006>.
53. Garozzo, D.; Ferraresi, S.; Buffatti, T. Surgical Treatment of Common Peroneal Nerve Injuries: Indications and Results. A Series of 62 Cases. *J. Neurosurg. Sci.* **2004**, *48*, 105–112.
54. Kasper, M.; Deister, C.; Beck, F.; Schmidt, C.E. Bench-to-Bedside Lessons Learned: Commercialization of an Acellular Nerve Graft. *Adv. Healthc. Mater.* **2020**, *9*, e2000174. <https://doi.org/10.1002/adhm.202000174>.
55. Safa, B.; Jain, S.; Desai, M.J.; Greenberg, J.A.; Niaccaris, T.R.; Nydick, J.A.; Leversedge, F.J.; Megee, D.M.; Zoldos, J.; Rinker, B.D.; et al. Peripheral Nerve Repair throughout the Body with Processed Nerve Allografts: Results from a Large Multicenter Study. *Microsurgery* **2020**, *40*, 527–537. <https://doi.org/10.1002/micr.30574>.
56. Peters, B.R.; Wood, M.D.; Hunter, D.A.; Mackinnon, S.E. Acellular Nerve Allografts in Major Peripheral Nerve Repairs: An Analysis of Cases Presenting With Limited Recovery. *Hand (N. Y.)* **2021**, 15589447211003175. <https://doi.org/10.1177/15589447211003175>.
57. Hudson, A.R.; Hunter, D.; Kline, D.G.; Bratton, B.R. Histological Studies of Experimental Interfascicular Graft Repairs. *J. Neurosurg.* **1979**, *51*, 333–340. <https://doi.org/10.3171/jns.1979.51.3.0333>.

VIII. GENERAL DISCUSSION

Sheep as a large animal model of PNI

Despite the advances in surgical techniques for the repair of PNI resulting in long gap resections, the autologous nerve graft remains the gold standard. Due to some limitations of this type of graft, it is necessary to find alternatives to this repair technique. Experimental models are a good tool to investigate new therapeutical strategies for the repair of nerve injuries. In this thesis, we have used both a small animal model, in the rat, and a large animal model of PNI, in the sheep, to test decellularized allografts with two optimized protocols from two different biomedical companies, VERI and the BST, that aimed to set up a decellularized protocol for human cadaveric nerves to repair long nerve defects in the clinic.

Small animal models, such as rodents, can be used in proof-of-concept studies, with the advantages that there is a well established model to evaluate nerve regeneration using the sciatic nerve. However, these species do not replicate the complex neurobiological processes found in humans and therefore, there is a limitation for the clinical translation. On the other hand, the length of the gaps that can be assessed is quite short. This is an important limitation, since the graft length and the total regenerative distance required to reinnervate the target organs and ensure functional recovery are two of the main factors determining successful regeneration. Use of large animal models allow to study long nerve defects. Moreover, these models replicate the biological processes and physical features in humans, allowing to test new therapies with potential translation to the clinic.

Currently, there is only one commercial decellularized allograft, approved by the FDA, to repair nerve defects, the Axogen's Avance® nerve graft. Clinical studies have demonstrated that this graft can successfully sustain regeneration in 87% of the patients when repairing gaps of up to 5 cm (Brooks et al. 2012; Kornfeld et al., 2019), but the effectivity decreases as the length of the gap increases.

Therefore, in this thesis we aimed to evaluate allograft alternatives to repair long gap lesions, from 5 to 7 cm, using the sheep peroneal nerve as an experimental model. We chose the sheep among other large animal models, like rabbits, pigs

GENERAL DISCUSSION

or dogs because this animal species has similar peripheral nerves length and similar body weight to humans. They also have plurifascicular nerves with multiple fascicles and the regeneration rate is similar as in the humans. Comparing to other large animals, sheep are calm, easy to obtain and house, and are cost-effective. Moreover, they allow long-term studies that mimic the timing of human PNI and the use of similar methods to evaluate motor and sensory functions than those used in humans. Conventional pigs are also easy to obtain but cannot be used for long-term studies as they have a fast growing to a large weight. Alternatively, the use of minipigs is very expensive relative to sheep, and their size is quite smaller. Finally, the use of dogs or primates for research purposes implies more ethical concerns and higher costs.

The injured nerve used in the model must be also relevant. In humans, the most commonly injured nerve in lower limbs is the common peroneal nerve (Al Abri et al., 2014; Lezak et al., 2022). It is a plurifascicular nerve that innervates the muscles in the anterior compartment of the hindleg and the dorsum of the foot and is similar in size to the peroneal nerve in the sheep (Lawson and Glasby, 1995; Roballo et al., 2020). We compared two gap injuries induced by resection, 5 or 7 cm long, since they are relevant for clinical situations and are considered as the limit for effective regeneration along decellularized grafts, and duplicate the length that can be regenerated with synthetic conduits in large nerves. Although the progression of functional recovery in both experimental groups was parallel, we found a slight delay in animals repaired with a 7 cm autograft, pointing out a relationship between the graft length and the timing of functional recovery. In accordance with several previous studies, the length of the injury is one of the factors that affects the expected recovery rate after PNI (Horch and Lisney, 1981; Buti et al., 1996; Brooks et al., 2012).

Apart of the animal model, it is essential to standardize the evaluation methods of the preclinical studies according to the clinical signs produced by the peroneal nerve transection. In humans, as in sheep, this lesion causes dorsiflexion weakness and foot drop (Marciniak, 2013), as well as sensory loss in the dorsal metatarsal area (Alvites et al., 2021). We tested different functional tests that allowed us to assess nerve regeneration and reinnervation throughout the study;

some of them, such as the muscle loss by palpation, proprioceptive replacement of the foot, or the flexor withdrawal test at proximal and middle points, were discarded for further use because they did not provide useful information, probably due to compensations produced by the tibial and sural nerves that remained intact. For this reason, some of the tests proposed by Alvites et al. (2021) such as the dynamic repositioning, should not be considered because the intact limb nerves influence the results of the tests. Likewise, it is important to adapt the tests to the species, in this case, the sheep. In our case the withdrawal reflex was performed on the skin of the dorsal area of the metatarsus area in comparison with Alvites et al. (2021) who performed the same test on the hoof. Nonetheless, the most useful method to evaluate nerve regeneration was the electrophysiological tests, nerve conduction and EMG of the target muscles. As innovative technique, we introduced the muscle ultrasound that allows the measurement of denervated muscle atrophy and changes in muscle echogenicity, as there is an increase in hyperechoic tissue due to an increase in connective tissue (Simon et al., 2016; Strakowski and Chiou-Tan, 2020).

Decellularization protocols

The nerve microstructure and the composition of the ECM are highly complex and, therefore, the generation of nerve substitutes with the appropriate microstructural characteristics remains a challenge. During the last years, different bioengineered conduits showed promising results experimentally, although they were less efficient than the autograft repair (Deumens et al., 2010; Houshyar et al., 2019; García-García et al., 2023).

The generation of acellular nerves emerged as a promising alternative to the autograft repair since they may be stored on the shelf, and do not cause the immunologic rejection observed in cellular allografts. However, for a generalized use, it is essential to optimize the decellularization protocols for preserving the 3D structure and the molecular composition of the ECM apart from removing efficiently the cellular contents to respond to the limitations and drawbacks of the current gold standard treatment for long-gap PNI.

GENERAL DISCUSSION

The process of decellularization implies different phases, from the preservation of the native tissue, the decellularization process itself and the preservation for long-term storage.

Decellularization protocols must allow the elimination of the antigens responsible for immunological rejection and the preservation of the natural nerve architecture and the ECM components after the decellularization, providing an ideal substrate for newly formed axons (Philips et al., 2018a). In addition, the protocol should be simple, efficient and cost-effective. There are different methods for decellularizing peripheral nerves, such as freeze-thawing, detergent-based or cold preservation. The most efficient is the detergent-based method which was developed first by Sondel et al. (1998). This protocol was based on Triton X-100 solutions, but it did not allow for structural preservation. Later, Hudson et al. (2004) proposed a less toxic protocol based on combining Triton X-200 solutions with amphoteric detergents such as sulfobetaines, which made it possible to better preserve the ECM. The Avance® nerve graft decellularization protocol is also based on detergents such as Triton and sulfobetaines, being considered the most effective until now since it also incorporates the degradation of CSPG, which inhibits axonal growth.

In this thesis we have tested nerve decellularization protocols from two different companies, VERI and BST. In both cases, the enzymatic-based decellularization protocols have been optimized for peripheral nerves of rats, sheep and humans. VERI based its protocol on DNase, PBS and NaCl, whereas the BST protocol used non-ionic detergent and zwitterionic agents, optimized with the addition of hypertonic NaCl 1M and DNase. The process used by BST is slower, taking 10 days to decellularize the nerves, while the process used by VERI lasts only 6 days. Both protocols were assessed for DNA content after decellularization with the DNeasy Blood and Tissue Kit from Qiagen, and demonstrated that the DNA content of the decellularized nerves was much lower than in native nerves. The immunofluorescence results (Figure 6), showed that the BST protocol removed more efficiently remnants of myelinated axons and SCs after the decellularization.

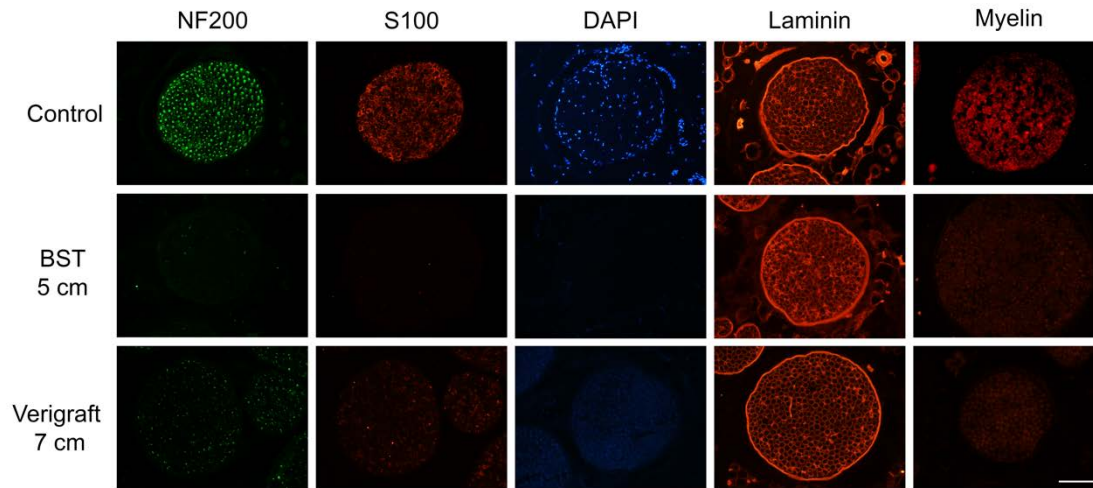


Figure 6. Representative micrographs showing immunofluorescence of myelinated axons (NF200), SC (S100), nuclei (DAPI), ECM proteins (Laminin) and myelin (Myelin) in a control nerve, in a decellularized sheep nerve from BST and in a decellularized sheep nerve from VERI. Scale bar 150 μm .

Although immunofluorescence showed ECM preservation in both cases, histological analysis after the implantation and in vivo follow up indicated better preservation of the fascicular structure with the BST decellularization protocol. In the case of the VERI protocol, some regenerated axons were seen following an extrafascicular route, as shown by other authors with nerve grafts (Gómez et al., 1996; Evans et al., 1999; Forden et al., 2011), suggesting that the ECM was not consistent enough after the decellularization process (see figure 9 Chapter I).

Nerve regeneration in long-gap injuries in the rat

In this thesis, we have performed two different in vivo assays of optimized decellularized allografts in a very long gap in rat, i.e. 15 mm gap, as the first step for testing the decellularized grafts in vivo. The limiting gap is defined as the distance from which the peripheral nerve cannot regenerate within synthetic conduits; it is dependent on the size of the nerve and the species, being considered 10 mm in the case of the rat sciatic nerve (Yannas and Hill, 2004). In our studies, the repair was carried out with a decellularized nerve allograft of 15 mm as an alternative to the use of the autograft. In both cases, the decellularized

GENERAL DISCUSSION

nerves allowed successful regeneration, although the recovery was slower than in the autograft due to the lack of the cellular component.

Despite using the same lesion model, in the study with VERI decellularized allografts, regeneration and reinnervation were slower than in the study with BST grafts. The animals repaired with the decellularized allograft provided by BST showed evidence of reinnervation of the tibialis anterior (TA) muscle at 30 days post-injury (dpi), while only 16.6% of the animals repaired with the decellularized allograft from VERI showed positive TA EMG values at 30 dpi. At the distal level, animals repaired with BST allograft showed first evidence of reinnervation of the PL muscle at 60 dpi, while animals repaired with VERI allograft did not do so until 90 dpi. At the end of the study, set up at 120 dpi, all the animals from both experimental groups had positive PL CMAP values although the amplitude of the CMAP in the PL muscle was statistically lower in the VERI group compared to the BST treated group ($p < 0.001$). Quantitative results of myelinated axons were similar in both studies.

On the other hand, the results achieved with both decellularized allografts were superior to the ones obtained by repairing the same gap with nerve conduits of different materials, previously tested in our laboratory by using similar assessment methods. Thus, none of the animals repaired with a silicone tube regenerated after 120 dpi, whereas 57% and 50% of the animals repaired with chitosan tubes or polyactive tubes, respectively, showed signs of reinnervation and regeneration (Gonzalez-Perez et al., 2015; Santos et al., 2017). Novel hybrid conduits that mix synthetic materials, such as PLC poly(L-lactide-co- ϵ -caprolactone), and natural materials such as chitosan have been tested recently to repair 15 mm lesions in the sciatic nerve of rats (unpublished results). However, these last conduits only guarantee target reinnervation and distal regeneration in 25% of the rats, in front of the 100% observed with the decellularized allografts, This highlights the potential of decellularized allograft as a better alternative than nerve conduits to the autograft for repairing long gaps.

We have also compared the capability to support nerve regeneration of decellularized grafts, using the BST protocol, coming from the same species, the

rat, although from non-related animals of an outbred strain (allograft), and from another species, the human (xenograft). Of interest, the outcomes were significantly better for the decellularized allograft than for the decellularized xenograft, indicating that beyond the cellular contribution, the ECM composition exerts influences on the regenerating axons. This is of relevance for considering the origin of the nerve for decellularization. Our results suggest that it is more suitable to use nerves from the same species, and maybe from immune-compatible subjects.

Nerve regeneration in long-gap injuries in the sheep

In the sheep, we have evaluated the regenerative capacity of the two decellularized nerve allografts provided by BST and VERI as an alternative to the autograft when repairing 5 and 7 cm gap in the common peroneal nerve respectively. Again, both nerve defects have clinical relevance, since the maximal gap length for conduits is limited to 2-3 cm in human subjects (Kornfeld et al., 2019). The Avance® Nerve Graft is indicated for the repair of nerve defects up to 5 cm, whereas for the repair of defects from 5 to 7 cm, only a third of the patients show some functional recovery. Previous studies in the sheep peroneal nerve showed effective regeneration with recellularized allografts to repair nerve gaps of 3 cm (Tamez-Mata et al., 2021). Other studies in sheep used nerve conduits to repair a 6 mm gap in the tibial nerve (Radtke et al., 2011), and the sciatic nerve (Kornfeld et al., 2021) or recellularized allografts to repair 2 cm gap in the sciatic nerve (Pedroza-Montoya et al., 2022).

In the BST study the repair was carried out in a 5 cm gap while in the VERI study in a 7 cm gap. At the end of the studies, set up at 9 mps, all of the animals repaired with the BST decellularized allograft showed evidence of reinnervation of the TA muscle while 20% of the animals repaired with the VERI decellularized allograft did not show positive TA EMG results. The mean weight of the TA muscle was similar in both experimental groups, although this parameter is less sensitive.

The growth of myelinated axons in the decellularized graft provided by the BST was circumscribed to the endoneurium of the preserved fascicles, while in the

GENERAL DISCUSSION

VERI decellularized graft some axons regenerated extrafascicularly, forming small regenerative units. Previous studies with different allografts (Gomez et al., 1996; Strasberg et al., 1996; Evans et al., 1999; Forden et al., 2011), found that, unlike the BST group, there were some axons that regenerated following an extrafascicular route. Although the results of the two studies suggest that the BST decellularization protocol is less aggressive, since there is better preservation of the ECM, the number of myelinated axons both at the middle of the graft and distal to the nerve graft were similar in both studies.

Decellularized allografts have limitations related to slower regeneration compared to autografts, basically due to the lack of cellularity to prevent an immune response. It is important to take into account the important role of the SCs in nerve regeneration (Allodi et al., 2012; Jessen and Mirsky, 2016). Therefore, the lack of cellular support in decellularized allografts limit their regenerative capacity, particularly when used to repair long gaps, as shown in our studies. Nevertheless, the decellularized allograft still provides better support for regeneration and better outcomes than any of the nerve conduits reported in the literature, thus representing the best alternative option to the gold standard, the autograft. To overcome the limitation of the lack of cellularity and to improve their regenerative capacity, decellularized allografts can be enriched with trophic factors or with pro-regenerative cells, such as Schwann cells or Mesenchymal Stem Cells (Peters et al., 2021; Contreras et al., 2022), with the aim to better mimic the autograft environment and therefore, to reach similar regenerative capabilities than the gold standard technique to repair nerve resections in clinics. Certainly, the origin of the cells used should be carefully considered, so to avoid possible immune-rejection. Further preclinical research on recellularized nerve allografts is needed to investigate which type of cells, which pretreatment in vitro, and the optimal density are the best options for improving nerve regeneration in well standardized long gap nerve injury models before clinical translation can be proposed.

IX. CONCLUSIONS

1. The decellularization protocols optimized by the companies BST and Verigraft that were evaluated in this thesis were efficient and showed similar performance. They consist in enzymatical digestion, that in the case of the BST was combined with detergents. Both methods are efficient in removing cell debris, preserving both the structure and the biochemical and biomechanical properties of the extracellular matrix in nerves from rat, sheep and human donors.
2. *In vivo* studies performed on 15 mm limiting gaps in the sciatic nerve of rats showed that the decellularized nerve allografts can successfully support nerve regeneration, although lack of cellularity implies a slight delay in the regenerative process compared to the ideal autografts.
3. The use of a decellularized xenograft from human origin used to repair a 15 mm limiting gap in the sciatic nerve of rats did not sustain nerve regeneration, due to a notorious inflammatory response and a fibrotic reaction during the early phases of regeneration. These responses could be due to inter-species differences and also to the lower capacity of extracellular matrix components to sustain axon growth from another species, as suggested in the *in vitro* studies.
4. The sheep model has been optimized for two different severe gap lesions of 5 and 7 cm in the peroneal nerve. The clinical protocol developed is useful, but has some limitations to assess nerve regeneration. Quantitative tests by electrophysiology and echography of the tibialis anterior muscle along with histological analysis at the end of the study are the most sensitive tools for evaluating nerve regeneration and reinnervation of long-gap nerve injuries.
5. The *in vivo* evaluation of the decellularized allografts in a limiting gap lesion of 5 cm in the peroneal nerve of the sheep demonstrated their ability to support axonal regeneration and functional recovery, indicating their potential for clinical translation in the treatment of severe long-gap nerve injuries.
6. When the repair was carried out in a larger nerve gap, specifically of 7 cm, using a decellularized nerve allograft in the peroneal nerve of the sheep, lower regenerative capability was observed in comparison to the 5 cm nerve defects,

CONCLUSIONS

although these grafts had the capacity to sustain regeneration and to reinnervate target organs. However, the outcomes were inferior to the ones reached by autograft repair.

X. REFERENCES

- Agius E, Cochard P. Comparison of neurite outgrowth induced by intact and injured sciatic nerves: a confocal and functional analysis. *J Neurosci*. 1998 Jan 1;18(1):328-38.
- Al Abri R, Koletheekkat AA, Kelleher MO, Myles LM, Glasby MA. Effect of locally administered ciliary neurotrophic factor on the survival of transected and repaired adult sheep facial nerve. *Oman Med J*. 2014 May;29(3):208-13.
- Allodi I, Udina E, Navarro X. Specificity of peripheral nerve regeneration: interactions at the axon level. *Prog Neurobiol*. 2012 Jul;98(1):16-37.
- Alvites RD, V Branquinho M, Sousa AC, Zen F, Maurina M, Raimondo S, Mendonça C, Atayde L, Geuna S, Varejão ASP, Maurício AC. Establishment of a Sheep Model for Hind Limb Peripheral Nerve Injury: Common Peroneal Nerve. *Int J Mol Sci*. 2021 Jan 30;22(3):1401.
- Angius D, Wang H, Spinner RJ, Gutierrez-Cotto Y, Yaszemski MJ, Windebank AJ. A systematic review of animal models used to study nerve regeneration in tissue-engineered scaffolds. *Biomaterials*. 2012 Nov;33(32):8034-9.
- Archibald SJ, Shefner J, Krarup C, Madison RD. Monkey median nerve repaired by nerve graft or collagen nerve guide tube. *J Neurosci*. 1995 May;15(5 Pt 2):4109-23.
- Asplund M, Nilsson M, Jacobsson A, von Holst H. Incidence of traumatic peripheral nerve injuries and amputations in Sweden between 1998 and 2006. *Neuroepidemiology*. 2009;32(3):217-28.
- Atchabahian A, Genden EM, MacKinnon SE, Doolabh VB, Hunter DA. Regeneration through long nerve grafts in the swine model. *Microsurgery*. 1998;18(6):379-82.
- Aubá C, Hontanilla B, Arcocha J, Gorría O. Peripheral nerve regeneration through allografts compared with autografts in FK506-treated monkeys. *J Neurosurg*. 2006 Oct;105(4):602-9.
- Babington EJ, Vatanparast J, Verrall J, Blackshaw SE. Three-dimensional culture of leech and snail ganglia for studies of neural repair. *Invert Neurosci*. 2005 Nov;5(3-4):173-82.
- Bae JY, Park SY, Shin YH, Choi SW, Kim JK. Preparation of human decellularized

REFERENCES

- peripheral nerve allograft using amphoteric detergent and nuclease. *Neural Regen Res*. 2021 Sep;16(9):1890-1896.
- Baron-Van Evercooren A, Gansmüller A, Gumpel M, Baumann N, Kleinman HK. Schwann cell differentiation in vitro: extracellular matrix deposition and interaction. *Dev Neurosci*. 1986;8(3):182-96.
- Bedar M, Jerez S, Pulos N, van Wijnen AJ, Shin AY. Dynamic seeding versus microinjection of mesenchymal stem cells for acellular nerve allograft: an in vitro comparison. *J Plast Reconstr Aesthet Surg*. 2022 Aug;75(8):2821-2830.
- Bell JH, Haycock JW. Next generation nerve guides: materials, fabrication, growth factors, and cell delivery. *Tissue Eng Part B Rev*. 2012 Apr;18(2):116-28.
- Brenner MJ, Lowe JB 3rd, Fox IK, Mackinnon SE, Hunter DA, Darcy MD, Duncan JR, Wood P, Mohanakumar T. Effects of Schwann cells and donor antigen on long-nerve allograft regeneration. *Microsurgery*. 2005;25(1):61-70.
- Brooks DN, Weber RV, Chao JD, Rinker BD, Zoldos J, Robichaux MR, Ruggeri SB, Anderson KA, Bonatz EE, Wisotsky SM, Cho MS, Wilson C, Cooper EO, Ingari JV, Safa B, Parrett BM, Buncke GM. Processed nerve allografts for peripheral nerve reconstruction: a multicenter study of utilization and outcomes in sensory, mixed, and motor nerve reconstructions. *Microsurgery*. 2012 Jan;32(1):1-14.
- Brushart TM, Tarlov EC, Mesulam MM. Specificity of muscle reinnervation after epineurial and individual fascicular suture of the rat sciatic nerve. *J Hand Surg Am*. 1983 May;8(3):248-53.
- Butí M, Verdú E, Labrador RO, Vilches JJ, Forés J, Navarro X. Influence of physical parameters of nerve chambers on peripheral nerve regeneration and reinnervation. *Exp Neurol*. 1996 Jan;137(1):26-33.
- Burrell JC, Browne KD, Dutton JL, Laimo FA, Das S, Brown DP, Roberts S, Petrov D, Ali Z, Ledebur HC, Rosen JM, Kaplan HM, Wolf JA, Smith DH, Chen HI, Cullen DK. A Porcine Model of Peripheral Nerve Injury Enabling Ultra-Long Regenerative Distances: Surgical Approach, Recovery Kinetics, and Clinical Relevance. *Neurosurgery*. 2020 Sep 15;87(4):833-846.
- Caissie R, Gingras M, Champigny MF, Berthod F. In vivo enhancement of sensory perception recovery in a tissue-engineered skin enriched with laminin.

- Biomaterials. 2006 May;27(15):2988-93.
- Campbell WW. Evaluation and management of peripheral nerve injury. Clin Neurophysiol. 2008 Sep;119(9):1951-65.
- Chernousov MA, Carey DJ. Schwann cell extracellular matrix molecules and their receptors. Histol Histopathol. 2000 Apr;15(2):593-601.
- Cho Y, Sloutsky R, Naegle KM, Cavalli V. Injury-induced HDAC5 nuclear export is essential for axon regeneration. Cell. 2013 Nov 7;155(4):894-908.
- Contreras E, Bolívar S, Navarro X, Udina E. New insights into peripheral nerve regeneration: The role of secretomes. Exp Neurol. 2022 Aug;354:114069.
- Costa D, Diogo CC, Costa LMD, Pereira JE, Filipe V, Couto PA, Geuna S, Armada-Da-Silva PA, Maurício AC, Varejão ASP. Kinematic patterns for hindlimb obstacle avoidance during sheep locomotion. Neurol Res. 2018 Nov;40(11):963-971.
- Curtis R, Adryan KM, Zhu Y, Harkness PJ, Lindsay RM, DiStefano PS. Retrograde axonal transport of ciliary neurotrophic factor is increased by peripheral nerve injury. Nature. 1993 Sep 16;365(6443):253-5.
- Curtis R, Scherer SS, Somogyi R, Adryan KM, Ip NY, Zhu Y, Lindsay RM, DiStefano PS. Retrograde axonal transport of LIF is increased by peripheral nerve injury: correlation with increased LIF expression in distal nerve. Neuron. 1994 Jan;12(1):191-204.
- Curtis R, Tonra JR, Stark JL, Adryan KM, Park JS, Cliffer KD, Lindsay RM, DiStefano PS. Neuronal injury increases retrograde axonal transport of the neurotrophins to spinal sensory neurons and motor neurons via multiple receptor mechanisms. Mol Cell Neurosci. 1998 Oct;12(3):105-18.
- Deumens R, Bozkurt A, Meek MF, Marcus MA, Joosten EA, Weis J, Brook GA. Repairing injured peripheral nerves: Bridging the gap. Prog Neurobiol. 2010 Nov;92(3):245-76.
- Diogo CC, Camassa JA, Pereira JE, Costa LMD, Filipe V, Couto PA, Geuna S, Maurício AC, Varejão AS. The use of sheep as a model for studying peripheral nerve regeneration following nerve injury: review of the literature. Neurol Res. 2017 Oct;39(10):926-939.

REFERENCES

- Doolabh VB, Hertl MC, Mackinnon SE. The role of conduits in nerve repair: a review. *Rev Neurosci*. 1996 Jan-Mar;7(1):47-84.
- Dudanova I, Klein R. Integration of guidance cues: parallel signaling and crosstalk. *Trends Neurosci*. 2013 May;36(5):295-304.
- Ducic I, Fu R, Iorio ML. Innovative treatment of peripheral nerve injuries: combined reconstructive concepts. *Ann Plast Surg*. 2012 Feb;68(2):180-7.
- Dumont CE, Hentz VR. Enhancement of axon growth by detergent-extracted nerve grafts. *Transplantation*. 1997 May 15;63(9):1210-5.
- Erlanger, J., Gasser, H.S., 1937. Electrical signs of nervous activity.
- Evans PJ, Midha R, Mackinnon SE. The peripheral nerve allograft: a comprehensive review of regeneration and neuroimmunology. *Prog Neurobiol*. 1994 Jun;43(3):187-233. .
- Evans PJ, Mackinnon SE, Levi AD, Wade JA, Hunter DA, Nakao Y, Midha R. Cold preserved nerve allografts: changes in basement membrane, viability, immunogenicity, and regeneration. *Muscle Nerve*. 1998 Nov;21(11):1507-22.
- Evans PJ, MacKinnon SE, Midha R, Wade JA, Hunter DA, Nakao Y, Hare GM. Regeneration across cold preserved peripheral nerve allografts. *Microsurgery*. 1999;19(3):115-27.
- Fansa H, Keilhoff G, Förster G, Seidel B, Wolf G, Schneider W. Acellular muscle with Schwann-cell implantation: an alternative biologic nerve conduit. *J Reconstr Microsurg*. 1999 Oct;15(7):531-7.
- Fansa H, Schneider W, Wolf G, Keilhoff G. Host responses after acellular muscle basal lamina allografting used as a matrix for tissue engineered nerve grafts1. *Transplantation*. 2002 Aug 15;74(3):381-7.
- Forden J, Xu QG, Khu KJ, Midha R. A long peripheral nerve autograft model in the sheep forelimb. *Neurosurgery*. 2011 May;68(5):1354-62; discussion 1362.
- Fox IK, Jaramillo A, Hunter DA, Rickman SR, Mohanakumar T, Mackinnon SE. Prolonged cold-preservation of nerve allografts. *Muscle Nerve*. 2005 Jan;31(1):59-69.
- Fox IK, Mackinnon SE. Experience with nerve allograft transplantation. *Semin Plast Surg*. 2007 Nov;21(4):242-9.

- Fox MA. Novel roles for collagens in wiring the vertebrate nervous system. *Curr Opin Cell Biol.* 2008 Oct;20(5):508-13.
- Frerichs O, Fansa H, Schicht C, Wolf G, Schneider W, Keilhoff G. Reconstruction of peripheral nerves using acellular nerve grafts with implanted cultured Schwann cells. *Microsurgery.* 2002;22(7):311-5.
- Fu SY, Gordon T. The cellular and molecular basis of peripheral nerve regeneration. *Mol Neurobiol.* 1997 Feb-Apr;14(1-2):67-116.
- García-García OD, El Soury M, Campos F, Sánchez-Porras D, Geuna S, Alaminos M, Gambarotta G, Chato-Astrain J, Raimondo S, Carriel V. Comprehensive ex vivo and in vivo preclinical evaluation of novel chemo enzymatic decellularized peripheral nerve allografts. *Front. Bioeng. Biotechnol.* 2023, 11:1162684.
- Gardiner NJ, Moffatt S, Fernyhough P, Humphries MJ, Streuli CH, Tomlinson DR. Preconditioning injury-induced neurite outgrowth of adult rat sensory neurons on fibronectin is mediated by mobilisation of axonal alpha5 integrin. *Mol Cell Neurosci.* 2007 Jun;35(2):249-60.
- Gerdts J, Summers DW, Milbrandt J, DiAntonio A. Axon Self-Destruction: New Links among SARM1, MAPKs, and NAD⁺ Metabolism. *Neuron.* 2016 Feb 3;89(3):449-60.
- Geuna S. The sciatic nerve injury model in pre-clinical research. *J Neurosci Methods.* 2015 Mar 30;243:39-46.
- Ghosh A, Greenberg ME. Calcium signaling in neurons: molecular mechanisms and cellular consequences. *Science.* 1995 Apr 14;268(5208):239-47.
- Glasby MA, Gilmour JA, Gschmeissner SE, Hems TE, Myles LM. The repair of large peripheral nerves using skeletal muscle autografts: a comparison with cable grafts in the sheep femoral nerve. *Br J Plast Surg.* 1990 Mar;43(2):169-78.
- Glasby MA, Mountain RE, Murray JA. Repair of the facial nerve using freeze-thawed muscle autografts. A surgical model in the sheep. *Arch Otolaryngol Head Neck Surg.* 1993 Apr;119(4):461-5.
- Godinho MJ, Teh L, Pollett MA, Goodman D, Hodgetts SI, Sweetman I, Walters M, Verhaagen J, Plant GW, Harvey AR. Immunohistochemical, ultrastructural and functional analysis of axonal regeneration through peripheral nerve grafts

REFERENCES

- containing Schwann cells expressing BDNF, CNTF or NT3. *PLoS One*. 2013 Aug 9;8(8):e69987.
- Godinho MJ, Staal JL, Krishnan VS, Hodgetts SI, Pollett MA, Goodman DP, Teh L, Verhaagen J, Plant GW, Harvey AR. Regeneration of adult rat sensory and motor neuron axons through chimeric peroneal nerve grafts containing donor Schwann cells engineered to express different neurotrophic factors. *Exp Neurol*. 2020 Aug;330:113355.
- Goldberg JL. How does an axon grow? *Genes Dev*. 2003 Apr 15;17(8):941-58.
- Gómez N, Cuadras J, Butí M, Navarro X. Histologic assessment of sciatic nerve regeneration following resection and graft or tube repair in the mouse. *Restor Neurol Neurosci*. 1996 Jan 1;10(4):187-96.
- Gonzalez-Perez F, Udina E, Navarro X. Extracellular matrix components in peripheral nerve regeneration. *Int Rev Neurobiol*. 2013;108:257-75.
- Gonzalez-Perez F, Cobianchi S, Geuna S, Barwig C, Freier T, Udina E, Navarro X. Tubulization with chitosan guides for the repair of long gap peripheral nerve injury in the rat. *Microsurgery*. 2015 May;35(4):300-8. doi: 10.1002/micr.22362. Epub 2014 Dec 4. PMID: 25471200.
- Gordon T, Borschel GH. The use of the rat as a model for studying peripheral nerve regeneration and sprouting after complete and partial nerve injuries. *Exp Neurol*. 2017 Jan;287(Pt 3):331-347.
- Gulati AK. Evaluation of acellular and cellular nerve grafts in repair of rat peripheral nerve. *J Neurosurg*. 1988 Jan;68(1):117-23.
- Gulati AK, Cole GP. Immunogenicity and regenerative potential of acellular nerve allografts to repair peripheral nerve in rats and rabbits. *Acta Neurochir (Wien)*. 1994;126(2-4):158-64.
- Gulati AK. Immunological fate of Schwann cell-populated acellular basal lamina nerve allografts. *Transplantation*. 1995 Jun 15;59(11):1618-22.
- Gulati AK, Rai DR, Ali AM. The influence of cultured Schwann cells on regeneration through acellular basal lamina grafts. *Brain Res*. 1995 Dec 24;705(1-2):118-24.
- Hall SM. Regeneration in cellular and acellular autografts in the peripheral nervous

- system. *Neuropathol Appl Neurobiol*. 1986 Jan-Feb;12(1):27-46.
- Haase SC, Rovak JM, Dennis RG, Kuzon WM Jr, Cederna PS. Recovery of muscle contractile function following nerve gap repair with chemically acellularized peripheral nerve grafts. *J Reconstr Microsurg*. 2003 May;19(4):241-8.
- Heinzel JC, Quyen Nguyen M, Kefalianakis L, Prahm C, Daigeler A, Hercher D, Kolbenschlag J. A systematic review and meta-analysis of studies comparing muscle-in-vein conduits with autologous nerve grafts for nerve reconstruction. *Sci Rep*. 2021 Jun 3;11(1):11691.
- Hems TE, Glasby MA. Repair of cervical nerve roots proximal to the root ganglia. An experimental study in sheep. *J Bone Joint Surg Br*. 1992 Nov;74(6):918-22.
- Hems TE, Glasby MA. The limit of graft length in the experimental use of muscle grafts for nerve repair. *J Hand Surg Br*. 1993 Apr;18(2):165-70.
- Herdegen T, Kummer W, Fiallos CE, Leah J, Bravo R. Expression of c-JUN, JUN B and JUN D proteins in rat nervous system following transection of vagus nerve and cervical sympathetic trunk. *Neuroscience*. 1991;45(2):413-22.
- Hess JR, Brenner MJ, Fox IK, Nichols CM, Myckatyn TM, Hunter DA, Rickman SR, Mackinnon SE. Use of cold-preserved allografts seeded with autologous Schwann cells in the treatment of a long-gap peripheral nerve injury. *Plast Reconstr Surg*. 2007 Jan;119(1):246-259.
- Hoffman PN, Cleveland DW, Griffin JW, Landes PW, Cowan NJ, Price DL. Neurofilament gene expression: a major determinant of axonal caliber. *Proc Natl Acad Sci U S A*. 1987 May;84(10):3472-6.
- Hökfelt T, Broberger C, Xu ZQ, Sergeev V, Ubink R, Diez M. Neuropeptides--an overview. *Neuropharmacology*. 2000 Jun 8;39(8):1337-56.
- Horch KW, Lisney SJ. On the number and nature of regenerating myelinated axons after lesions of cutaneous nerves in the cat. *J Physiol*. 1981;313:275-86.
- Houshyar S, Bhattacharyya A, Shanks R. Peripheral Nerve Conduit: Materials and Structures. *ACS Chem Neurosci*. 2019 Aug 21;10(8):3349-3365.
- Hu J, Zhu QT, Liu XL, Xu YB, Zhu JK. Repair of extended peripheral nerve lesions in rhesus monkeys using acellular allogenic nerve grafts implanted with

REFERENCES

- autologous mesenchymal stem cells. *Exp Neurol*. 2007 Apr;204(2):658-66.
- Hudson TW, Zawko S, Deister C, Lundy S, Hu CY, Lee K, Schmidt CE. Optimized acellular nerve graft is immunologically tolerated and supports regeneration. *Tissue Eng*. 2004 Nov-Dec;10(11-12):1641-51.
- Hundepool CA, Nijhuis TH, Kotsougiani D, Friedrich PF, Bishop AT, Shin AY. Optimizing decellularization techniques to create a new nerve allograft: an in vitro study using rodent nerve segments. *Neurosurg Focus*. 2017 Mar;42(3):E4.
- Ide C, Tohyama K, Tajima K, Endoh K, Sano K, Tamura M, Mizoguchi A, Kitada M, Morihara T, Shirasu M. Long acellular nerve transplants for allogeneic grafting and the effects of basic fibroblast growth factor on the growth of regenerating axons in dogs: a preliminary report. *Exp Neurol*. 1998 Nov;154(1):99-112.
- Isaacs J. Treatment of acute peripheral nerve injuries: current concepts. *J Hand Surg Am*. 2010 Mar;35(3):491-7; quiz 498.
- Jensen JN, Brenner MJ, Tung TH, Hunter DA, Mackinnon SE. Effect of FK506 on peripheral nerve regeneration through long grafts in inbred swine. *Ann Plast Surg*. 2005 Apr;54(4):420-7.
- Jessen KR, Mirsky R. The repair Schwann cell and its function in regenerating nerves. *J Physiol*. 2016 Jul 1;594(13):3521-31.
- Jesuraj NJ, Santosa KB, Newton P, Liu Z, Hunter DA, Mackinnon SE, Sakiyama-Elbert SE, Johnson PJ. A systematic evaluation of Schwann cell injection into acellular cold-preserved nerve grafts. *J Neurosci Methods*. 2011 Apr 30;197(2):209-15.
- Jesuraj NJ, Santosa KB, Macewan MR, Moore AM, Kasukurthi R, Ray WZ, Flagg ER, Hunter DA, Borschel GH, Johnson PJ, Mackinnon SE, Sakiyama-Elbert SE. Schwann cells seeded in acellular nerve grafts improve functional recovery. *Muscle Nerve*. 2014 Feb;49(2):267-76.
- Kettle SJ, Starritt NE, Glasby MA, Hems TE. End-to-side nerve repair in a large animal model: how does it compare with conventional methods of nerve repair? *J Hand Surg Eur Vol*. 2013 Feb;38(2):192-202.
- Kline DG. Nerve surgery as it is now and as it may be. *Neurosurgery*. 2000 Jun;46(6):1285-93.

- Koller R, Rab M, Todoroff BP, Neumayer C, Haslik W, Stöhr HG, Frey M. The influence of the graft length on the functional and morphological result after nerve grafting: an experimental study in rabbits. *Br J Plast Surg.* 1997 Dec;50(8):609-14.
- Kornfeld T, Vogt PM, Radtke C. Nerve grafting for peripheral nerve injuries with extended defect sizes. *Wien Med Wochenschr.* 2019 Jun;169(9-10):240-251.
- Kornfeld T, Nessler J, Helmer C, Hannemann R, Waldmann KH, Peck CT, Hoffmann P, Brandes G, Vogt PM, Radtke C. Spider silk nerve graft promotes axonal regeneration on long distance nerve defect in a sheep model. *Biomaterials.* 2021 Apr;271:120692.
- Lawson GM, Glasby MA. A comparison of immediate and delayed nerve repair using autologous freeze-thawed muscle grafts in a large animal model. The simple injury. *J Hand Surg Br.* 1995 Oct;20(5):663-700.
- Leah JD, Herdegen T, Bravo R. Selective expression of Jun proteins following axotomy and axonal transport block in peripheral nerves in the rat: evidence for a role in the regeneration process. *Brain Res.* 1991 Dec 6;566(1-2):198-207.
- Lee SE, Shen H, Tagliabatella G, Chung JM, Chung K. Expression of nerve growth factor in the dorsal root ganglion after peripheral nerve injury. *Brain Res.* 1998 Jun 15;796(1-2):99-106.
- Lefcort F, Venstrom K, McDonald JA, Reichardt LF. Regulation of expression of fibronectin and its receptor, alpha 5 beta 1, during development and regeneration of peripheral nerve. *Development.* 1992 Nov;116(3):767-82. .
- Levi AD, Guénard V, Aebischer P, Bunge RP. The functional characteristics of Schwann cells cultured from human peripheral nerve after transplantation into a gap within the rat sciatic nerve. *J Neurosci.* 1994 Mar;14(3 Pt 1):1309-19.
- Levi AD. Characterization of the technique involved in isolating Schwann cells from adult human peripheral nerve. *J Neurosci Methods.* 1996 Sep;68(1):21-6.
- Lezak B, Massel DH, Varacallo M. Peroneal Nerve Injury. 2022 Nov 14. In: StatPearls [Internet]. Treasure Island (FL): StatPearls Publishing; 2023 Jan–.
- Li H, Terenghi G, Hall SM. Effects of delayed re-innervation on the expression of c-erbB receptors by chronically denervated rat Schwann cells in vivo. *Glia.* 1997

REFERENCES

- Aug;20(4):333-47.
- Liu HM. Growth factors and extracellular matrix in peripheral nerve regeneration, studied with a nerve chamber. *J Peripher Nerv Syst.* 1996;1(2):97-110.
- Lovati AB, D'Arrigo D, Odella S, Tos P, Geuna S, Raimondo S. Nerve Repair Using Decellularized Nerve Grafts in Rat Models. A Review of the Literature. *Front Cell Neurosci.* 2018 Nov 19;12:427.
- Lundborg G, Dahlin LB, Danielsen N, Gelberman RH, Longo FM, Powell HC, Varon S. Nerve regeneration in silicone chambers: influence of gap length and of distal stump components. *Exp Neurol.* 1982 May;76(2):361-75.
- Lundborg G, Dahlin LB, Danielsen N, Gelberman RH, Longo FM, Powell HC, Varon S. Nerve regeneration in silicone chambers: influence of gap length and of distal stump components. *Exp Neurol.* 1982 May;76(2):361-75. Lundborg G. Nerve injury and repair. Churchill Livingstone. 1988
- Lundborg G. A 25-year perspective of peripheral nerve surgery: evolving neuroscientific concepts and clinical significance. *J Hand Surg Am.* 2000 May;25(3):391-414.
- Lundborg G, Rosén B. Sensory relearning after nerve repair. *Lancet.* 2001 Sep 8;358(9284):809-10.
- Lundborg G, Richard P. Bunge memorial lecture. Nerve injury and repair--a challenge to the plastic brain. *J Peripher Nerv Syst.* 2003 Dec;8(4):209-26.
- Mackinnon SE, Dellon AL. A study of nerve regeneration across synthetic (Maxon) and biologic (collagen) nerve conduits for nerve gaps up to 5 cm in the primate. *J Reconstr Microsurg.* 1990 Apr;6(2):117-21.
- Mao Y, Schwarzbauer JE. Stimulatory effects of a three-dimensional microenvironment on cell-mediated fibronectin fibrillogenesis. *J Cell Sci.* 2005 Oct 1;118(Pt 19):4427-36.
- Marciniak C. Fibular (peroneal) neuropathy: electrodiagnostic features and clinical correlates. *Phys Med Rehabil Clin N Am.* 2013 Feb;24(1):121-37.
- Mathot F, Saffari TM, Rbia N, Nijhuis THJ, Bishop AT, Hovius SER, Shin AY. Functional Outcomes of Nerve Allografts Seeded with Undifferentiated and Differentiated Mesenchymal Stem Cells in a Rat Sciatic Nerve Defect Model.

- Plast Reconstr Surg. 2021 Aug 1;148(2):354-365.
- Matsumoto K, Ohnishi K, Kiyotani T, Sekine T, Ueda H, Nakamura T, Endo K, Shimizu Y. Peripheral nerve regeneration across an 80-mm gap bridged by a polyglycolic acid (PGA)-collagen tube filled with laminin-coated collagen fibers: a histological and electrophysiological evaluation of regenerated nerves. *Brain Res.* 2000 Jun 23;868(2):315-28.
- Matsuyama T, Midha R, Mackinnon SE, Munro CA, Wong PY, Ang LC. Long nerve allografts in sheep with Cyclosporin A immunosuppression. *J Reconstr Microsurg.* 2000 Apr;16(3):219-25.
- Moore AM, MacEwan M, Santosa KB, Chenard KE, Ray WZ, Hunter DA, Mackinnon SE, Johnson PJ. Acellular nerve allografts in peripheral nerve regeneration: a comparative study. *Muscle Nerve.* 2011 Aug;44(2):221-34.
- Moradzadeh A, Borschel GH, Luciano JP, Whitlock EL, Hayashi A, Hunter DA, Mackinnon SE. The impact of motor and sensory nerve architecture on nerve regeneration. *Exp Neurol.* 2008 Aug;212(2):370-6.
- Mueller BK. Growth cone guidance: first steps towards a deeper understanding. *Annu Rev Neurosci.* 1999;22:351-88.
- Mukhopadhyay G, Doherty P, Walsh FS, Crocker PR, Filbin MT. A novel role for myelin-associated glycoprotein as an inhibitor of axonal regeneration. *Neuron.* 1994 Sep;13(3):757-67.
- Nagao RJ, Lundy S, Khaing ZZ, Schmidt CE. Functional characterization of optimized acellular peripheral nerve graft in a rat sciatic nerve injury model. *Neurol Res.* 2011 Jul;33(6):600-8.
- Navarro X, Rodríguez FJ, Ceballos D, Verdú E. Engineering an artificial nerve graft for the repair of severe nerve injuries. *Med Biol Eng Comput.* 2003 Mar;41(2):220-6.
- Navarro X, Verdú E. Cell Transplants and Artificial Guides for Nerve Repair. In: Herdegen T, Delgado-García J (eds) *Brain Damage and Repair.* 2004. Springer, Dordrecht.
- Navarro X. Functional evaluation of peripheral nerve regeneration and target reinnervation in animal models: a critical overview. *Eur J Neurosci.* 2016 Feb;43(3):271-86.

REFERENCES

- Navarro X, Vivó M, Valero-Cabré A. Neural plasticity after peripheral nerve injury and regeneration. *Prog Neurobiol.* 2007 Jul;82(4):163-201.
- Neubauer D, Graham JB, Muir D. Nerve grafts with various sensory and motor fiber compositions are equally effective for the repair of a mixed nerve defect. *Exp Neurol.* 2010 May;223(1):203-6.
- Nieto-Nicolau N, López-Chicón P, Fariñas O, Bolívar S, Udina E, Navarro X, Casaroli-Marano RP, Vilarrodona A. Effective decellularization of human nerve matrix for regenerative medicine with a novel protocol. *Cell Tissue Res.* 2021 Apr;384(1):167-177.
- Ozturk C, Uygur S, Lukaszuk M. Sheep as a Large Animal Model for Nerve Regeneration Studies. In *Plastic and Reconstructive surgery: Experimental models and research designs.* London: Springer, UK. 2015 pp 507-511. ISBN 9781447163350
- Pan J, Zhao M, Yi X, et al. Acellular nerve grafts supplemented with induced pluripotent stem cell-derived exosomes promote peripheral nerve reconstruction and motor function recovery. *Bioact Mater.* 2021;15:272-287. Published 2021 Dec 20.
- Papalia I, Geuna S, D'Alcontres FS, Tos P. Origin and history of end-to-side neurorrhaphy. *Microsurgery.* 2007;27(1):56-61.
- Pedrini FA, Boriani F, Bolognesi F, Fazio N, Marchetti C, Baldini N. Cell-Enhanced Acellular Nerve Allografts for Peripheral Nerve Reconstruction: A Systematic Review and a Meta-Analysis of the Literature. *Neurosurgery.* 2019 Nov 1;85(5):575-604.
- Pedroza-Montoya FE, Tamez-Mata YA, Simental-Mendía M, Soto-Domínguez A, García-Pérez MM, Said-Fernández S, Montes-de-Oca-Luna R, González-Flores JR, Martínez-Rodríguez HG, Vilchez-Cavazos F. Repair of ovine peripheral nerve injuries with xenogeneic human acellular sciatic nerves prerecellularized with allogeneic Schwann-like cells-an innovative and promising approach. *Regen Ther.* 2022 Feb 12;19:131-143.
- Peters BR, Wood MD, Hunter DA, Mackinnon SE. Acellular Nerve Allografts in Major Peripheral Nerve Repairs: An Analysis of Cases Presenting With Limited Recovery. *Hand (N Y).* 2023 Mar;18(2):236-243.

- Philips C, Cornelissen M, Carriel V. Evaluation methods as quality control in the generation of decellularized peripheral nerve allografts. *J Neural Eng.* 2018a Apr;15(2):021003.
- Philips C, Campos F, Roosens A, Sánchez-Quevedo MDC, Declercq H, Carriel V. Qualitative and Quantitative Evaluation of a Novel Detergent-Based Method for Decellularization of Peripheral Nerves. *Ann Biomed Eng.* 2018b Nov;46(11):1921-1937.
- Radtke C, Allmeling C, Waldmann KH, Reimers K, Thies K, Schenk HC, Hillmer A, Guggenheim M, Brandes G, Vogt PM. Spider silk constructs enhance axonal regeneration and remyelination in long nerve defects in sheep. *PLoS One.* 2011 Feb 25;6(2):e16990.
- Raivich G, Hellweg R, Kreutzberg GW. NGF receptor-mediated reduction in axonal NGF uptake and retrograde transport following sciatic nerve injury and during regeneration. *Neuron.* 1991 Jul;7(1):151-64.
- Reyes O, Sosa I, Kuffler DP. Promoting neurological recovery following a traumatic peripheral nerve injury. *P R Health Sci J.* 2005 Sep;24(3):215-23.
- Rbia N, Bulstra LF, Bishop AT, van Wijnen AJ, Shin AY. A Simple Dynamic Strategy to Deliver Stem Cells to Decellularized Nerve Allografts. *Plast Reconstr Surg.* 2018 Aug;142(2):402-413.
- Rbia N, Bulstra LF, Thaler R, Hovius SER, van Wijnen AJ, Shin AY. In Vivo Survival of Mesenchymal Stromal Cell-Enhanced Decellularized Nerve Grafts for Segmental Peripheral Nerve Reconstruction. *J Hand Surg Am.* 2019 Jun;44(6):514.e1-514.e11.
- Rishal I, Fainzilber M. Axon-soma communication in neuronal injury. *Nat Rev Neurosci.* 2014 Jan;15(1):32-42.
- Roballo KCS, Burns DT, Ghnenis AB, Osimanjiang W, Bushman JS. Long-term neural regeneration following injury to the peroneal branch of the sciatic nerve in sheep. *Eur J Neurosci.* 2020 Nov;52(10):4385-4394.
- Rodríguez FJ, Gómez N, Labrador RO, Butí M, Ceballos D, Cuadras J, Verdú E, Navarro X. Improvement of regeneration with predegenerated nerve transplants in silicone chambers. *Restor Neurol Neurosci.* 1999;14(1):65-79.
- Rodríguez FJ, Valero-Cabré A, Navarro X. Regeneration and functional recovery

REFERENCES

- following peripheral nerve injuries. *Drug Discovery Today: Disease Models* 2004,1:177-185.
- Rovak JM, Bishop DK, Boxer LK, Wood SC, Mungara AK, Cederna PS. Peripheral nerve transplantation: the role of chemical acellularization in eliminating allograft antigenicity. *J Reconstr Microsurg.* 2005 Apr;21(3):207-13.
- Saheb-Al-Zamani M, Yan Y, Farber SJ, Hunter DA, Newton P, Wood MD, Stewart SA, Johnson PJ, Mackinnon SE. Limited regeneration in long acellular nerve allografts is associated with increased Schwann cell senescence. *Exp Neurol.* 2013 Sep;247:165-77.
- Sameem M, Wood TJ, Bain JR. A systematic review on the use of fibrin glue for peripheral nerve repair. *Plast Reconstr Surg.* 2011 Jun;127(6):2381-2390.
- Santos D, Wieringa P, Moroni L, Navarro X, Valle JD. PEOT/PBT Guides Enhance Nerve Regeneration in Long Gap Defects. *Adv Healthc Mater.* 2017 Feb;6(3).
- Schwaiger FW, Hager G, Schmitt AB, Horvat A, Hager G, Streif R, Spitzer C, Gamal S, Breuer S, Brook GA, Nacimiento W, Kreutzberg GW. Peripheral but not central axotomy induces changes in Janus kinases (JAK) and signal transducers and activators of transcription (STAT). *Eur J Neurosci.* 2000 Apr;12(4):1165-76.
- Schmidt CE, Leach JB. Neural tissue engineering: strategies for repair and regeneration. *Annu Rev Biomed Eng.* 2003;5:293-347.
- Seddon HJ. A Classification of Nerve Injuries. *Br Med J.* 1942 Aug 29;2(4260):237-9.
- Shenaq JM, Shenaq SM, Spira M. Reliability of sciatic function index in assessing nerve regeneration across a 1 cm gap. *Microsurgery.* 1989;10(3):214-9.
- Shin YH, Park SY, Kim JK. Comparison of systematically combined detergent and nuclease-based decellularization methods for acellular nerve graft: An ex vivo characterization and in vivo evaluation. *J Tissue Eng Regen Med.* 2019 Jul;13(7):1241-1252.
- Siemionow M, Brzezicki G. Chapter 8: Current techniques and concepts in peripheral nerve repair. *Int Rev Neurobiol.* 2009;87:141-72.
- Simon NG, Noto YI, Zaidman CM. Skeletal muscle imaging in neuromuscular

- disease. *J Clin Neurosci*. 2016 Nov;33:1-10.
- Skene JH. Axonal growth-associated proteins. *Annu Rev Neurosci*. 1989;12:127-56.
- Sondell M, Lundborg G, Kanje M. Regeneration of the rat sciatic nerve into allografts made acellular through chemical extraction. *Brain Res*. 1998 Jun 8;795(1-2):44-54.
- Squintani G, Bonetti B, Paolin A, Vici D, Cogliati E, Murer B, Stevanato G. Nerve regeneration across cryopreserved allografts from cadaveric donors: a novel approach for peripheral nerve reconstruction. *J Neurosurg*. 2013 Oct;119(4):907-13.
- Sridharan R, Reilly RB, Buckley CT. Decellularized grafts with axially aligned channels for peripheral nerve regeneration. *J Mech Behav Biomed Mater*. 2015 Jan;41:124-35.
- Stoll G, Müller HW. Nerve injury, axonal degeneration and neural regeneration: basic insights. *Brain Pathol*. 1999 Apr;9(2):313-25.
- Strakowski JA, Chiou-Tan FY. Musculoskeletal ultrasound for traumatic and torsional alterations. *Muscle Nerve*. 2020 Dec;62(6):654-663.
- Strasberg SR, Mackinnon SE, Genden EM, Bain JR, Purcell CM, Hunter DA, Hay JB. Long-segment nerve allograft regeneration in the sheep model: experimental study and review of the literature. *J Reconstr Microsurg*. 1996 Nov;12(8):529-37.
- Strauch B, Ferder M, Lovelle-Allen S, Moore K, Kim DJ, Llana J. Determining the maximal length of a vein conduit used as an interposition graft for nerve regeneration. *J Reconstr Microsurg*. 1996 Nov;12(8):521-7.
- Strauch B, Rodriguez DM, Diaz J, Yu HL, Kaplan G, Weinstein DE. Autologous Schwann cells drive regeneration through a 6-cm autogenous venous nerve conduit. *J Reconstr Microsurg*. 2001 Nov;17(8):589-95; discussion 596-7.
- Sufan W, Suzuki Y, Tanihara M, Ohnishi K, Suzuki K, Endo K, Nishimura Y. Sciatic nerve regeneration through alginate with tubulation or nontubulation repair in cat. *J Neurotrauma*. 2001 Mar;18(3):329-38.
- Sunderland S. The anatomy and physiology of nerve injury. *Muscle Nerve*. 1990

REFERENCES

- Sep;13(9):771-84.
- Suss PH, Ribeiro VST, Motooka CE, de Melo LC, Tuon FF. Comparative study of decellularization techniques to obtain natural extracellular matrix scaffolds of human peripheral-nerve allografts. *Cell Tissue Bank*. 2022 Sep;23(3):511-520.
- Suzuki Y, Tanihara M, Ohnishi K, Suzuki K, Endo K, Nishimura Y. Cat peripheral nerve regeneration across 50 mm gap repaired with a novel nerve guide composed of freeze-dried alginate gel. *Neurosci Lett*. 1999 Jan 8;259(2):75-8.
- Szynkaruk M, Kemp SW, Wood MD, Gordon T, Borschel GH. Experimental and clinical evidence for use of decellularized nerve allografts in peripheral nerve gap reconstruction. *Tissue Eng Part B Rev*. 2013 Feb;19(1):83-96.
- Tamez-Mata Y, Pedroza-Montoya FE, Martínez-Rodríguez HG, García-Pérez MM, Ríos-Cantú AA, González-Flores JR, Soto-Domínguez A, Montes-de-Oca-Luna R, Simental-Mendía M, Peña-Martínez VM, Vílchez-Cavazos F. Nerve gaps repaired with acellular nerve allografts recellularized with Schwann-like cells: Preclinical trial. *J Plast Reconstr Aesthet Surg*. 2022 Jan;75(1):296-306.
- Tanaka K, Zhang QL, Webster HD. Myelinated fiber regeneration after sciatic nerve crush: morphometric observations in young adult and aging mice and the effects of macrophage suppression and conditioning lesions. *Exp Neurol*. 1992 Oct;118(1):53-61.
- Tang BL. Inhibitors of neuronal regeneration: mediators and signaling mechanisms. *Neurochem Int*. 2003 Feb;42(3):189-203.
- Taylor CA, Braza D, Rice JB, Dillingham T. The incidence of peripheral nerve injury in extremity trauma. *Am J Phys Med Rehabil*. 2008 May;87(5):381-5.
- Tetzlaff W, Leonard C, Krekoski CA, Parhad IM, Bisby MA. Reductions in motoneuronal neurofilament synthesis by successive axotomies: a possible explanation for the conditioning lesion effect on axon regeneration. *Exp Neurol*. 1996 May;139(1):95-106.
- Tos P, Ronchi G, Papalia I, Sallen V, Legagneux J, Geuna S, Giacobini-Robecchi MG. Chapter 4: Methods and protocols in peripheral nerve regeneration experimental research: part I-experimental models. *Int Rev Neurobiol*.

- 2009;87:47-79.
- Turner AS. Experiences with sheep as an animal model for shoulder surgery: strengths and shortcomings. *J Shoulder Elbow Surg.* 2007 Sep-Oct;16(5 Suppl):S158-63.
- Udina E, Voda J, Gold BG, Navarro X. Comparative dose-dependence study of FK506 on transected mouse sciatic nerve repaired by allograft or xenograft. *J Peripher Nerv Syst.* 2003a Sep;8(3):145-54.
- Udina E, Ceballos D, Gold BG, Navarro X. FK506 enhances reinnervation by regeneration and by collateral sprouting of peripheral nerve fibers. *Exp Neurol.* 2003b Sep;183(1):220-31.
- Usoskin D, Furlan A, Islam S, Abdo H, Lönnerberg P, Lou D, Hjerling-Leffler J, Haeggström J, Kharchenko O, Kharchenko PV, Linnarsson S, Ernfors P. Unbiased classification of sensory neuron types by large-scale single-cell RNA sequencing. *Nat Neurosci.* 2015 Jan;18(1):145-53.
- Valero-Cabré A, Navarro X. Functional impact of axonal misdirection after peripheral nerve injuries followed by graft or tube repair. *J Neurotrauma.* 2002 Nov;19(11):1475-85.
- Valero-Cabré A, Tsironis K, Skouras E, Navarro X, Neiss WF. Peripheral and spinal motor reorganization after nerve injury and repair. *J Neurotrauma.* 2004 Jan;21(1):95-108.
- Varejão AS, Meek MF, Ferreira AJ, Patrício JA, Cabrita AM. Functional evaluation of peripheral nerve regeneration in the rat: walking track analysis. *J Neurosci Methods.* 2001 Jul 15;108(1):1-9.
- Wallquist W, Patarroyo M, Thams S, Carlstedt T, Stark B, Cullheim S, Hammarberg H. Laminin chains in rat and human peripheral nerve: distribution and regulation during development and after axonal injury. *J Comp Neurol.* 2002 Dec 16;454(3):284-93.
- Walsh S, Biernaskie J, Kemp SW, Midha R. Supplementation of acellular nerve grafts with skin derived precursor cells promotes peripheral nerve regeneration. *Neuroscience.* 2009 Dec 15;164(3):1097-107.
- Wang GY, Hirai K, Shimada H, Taji S, Zhong SZ. Behavior of axons, Schwann cells and perineurial cells in nerve regeneration within transplanted nerve grafts:

REFERENCES

- effects of anti-laminin and anti-fibronectin antisera. *Brain Res.* 1992 Jun 26;583(1-2):216-26.
- Wang H, Zhao Q, Zhao W, Liu Q, Gu X, Yang Y. Repairing rat sciatic nerve injury by a nerve-growth-factor-loaded, chitosan-based nerve conduit. *Biotechnol Appl Biochem.* 2012 Sep-Oct;59(5):388-94.
- Werner A, Willem M, Jones LL, Kreutzberg GW, Mayer U, Raivich G. Impaired axonal regeneration in alpha7 integrin-deficient mice. *J Neurosci.* 2000 Mar 1;20(5):1822-30.
- Whitlock EL, Tuffaha SH, Luciano JP, Yan Y, Hunter DA, Magill CK, Moore AM, Tong AY, Mackinnon SE, Borschel GH. Processed allografts and type I collagen conduits for repair of peripheral nerve gaps. *Muscle Nerve.* 2009 Jun;39(6):787-99.
- Williams LR, Longo FM, Powell HC, Lundborg G, Varon S. Spatial-temporal progress of peripheral nerve regeneration within a silicone chamber: parameters for a bioassay. *J Comp Neurol.* 1983 Aug 20;218(4):460-70.
- Wong J, Oblinger MM. A comparison of peripheral and central axotomy effects on neurofilament and tubulin gene expression in rat dorsal root ganglion neurons. *J Neurosci.* 1990 Jul;10(7):2215-22.
- Wu X, Jiang J, Gu Z, Zhang J, Chen Y, Liu X. Mesenchymal stromal cell therapies: immunomodulatory properties and clinical progress. *Stem Cell Res Ther.* 2020 Aug 8;11(1):345.
- Yannas IV, Hill BJ. Selection of biomaterials for peripheral nerve regeneration using data from the nerve chamber model. *Biomaterials.* 2004 Apr;25(9):1593-600.
- Zalewski AA, Gulati AK. Evaluation of histocompatibility as a factor in the repair of nerve with a frozen nerve allograft. *J Neurosurg.* 1982 Apr;56(4):550-4.
- Zhang F, Blain B, Beck J, Zhang J, Chen Z, Chen ZW, Lineaweaver WC. Autogenous venous graft with one-stage prepared Schwann cells as a conduit for repair of long segmental nerve defects. *J Reconstr Microsurg.* 2002 May;18(4):295-300.
- Zochodne DW. The challenges and beauty of peripheral nerve regrowth. *J Peripher Nerv Syst.* 2012 Mar;17(1):1-18.

XI. ACKNOWLEDGMENTS

En primer lloc, agrair als meus directors de tesi, el Xavi i l'Esther per fer possible aquesta tesi. Xavi, gràcies per tot el que m'has ensenyat, ha estat un plaer poder aprendre de la teva passió. Gràcies també per totes les hores a granja, fins i tot en vigília de cap d'any. Esther, han sigut moltes les hores a cultius, fent tècniques que no dominàvem però que acabàvem resolent ningú sap com, de manera exitosa. Gràcies per acompanyar-me i ajudar-me sempre que ho he necessitat.

Al Banc de Sang i Teixits, per tota la feina i tota l'ajuda rebuda, en especial agrair a la Núria tota la optimització dels nervis d'ovella durant la pandèmia i tota l'ajuda que m'has donat sempre que ho he necessitat amb els protocols de descel·lularització.

To Verigraft, for helping to carry out the studies of this thesis.

A todo el equipo NFIS, por vuestra inestimable ayuda siempre que la he necesitado, especialmente a todos aquellos que os habéis puesto un mono de granja. A Sara B, por tu ayuda desde el minuto cero con todos los estudios y todas las dudas. A Jessica, porque aunque te lo he puesto difícil con mis nervios de oveja, los hemos sacado adelante siempre entre risas. Incluso se podría decir que hemos optimizado nuestros propios protocolos Jaramillo et al. A Míriam, mi mastercita, porque aunque sufrimos lo nuestro para sacar adelante tu TFM, lo hicimos, por todas las horas aprendiendo contigo. Te deseo lo mejor en esta nueva etapa.

A Patri, por darme la oportunidad de entrar en el mundo de la investigación, por animarnos siempre a obtener el mayor provecho a esta etapa de residencia y tesis conjunta. Gracias a todo el equipo del SIAL y de fisiología veterinaria, del que me llevo una gran experiencia, tanto personal como laboral. Sara, a tu especialment, aquesta tesi porta un tros teu. Gràcies per tota l'ajuda, per donar-me suport i ànims en moments difícils.

A todo el equipo de cirugía, por su trabajo y predisposición. En especial al Dr. Forés. Quim, gràcies pel teu temps, no només a quiròfans, sino durant tot l'estudi, ha estat un plaer compartir aquesta tesi amb tu. A l'Eduard, per la seva

ACKNOWLEDGMENTS

col·laboració en aquesta tesi, per la implementació del tests ecogràfics, la fabricació de les fèrules caseres i tota la revisió dels papers.

A l'equip de granges, sou genials. Pepe, Ramón, Sergi, un llarg etç. Sense vosaltres tot això no hagues estat possible. Gràcies per estar sempre al nostre costat, donant-nos un cop de mà. Us trobem a faltar.

A la família y amigos que han estado dando ánimos en esta etapa, que no ha sido muy relajada. En especial a mi pareja, Juan Carlos, gracias por todo y más.

I finalment agraïr a totes les Dawley, Jumping, Minnie, Shy, Unicornio, Malefica i un llarg etç, sense elles aquesta tesi no hauria estat possible.